

**URBAN SPRAWL IN THE STATE OF MISSOURI:
CURRENT TRENDS, DRIVING FORCES, AND
PREDICTED GROWTH ON MISSOURI'S NATURAL
LANDSCAPE**

A Dissertation
presented to
the Faculty of Forestry Department
University of Missouri

In Partial Fulfillment
of the Requirements for the Degree

Doctor of Philosophy

By
Bo ZHOU

Dr. Hong S. He, Dissertation Supervisor

December 2012

The undersigned, appointed by the dean of the graduate school, have examined the
dissertation entitled

URBAN SPRAWL IN THE STATE OF MISSOURI: CURRENT
TRENDS, DRIVING FORCES, AND PREDICTED GROWTH ON
MISSOURI'S NATURAL LANDSCAPE

Presented by Bo Zhou

A candidate for the degree of

Doctor of Philosophy

And hereby certify that, in their opinion, it is worthy of acceptance

Hong S. He

Professor

Department of Forestry

David R. Larsen

Professor

Department of Forestry

Francisco X. Aguilar

Assistant Professor

Department of Forestry

Cuizhen Wang

Associate Professor

Department of Geography

John Fresen

Assistant Teaching Professor

Department of Statistics

ACKNOWLEDGMENTS

This study was funded by the Missouri Department of Conservation, which also provided Landsat imageries and road network GIS files covering the whole study area of Missouri. The University of Missouri Department of Forestry faculty and staff were a valuable resource of information and support. The GIS and Spatial Analysis Lab provided a wonderful place to conduct my research and exchange ideas with my colleagues.

I would like to give a special acknowledgment to my advisor, Dr. Hong S. He for his continuous support, knowledge, and feedback. I would also like to thank my committee members, Dr. David R. Larsen, Dr. Francisco X. Aguilar, Dr Susan Wang and Dr. John Fresen for their wonderful recommendations and remarks. Besides my committee members, I would like to thank Dr. Jason A. Hubbard for his continuous interest and support in my research not to mention his fabulous editing of the manuscript of my second chapter. Outside the university, I would also like to thank Tim Nigh and John H. Schulz with the Missouri Department of Conservation for their expertise and support throughout the progress of my research.

My current colleagues and past alumni in the GIS and Spatial Analysis Lab have been a tremendous part of my support both academically and psychologically. Thanks to Zhenqian Lu and Jackie Schneiderman in my early stage of GIS learning. Thanks to Jian Yang and Yangjian Zhang for their guidance in my overall direction of research. Thanks to Erica Serna for always backing me up when I am not in a good mood. Thanks to Jacob Fraser, Wenjuan Wang, Jeffrey Schneiderman, Chris Bobryk, Shannon Bobryk, Michael Sunde, Qia Wang and Wenchi Jin for providing me an enjoyable environment to do research in this lab.

Finally, I would like to thank my parents for always believing me and supporting me unconditionally. They gave me the name 'Bo' when I was born so that I know I am destined to have a Ph. D. Degree when I grow up. It is my pleasure to accomplish my dream on their behave.

TABLE OF CONTENTS

ACKNOWLEDGMENTS	ii
TABLE OF CONTENTS.....	iv
LIST OF FIGURES	vii
LIST OF TABLES	x
ABSTRACT.....	xi
Introduction.....	1
1. Research problem.....	1
2. Objectives	3
3. Chapter outline.....	4
References.....	6
Chapter I. Mapping and analyzing change of impervious surface for two decades using multi-temporal Landsat imagery in Missouri	7
Abstract.....	7
1. Introduction.....	9
2. Approach and method	12
2.1. <i>Overview of impervious surface mapping approach</i>	12
2.2. <i>Data source and preprocessing</i>	15
2.3. <i>Procedure for mapping percent of impervious surface</i>	17
2.4. <i>Accuracy assessment</i>	19
2.5. <i>Impervious surface growth analysis</i>	20
3. Results.....	21
3.1. <i>Accuracy assessment</i>	21
3.2. <i>Statewide statistics of impervious surface growth</i>	22
3.3. <i>Spatial patterns of impervious surface growth</i>	23
3.4. <i>Sprawl affected area in relation to land cover, terrain, and road network</i>	24
3.5. <i>Impervious surface growth in relation to LTA, watershed, and county boundaries</i> ..	25
4. Discussion.....	27
4.1. <i>Approach implications</i>	27
4.2. <i>Result implications</i>	30
4.3. <i>Conclusions</i>	33
References.....	35
Tables.....	41
Figures	47
Chapter II. A pixel level approach of population estimation from Landsat derived impervious surface and Census data for the state of Missouri.....	54

Abstract.....	54
1. Introduction.....	55
2. Method	61
2.1. <i>Data</i>	61
2.2. <i>Identify the best range of imperviousness for population mapping</i>	63
2.3. <i>Regression relationship between population and imperviousness</i>	64
2.4. <i>Estimating per pixel population</i>	70
3. Results.....	72
3.1. <i>Results validation</i>	72
3.2. <i>Pixel-based regression model</i>	73
3.3. <i>Map results</i>	73
4. Discussion.....	75
4.1. <i>Approach implications</i>	75
4.2. <i>Data implications</i>	76
4.3. <i>Result implications</i>	77
5. Conclusions.....	78
References.....	80
Tables.....	83
Figures	86
Chapter III. A pixel-level approach of GIS simulation of urban growth from historical impervious surface and population in Jackson County, Missouri	96
Abstract.....	96
1. Introduction.....	97
2. Methodology	102
2.1. <i>Study area</i>	102
2.2. <i>Data preparation</i>	103
2.3. <i>Model design</i>	107
2.4. <i>Model structure</i>	109
2.5. <i>Model calibration</i>	111
2.6. <i>Model simulation</i>	112
3. Results.....	113
3.1. <i>Pattern of historical impervious surface growth</i>	113
3.2. <i>Model calibration</i>	114
3.3. <i>Future impervious surface growth prediction</i>	116
4. Discussion.....	117
5. Conclusion	120
References.....	122

Tables.....	126
Figures	127
VITA.....	142

LIST OF FIGURES

Figure 1-1. The 2 m NAIP image overlapped with a validation block inside the study area. Each outlined small box represents a 30 m by 30 m pixel corresponding to the Landsat pixel. The numbers inside each box is corresponding to the digitized and measured PIS inside each box. 47

Figure 1-2. Sub-pixel classifier (SPC) for percent of impervious surface (PIS) for the state of Missouri: a portion of Springfield in (a) 1980; (b) 1990; (c) 2000; and Jefferson City in (d) 1980; (e) 1990; (f) 2000. 48

Figure 1-3. Sub-pixel classifier (SPC) for percent of impervious surface (PIS) for the state of Missouri: a portion of Kansas City in (a) 1980; (b) 1990; (c) 2000 with A indicating leap frog, B indicating low density development on urban fringe of Kansas City, and C indicating low density development along the highway I-470; and a portion of St. Louis metro in (d) 1980; (e) 1990; (f) 2000 with A indicating development along highway I-70, B indicating infilling pattern, and C indicating rural sprawl. 49

Figure 1-4. Impervious surface growth (ISG) in the state of Missouri versus density of road networks for 1980s, and 1990s. 50

Figure 1-5. Percent of Impervious surface growth (ISG) summarized by Land type association (LTA) in the state of Missouri: a) 1980s; b) 1990s. ISG summarized by 10 digit watershed of the state of Missouri: c) 1980s; d) 1990s. 51

Figure 1-6. Per capita share of impervious surface (PCIS) summarized by county for 1980, 1990 and 2000 in the state of Missouri. 52

Figure 1-7. Impervious surface growth (ISG) by county in hectare: (a) 1980s; (b) 1990s. Percent change of per capita share of impervious surface (PCIS) by county: (c) 1980s; (d) 2000s. 53

Figure 2-1. Study area in Missouri, USA with preprocessed impervious surface data overlaid with Census block boundaries. A small area is magnified to show details. 86

Figure 2-2. Four different versions of preprocessed imperviousness: a) imperviousness with road network removed; b) imperviousness with road network and values larger than 80% removed; c) imperviousness with road network and values larger than 70% removed; d) imperviousness with road network and values larger than 60% removed. 87

Figure 2-3. GIS model diagram for attaching census population to each pixel inside based on the assumption that uniform population for each impervious surface pixel. 88

Figure 2-4. Census blocks classified into five categories based on population density with percent of impervious surface as background. 89

Figure 2-5. Census blocks classified into five categories based on adjusted population density with percent of impervious surface as background. 90

Figure 2-6. The distributions of population against percent of impervious surface class in each adjusted population density category based on the mean and standard deviation of population in Table 1. 91

Figure 2-7. Regression relationships between population and impervious surface for blocks of different adjusted population density. 92

Figure 2-8. GIS model diagram for calculating population estimates based Census population and percent of impervious surface plus four unique coefficients of γ , θ , κ , and λ derived from Missouri, USA.	93
Figure 2-9. Per-pixel population for Missouri, USA with four panels magnified for detail with the open space indicating no population and darker color indicating more population.....	94
Figure 2-10. Histogram of number of people per pixel for the whole state of Missouri, USA excluding pixels with zero population.	95
Figure 3-1. Graphic illustration to show the derivation of core urban areas using impervious surface generated binary urban and non-urban dataset. A morphological operation involving dilation and erosion is used to delineate the core urbanized areas. The core urban derived centroids are visibly better than the ones generated by Census designated place and urbanized areas by Census definition.	127
Figure 3-2. Overall model structure of the urban growth simulation model with a total of 6 sub-modules illustrated.	128
Figure 3-3. Diagram of the transition probability module, all the predictor variables are reclassified based on the statistical results generated from the multi-criteria evaluation of historical impervious surface coupled with default or expert input weights excluding the non-developable areas to generate the final transition probability surface output.	129
Figure 3-4. Diagram of the urban growth simulation module, the generation of new impervious surface pixels is based on an iteration loop controlled by the input of preset total growth. The module is stopped by a Boolean logic once the designated growth total is met. The output can be impervious surface density based on the location of new urban and historical density distribution of impervious surface or simply the location of new urban growth.	130
Figure 3-5. Flowchart of overall model simulation of future urban growth.	131
Figure 3-6. Output of distance analysis and terrain analysis module normalized predictor variables: elevation, slope, distance to centroids, distance to road, distance to major road, distance to water, distance to major water, distance to 1980 imperviousness and distance to 1990 imperviousness.....	132
Figure 3-7. The frequencies of impervious surface growth summarized by normalized elevation in 1980s and 1990s (A). The frequencies of impervious surface growth summarized by normalized slope in the 1980s and 1990s (B).	133
Figure 3-8. The frequencies of impervious surface growth summarized by normalized distance to growth centroids (A), major road (B), historical impervious surface (C), and major water (D) in the 1980s and 1990s.....	134
Figure 3-9. Reclassified transition probability surface values based on normalized elevation, slope, distance to centroids, distance to major road, distance to major water and distance to 1980 impervious surface and multi-criteria evaluation derived statistical results. High values are corresponding to high possibility to change from non-urban to urban based on historical impervious surface growth in the 1980s.	135
Figure 3-10. Reclassified transition probability values based on normalized elevation, slope, distance to centroids, distance to major road, distance to major water and distance to 1990 impervious surface and multi-criteria evaluation derived statistical results. High values are corresponding to high possibility to change from non-urban to urban based on historical impervious surface growth in the 1990s.	136
Figure 3-11. Total transition probability values for all developable pixels for the decade of 1980s and 1990s. High total values are corresponding to high possibility to change from non-	

urban to urban based on historical impervious surface growth in the 1980s and 1990s correspondingly.	137
Figure 3-12. ROC curves for model simulation of impervious surface growth calibration in 1980s (upper) and 1990s (lower) for Jackson, Greene, and Boone Counties compared with random growth of impervious surface.	138
Figure 3-13. Model simulation for future urban growth in the form of impervious surface growth for Jackson County for 2010, 2020 and 2030 with historical impervious surface extent of 2000 for reference and an inset to illustrate the exact location of the simulation in the spatial context of Missouri.	139
Figure 3-14. Model simulation for future urban growth in the form of impervious surface growth for Greene County for 2010, 2020 and 2030 with historical impervious surface extent of 2000 for reference and an inset to illustrate the exact location of the simulation in the spatial context of Missouri.	140
Figure 3-15. Model simulation for future urban growth in the form of impervious surface growth for Boone County for 2010, 2020 and 2030 with historical impervious surface extent of 2000 for reference and an inset to illustrate the exact location of the simulation in the spatial context of Missouri.	141

LIST OF TABLES

Table 1-1. Landsat imagery utilized for impervious surface mapping	41
Table 1-2. Coefficients for conversion of Landsat 5 TM DN to Landsat 7 ETM+ DN.....	42
Table 1-3. Accuracy assessment	43
Table 1-4. Impervious surface growth (ISG) and total area of pixels with ISG in hectare.....	44
Table 1-5. The amount of land affected by impervious surface growth (ISG) by land cover in hectare.....	46
Table 2-1. Performance metrics of regression analysis versus dasymmetric mapping , comparison is made upon four different types of imperviousness datasets all of which have road network imperviousness removed.....	83
Table 2-2. Moran’s I values calculated for the census blocks population density classified based on the five population density categories and the five adjusted population density categories.	84
Table 2-3. Average and standard deviation of population for the pixels classified by both percent of impervious surfaces and adjusted population density (APD). Pixels with either zero population or zero percent impervious surfaces are not included to reduce confusion between the population and imperviousness relationship.	85
Table 3-1. Model simulation validation for the decade of 1980s and 1990s presented as (%) error.....	126

**URBAN SPRAWL IN THE STATE OF MISSOURI:
CURRENT TRENDS, DRIVING FORCES, AND
FUTURE GROWTH ON MISSOURI'S NATURAL
LANDSCAPE**

Bo Zhou

Dr. Hong S. He Dissertation Advisor

ABSTRACT

Human population growth and associated sprawl has rapidly converted open lands to developed use and affected their distinctive ecological characteristics. Missouri reflects a full range of sprawl characteristics that include large metropolitan centers, which led growth in 1980s, and smaller metropolitan and rural areas, which led growth in 1990s. In order to study the historical patterns of sprawl, there is a need to quantitatively and geographically depict the extent and density of impervious surface for three time periods of 1980, 1990, and 2000 for the entire state of Missouri. This research goes beyond the usual hot spots of metropolitan areas to include rural landscapes where negative impact was exerted to the ecosystem due to the low density development and larger affected areas.

Mapped impervious surface is the best candidate of ancillary data for dasymetric mapping of population in several comparison studies. The current research examines the performances of dasymetric mapping of population with imperviousness as ancillary data and regression analysis of population using imperviousness as a predictor. In the context of this comparison, this research also examines the performance of imperviousness with

road network removed versus imperviousness with road network and certain ranges of values removed. The assessment of approach and ancillary data performance is done by comparing estimated population for each block to the original Census block population. Results from this work can be aggregated to any geographical unit (hydrologic boundaries, administrative boundaries, etc.). More importantly, the aggregated population information will be crucial in the modeling of future urban growth.

A pilot future urban growth study for the two decades of 1980s and 1990s was done in Missouri. The historical urban growth of the two decades were analyzed then coupled with various predictor variables to investigate the influence of each predictor variables towards the process of urban growth. The knowledge learned from the process is then used to build an urban growth simulation model that is GIS-based with open framework for ease of management and improvement. The complexity of urban systems is making the holistic modeling approach obsolete. Because it is impossible for one omnipotent model to solve urban growth problems of different locations, in this research, we decided to group those problems by different physical and mathematical process to tackle them one by one. Correspondingly, we used multiple sub modules each responsible for different processes related to urban growth. The structure of this model ensures each individual module can be updated and improved, and more sub modules can be added. Pixel level urban growth was simulated for year 2010, 2020 and 2030. This model framework is developed with the ultimate goal of simulating urban growth for the entire state of Missouri.

Introduction

1. Research problem

In the domain of land use policy, sprawl may be define as “low-density development on the edges of cities and towns that is poorly planned, land consumptive, automobile dependent and designed without regards to its surroundings” (Freilich, 2003). It is often referred to as uncontrolled, scattered suburban development that increases traffic problems, depletes local resources, and destroys open space (Peiser, 2001). For larger metropolitan areas, urban sprawl tends to be relatively dense affecting a smaller area per housing unit; but the number of housing unit also tends to be greater, thus increasing local environmental impacts. In contrast, for mid-to small-size cities and towns, rural sprawl often occurs at lower densities and affects much larger areas than doe’s urban sprawl (Radeloff et al., 2004). In both cases, the effects of sprawl ripple through the economic, fiscal, social, government tax revenues, and quantity and quality of public services. Moreover, sprawl has cumulative ecological and environmental effects at large scales (e.g. ecoregion), effects which may often occur over long period of time (e.g. decades) before they are recognized (Mckinney, 2002; Liu et al., 2003). Such large scale effects include land use change, degradation of soil, air and water quality, fragmentation and loss of wildlife habitat, and ultimately the decline of the amenities and heritage values that enhance the quality of life and bestow a sense of place on regions and localities where people live (Knight et al., 1995; Theobald, 2001; Hansen et al., 2002). In light of the negative effects of sprawl, understanding sprawl and its spatial and temporal

trends is essential to establish scientifically sound conservation policies, as well as to raise the public awareness of the dark side of sprawl.

Situated in the heartland, Missouri reflects the full range of sprawl reality in the U.S. The state has a mixture of large metropolitan centers, namely Kansas City and St. Louis, and numerous small to mid size cities and towns, and vast rural agricultural, forest, and prairie (Brookings Institution, 2002). Missouri has experienced shifting patterns of population growth over the past decades. During the 1980s Kansas City and St. Louis metro areas accounted for the largest share of growth in the state (57.5%), followed by smaller metropolitan areas (23.6%) and rural areas (18.9%). In the 1990s the population growth in the state's rural areas has a share of (36.4%) versus smaller metropolitan area (23.3%) and metropolitan areas (40.2%) (Brookings Institution, 2002). This increase of rural population growth has been fueled by small metropolitan growth with four smaller metropolitan areas (Springfield, Joplin, Columbia, and St. Joseph) emerged as the fastest growing regions expanding their size into the rural areas at a rate of 18.3%.

Besides the shifting pattern of population growth, more recent urban growth, sprawl, has the tendency to consume open land faster and occur more often on distinctive or otherwise significant ecological land types (Johnson & Beale, 2002; Schnaiberg et al., 2002, Barlett et al., 2000; Heimlich & Anderson, 2001). Thus, poses great threat to the conservation of natural resources and environment.

At the same time of housing development spread out, other basic infrastructure and service facilities such as transportation, commercial, and other developments also spread out even though population growth is modest compared to the spread of urbanized areas. To sum up, the dispersal of population in Missouri required the conversion of

435,400 acres of fields, farmland, forests, and green space to “urban” use in the decade of 80s and 90s combined. The growth is equivalent to 35% increase of the state’s urbanized area, given the population growth of only 9.7% during the same period of time yielding an actual decrease in population density which is a strong sign of unhealthy urban sprawl (Brookings Institution, 2002). These urban growths occurred both at the fringe of urban areas and in forested rural amenity areas including southern Missouri. In fact, this phenomenon is not unique to the state of Missouri. Previous research have indicated this phenomenon to be common in most of U.S. Midwest, and about one-third of the growth in the form of housing growth occurred outside non-metropolitan areas in the Midwest from 1940 to 2000 (Radeloff et al., 2005).

Urban sprawl is gaining more and more recognition from policy makers. Although this phenomenon is much discussed though poorly defined, more often it is studied qualitatively than quantitatively not even to mention spatially. The negative effects of sprawl on the natural landscape are numerous, to name just a few: forest and habitat fragmentation and destruction, increased pollution and reliance on fossil fuel, decreased water quality and quantity. With such a problem so evident in the state of Missouri, it is necessary to study and understand this phenomenon better in order to balance economic development and urban land use growth. Such knowledge will ensure the set up of a healthy public policy and better decision making for the better future of Missouri.

2. Objectives

The objectives of my research are to (1) map the extent and density of impervious surface for the state of Missouri for three time periods of 1980, 1990, and 2000, (2) develop a

mapping approach for per pixel population estimation for the entire state of Missouri, and (3) develop and calibrate an urban growth simulation model based on historical urban growth to predict future urban growth. These three objectives correspond to the following three chapters in my dissertation.

3. Chapter outline

Chapter 1 presented a systematic approach to map impervious surface for 1980, 1990 and 2000. Accuracy of the impervious surface mapping is conducted by comparing the sub-pixel classifier derived percent of impervious versus the ground-truth percent of impervious surface derived with air photos. For the whole state of Missouri over three time periods, the assessed RMSE is between 24.89 to 25.75%, SE is between 5.89 to 8.22%, and MAE is between 14.28 to 14.64%. Considering the size of the study area, the obtained accuracy is satisfactory. Our results show that during 1980–2000, 129,853 ha of land were converted to impervious surface. While sprawl was prominent on urban fringe during 1980s with 23,674 ha of land converted to impervious surface, there was a temporal shift in the rural landscapes in the 1990s with 48,079 ha of land converted to impervious surface.

Chapter 2 presented a dasymetric and localized regression mapping approach to model per pixel population by imperviousness per pixel and Census population at Census unit level for the whole state of Missouri, USA. Unique relationships were discovered between population and imperviousness at pixel level for each census block. These relationships were used to assign the number of people to each individual pixel with the presence of impervious surface at Census block level. The findings inferred from the mapping result indicate that over 99% of the population pixels coincide with impervious

surface pixels have equal or less than six people. This mapping approach improves upon previous approaches for given flexibility in using Census data of different geographical levels and its insensitivity to the location and size of the study area. The mapping result is an improvement over the uniform distribution of population defined and used by U.S. Census. This approach also manages to map per pixel population for a large geographic area at a resolution not achieved before.

Chapter 3 presented an open, rule-based, modulated, GIS model that was developed using ModelBuilder in ArcGIS. Multiple independent variables are identified and analyzed as the predictor variables of this model. Model calibration was done using MCE of historical urban growth. A trial and error approach was used to derive weights for each predictor variable in order for the simulated urban growth to be consistent spatially with the actual urban growth. The calibrated model is used to simulate future urban growth for 2010, 2020 and 2030 under the historical growth trend during the 1990s.

References

- BARTLETT, J. G., MAGEEAN, D. M. & O'CONNOR, R. J. (2000) Residential expansion as a continental threat to U.S. coastal ecosystems. *Population and Environment*, 21, 429-468.
- BROOKING, I. (2002) Growth in the heartland: challenges and opportunities for Missouri. Washington, D.C., USA, Brookings Institution, Center on Urban and Metropolitan Policy.
- FREILICH, R. H. (2003) Smart growth in western metro areas. *Natural Resources Journal*, 43, 687-702.
- HANSEN, A. J., RASKER, R., MAXWELL, B., ROTELLA, J. J., JOHNSON, J. D., WRIGHT PARMENTER, A., LANGNER, U., COHEN, W. B., LAWRENCE, R. L. & KRASKA, M. P. V. (2002) Ecological causes and consequences of demographic change in the new west. *BioScience*, 52, 151-162.
- HEIMLICH, R. E. & ANDERSON, W. D. (2001) Development at the urban fringe and beyond: Impacts on agriculture and rural land. *Development at the Urban Fringe and Beyond: Impacts on Agriculture and Rural Land*.
- JOHNSON, K. M. & BEALE, C. L. (2002) Nonmetro recreation counties: Their identification and rapid growth. *Rural America*, 17, 12-19.
- KNIGHT, R. L., WALLACE, G. N. & RIEBSAME, W. E. (1995) Ranching the view: Subdivisions versus agriculture. *Conservation Biology*, 9, 459-461.
- LIU, J., DAILY, G. C., EHRLICHT, P. R. & LUCK, G. W. (2003) Effects of household dynamics on resource consumption and biodiversity. *Nature*, 421, 530-533.
- MCKINNEY, M. L. (2002) Urbanization, biodiversity, and conservation. *BioScience*, 52, 883-890.
- PEISER, R. (2001) Decomposing urban sprawl. *Town Planning Review*, 72, 275-298.
- RADELOFF, V. C., HAMMER, R. B. & STEWART, S. I. (2005) Rural and suburban sprawl in the U.S. Midwest from 1940 to 2000 and its relation to forest fragmentation. *Conservation Biology*, 19, 793-805.
- SCHNAIBERG, J., RIERA, J., TURNER, M. G. & VOSS, P. R. (2002) Explaining human settlement patterns in a recreational lake district: Vilas County, Wisconsin, USA. *Environmental Management*, 30, 24-34.
- THEOBALD, D. M. (2001) Land-use dynamics beyond the American urban fringe. *Geographical Review*, 91, 544-564.

Chapter I. Mapping and analyzing change of impervious surface for two decades using multi-temporal Landsat imagery in Missouri

Abstract

Human population growth and associated sprawl has rapidly converted open lands to developed use and affected their distinctive ecological characteristics. Missouri reflects a full range of sprawl characteristics that include large metropolitan centers, which led growth in 1980s, and smaller metropolitan and rural areas, which led growth in 1990s. In order to study the historical patterns of sprawl, there is a need to quantitatively and geographically depict the extent and density of impervious surface for three time periods of 1980, 1990, and 2000 for the entire state of Missouri. We mapped impervious surface using Sub-pixel Classifier™, an add-on module of Erdas Imagine for the three time periods, where impervious surface growth was derived as the subtraction of impervious surface mapped from the different time periods. Accuracy assessment was performed by comparing satellite derived impervious surface images with ground-truth acquired from high resolution air photos. Results show that during 1980–2000, 129,853 ha of land were converted to impervious surface. Sprawl was prominent on urban fringe (within the urban boundaries) during 1980s with 23,674 ha of land converted to impervious surface compared to 22,918 ha in 1990s. There was a temporal shift in the rural landscapes (outside the urban boundaries) in the 1990s with 48,079 ha of land converted to impervious surface compared to 35,180 ha in 1980s. Major findings based on analysis of the impervious surface growth include: i) new growth of impervious surfaces are concentrated on areas with 0.5 to 1.0 percent road cover; ii) most new growths are either

inside or close to urban watersheds; and iii) most new growths are either inside or close to counties with metropolitan cities. This research goes beyond the usual hot spots of metropolitan areas to include rural landscapes where negative impact was exerted to the ecosystem due to the low density development and larger affected areas.

Keywords: Impervious surface growth; Sub-pixel classification; Urban and rural sprawl; Missouri

1. Introduction

Sprawl can be defined as low-density development on the edge of cities and towns that are poorly planned, land consumptive, automobile dependent and designed without regards to its surroundings (Freilich, 2003). It is often referred to as uncontrolled, scattered suburban development that increases traffic problems, depletes local resources, and destroys open space (Peiser, 2001). Thus, by definition, most of the new growth can be classified as sprawl (Esch et al., 2009). The effects of sprawl ripple through the economic, fiscal, social/cultural, tax revenues, and quantity/quality of public services. Moreover, sprawl may have cumulative effects that occur at a very large region (e.g. ecoregion) and over a long period of time (e.g. decades) before they were recognized (Mckinney, 2002; Liu et al., 2003). Such large scale effects include land use change, degradation of soil, air and water quality, increased pollution, fragmentation and loss of wildlife habitat, and ultimately the loss of ecological services that sustain local or regional communities (Knight et al., 1995; Theobald, 2001; Hansen et al., 2002; Walker and Salt, 2006).

Humans are the dominant factor causing ecosystem degradation, land use change, pollution of streams, lakes and other surface waters, and depletion of natural resources. Successful management of ecosystems altered by human intervention is best achieved through cooperation between local communities, and state and federal agencies using reliable information. This requires an understanding of the complex interactions between hydrologic processes, climate, land use, water quality, ecology, and human socioeconomic considerations. Furthermore, a general lack of analytical tools and baseline information about urban and rural sprawl at state levels has lead to a serious lack

of progress identifying and prioritizing courses of action. It is therefore understandable that intense debates are occurring in communities regarding the nature of sprawl, and possible avenues for environmental amelioration (Law et al. 2008).

Situated in the mid-western portion of the United States, Missouri reflects a full range of sprawl characteristics (Brookings Institution 2002) that include large metropolitan centers (i.e., Kansas City, St. Louis) and numerous small to mid-size cities and towns. Coupled with the spectrum of urban areas are vast landscapes of rural agricultural, forest, and prairie environments (Nigh and Schroeder, 2002). Missouri has experienced shifting patterns of population growth over the past decades. During the 1980s, Kansas City and St. Louis metro areas accounted for the largest share of growth in the state (57.5%), followed by smaller metropolitan areas (23.6%) and rural areas (18.9%) (Brookings Institution, 2002). In the 1990s, the population growth in the state's rural areas had a share of (36.4%) versus smaller metropolitan areas (23.3%) and large metropolitan areas (40.2%) (Brookings Institution, 2002). This increase of rural population growth has been fueled by small metropolitan growth with four smaller metropolitan areas (Springfield, Joplin, Columbia, and St. Joseph) that emerged as the fastest growing regions expanding their size into the surrounding rural areas (Brookings Institution, 2002).

Human population growth and associated sprawl has rapidly converted open lands to developed uses that consequently affected their distinctive ecological characteristics (Johnson and Beale, 2002; Schnaiberg et al., 2002; Barlett et al., 2000; Heimlich and Anderson, 2001). In Missouri, this low-density development converted >71,000 ha of fields, farmland, forests, and green space to urban use during the 1980s and 1990s. This

type of growth was equivalent to a 35% increase of the state's urbanized area, given the population growth of only 9.7% during the same period of time (Brookings Institution, 2002). The low density growth is not unique to Missouri; For example, within the Midwest, about one-third of housing growth occurred outside non-metropolitan areas during 1940–2000 (Radeloff et al 2005). Other studies have found shifting trends of sprawl from suburban to rural areas throughout United States (Fuguitt, 1985; Johnson and Fuguitt, 2000).

Previous studies have identified various factors that were important in studying sprawl. For example, Behan (2008) and Patman (2003) determined that proximity to water and roads were highly correlated with sprawl. Also, there appears to be a close relationship between sprawl and certain types of land use and land cover (LULC), where LULC was used to predict new sprawl (Xian and Homer 2009). Radeloff et al. (2005) reported that sprawl was not spatially homogeneous and certain eco-regions were more inclined to experience sprawl than others. At the watershed scale, the amount of sprawl can serve as an indicator of watershed health (Brabec et al., 2002; Arnold and Gibbons, 1996). Sprawl is also influenced by municipal or political entities which enact land use regulations that ultimately affect lifestyle preferences of people within local jurisdictions (Carruthers, 2003). The objectives of this research are: i) map the extent and density of impervious surface for the state of Missouri for three time periods of 1980, 1990, and 2000, and ii) summarize the growth of impervious surfaces using various datasets with different geographical boundaries, and iii) find out whether rural sprawl has become more prominent than urban sprawl in the last two decades.

2. Approach and method

2.1. Overview of impervious surface mapping approach

Previous sprawl research has used housing density as an indicator for urban and rural sprawl (Theobald 2001; Radeloff et al., 2005); however, there are limitations when using census data to study sprawl. Census blocks were often too coarse and only updated at decadal intervals, which is not timely for monitoring purposes (Harris and Longley, 2000; Plane and Rogerson, 1994). Census block and block group boundaries change over time and this complicates sprawl studies by introducing a spatial mismatch between boundaries of different datasets (Hammer et al., 2004). Housing development also does not reflect other forms of development such as infrastructure construction. The nonlinear variation of the aggregated population density of urban areas as a function of total population are due to different measurement scales (i.e. block group) and complicates identification of urban sprawl in a uniform spatial context (Sutton, 2002).

Many studies have suggested that impervious surface is a reliable indicator of urbanization because it is closely tied to urban and rural development (e.g., Arnold and Gibbons, 1996; Powell et al., 2008). Impervious surface has distinct man-made features and can be detected and quantified by remote sensing over time to reflect urban and rural sprawl (Cronon 1991, Reisner 1993, Alberti et al. 2008, Anderson 2006). Other research indicates that remote sensing technology was an effective tool to overcome the limitations of census data with per-pixel classification (Chen, et al., 2000; Epstein et al., 2002; Ji et al., 2001; Lo and Yang, 2002; Ward et al., 2000; Yeh and Li, 2001). However, since virtually every pixel represents mixtures of different surface materials (e.g. concrete,

asphalt, metal, vegetation or water), numerous developments may be left undetected due to the 30m resolution of satellite image (Raup, 1982; Theobald, 2001; Clapham, 2003).

In order to overcome such limitations, more recent studies have focused on deriving and quantifying impervious surface at sub-pixel level using remotely sensed data with on-the-ground verification. Civco and Hurd (1997) derived impervious surfaces at sub-pixel level with artificial neural network processing. Carlson and Arthur (2000) calculated percent of impervious surface per pixel using fractional vegetation derived from scaled normalized difference vegetation index (NDVI). Yang et al. (2003) proposed a General Classification and Regression Tree (CART) approach that used Landsat satellite data derived Tasseled Cap transformed data. Bauer et al. (2007) used regression analysis to estimate impervious surface area per pixel.

Another approach included a vegetation-impervious-soil model that parameterized biophysical composition of urban environment (Ridd, 1995), which was later improved by Wu and Murray (2003) and Lu and Weng (2006) using four end-members: high-albedo and low-albedo, coupled with soil and vegetation extracted from the image. The impervious surface was extracted by adding the high and low-albedo fractions. However, confusion occurs among classification of dry soils that are mixed with high-albedo fractions, water, building shadows, vegetation shadows, and dark impervious surface materials which over-estimates the extent and density of impervious surface. The over-estimated impervious surface was removed by expert rules developed from sample plots using high spatial resolution aerial photos (Lu and Weng 2006). Most recently, Weng and Lu (2009) used the concept of landscape in the whole study area as a continuum by combining the benefits of Vegetation-Impervious Surface-Soil (VIS) and

Linear Spectral Mixture Analysis (LSMA) to better characterize and quantify the spatial and temporal changes of the urban landscape.

The majority of previous research has focused on the concept of validation for sub-pixel impervious surface mapping within small study areas, such as cities. The more recent direction of research in impervious surface densities has focused on larger areas with extents at state and country levels. For instance, Bauer et al. (2007) attempted to assess changes in impervious surfaces at large spatial (the state of Minnesota) and temporal (a decade between 1990 and 2000) scales. Haase et al. (2007) mapped impervious surface for the state of Pennsylvania to predict water quality in 42 watersheds. The National Land Cover Database (NLCD) project is another example of a large scale study that provides impervious surface densities at sub-pixel levels for the entire country for 1992 (Vogelmann et al., 2001b) and 2001 (Homer et al., 2002).

Although large scale impervious surface mapping have been implemented using various approaches with success, the mapping procedures are complicated due to inconsistent image quality and scale, where mixed pixels occurs over large geographical areas. The pixel unmixing approach is very sensitive to the end-member derivation process, which needs to be performed for each image individually (Lu and Weng 2006). The regression approach is very sensitive to calibration sites which also require individual image processing to ensure good mapping results (Bauer, 2007). Thus, in this research, a more efficient approach is chosen. Sub-pixel ClassifierTM (SPC), engineered by Applied Analysis Inc., is an add-on module to Leica Geosystems' Erdas Imagine software, and was selected due to its applicability and automated signature derivation capability. The classified pixel had percentage values of 0-20%, 20-30%, 30-40%, ~ 90-

100%, a total of 9 classes by default setting of the software, representing the percent of impervious surface inside each pixel.

2.2. Data source and preprocessing

For impervious surface mapping, 30m Landsat TM and ETM+ imageries were acquired from the U.S. Geological Survey (USGS) at decadal intervals (1980, 1990, and 2000) (Table 1). A total of 45 images were collected where 15 images represented each date and covered the entire state of Missouri. Images were selected based on the following criteria: i) winter season images with leaf-off for maximum impervious exposure; ii) image acquisition time (month and year) to be within a close range for minimum color difference; and iii) low cloud coverage. Compromises were made when good quality images were not available.

High spatial resolution air photos were collected to assist impervious surface mapping and provide accuracy assessments. For 1980 and 1990 satellite images, 2m resolution National High Altitude Photography (NHAP) black-and-white (B/W) and 1m resolution National Aerial Photography Program (NAPP) B/W images were used for error checking, respectively. The NHAP/NAPP archives were used because they are an invaluable source of high quality, cloud free, quad-based photography that covers the conterminous U.S. A total of 200 scenes were downloaded from USGS Global Visualization Viewer (GloVis) and were selected based on error checking sampling locations. Only NHAP and NAPP photos that were exclusively within the respective years (1980 and 1990) were selected for more accurate error checking. For 2000's impervious surface mapping, a total of 115 2m Digital Ortho Quarter Quad tiles (DOQQs) National Agriculture Imagery Program (NAIP) color photos were obtained from Missouri

Spatial Data Information Service (MSDIS). The selection of 2004 photos was due to the high image quality and low cloud cover (Timothy Nigh, personal communication).

Standard procedures were followed for satellite image preprocessing, which included: (a) navigation registration, (b) radiometric normalization, (c) relative radiometric calibration (Jensen, 1996), (d) rectification and geo-referencing to the UTM projection (NAD 83 datum, Zone 15 North). Navigation registration was performed by acquiring coordinate values of the four corners of an image from associated metadata. Radiometric normalization was performed for images because scenes were acquired by different sensors. To correct for inconsistencies among different sensors, the digital number (DN) of Landsat 5 TM was converted to a pseudo Landsat 7 ETM+ DN using calibration coefficients derived by Vogelmann et al. (2001a) (Table 2). Relative radiometric calibration was performed due to differences between image acquisition conditions. One ETM+ image with good quality from 2000 was used as a reference image. For all images overlapping with the reference images, pseudo-invariant features (PIFs) were selected from inside the overlapped areas. Image normalization was performed on those images using the PIF features. The normalized images were then treated as new references. This process was repeated until all year 2000 images were normalized. Images from the 1980 and 1990 used calibrated 2000 images of the corresponding paths and rows as references to perform relative radiometric calibration. Georeferencing was performed by selecting ground control points (GCPs) from TIGER/Line data from the U.S. Census Bureau in 1992 and 2000. Due to the lack of TIGER/Line data in the 1980, the 1992 data was used to georeference 1980 images. Coordinate locations, mostly road intersections, were identified by overlaying

TIGER/Line data on top of Landsat images. Because the state of Missouri is relatively flat, geometric correction was performed with 1st order polynomial and nearest neighbor resampling methods. The root-mean-square (RMS) error of the georeferenced images were less than 0.5 pixels (15 m). The processed images are then mosaiced and trimmed by Missouri state boundary into three state images representing the time periods of 1980, 1990, and 2000. The preprocessing of air photos included only geometric correction, which was performed with the same approach and projection properties used on Landsat images.

2.3. Procedure for mapping percent of impervious surface

The mapping of impervious surface included a procedure specifically tailored for sub-pixel classification, a procedure for signature derivation, and a procedure for material of interest (MOI) classification. The first procedure is called preprocessing. Preprocessing was automated by the software and prepares the images for sub-pixel classification. The output of preprocessing is an *.aasap* file that is an associated file to the image. The second procedure of signature derivation was conducted semi-automatically by manually creating a training set using areas-of-interest (AOIs) to represent pixels with 100% pure impervious surface. In cases where large man-made structures are available, this process can be done directly with Landsat images. If large man-made structures are not available, air photos were used together with Landsat images to better identify Landsat pixels with pure impervious surface. Since most Landsat pixels are mixed with more than one type of material, the identification of pure impervious surface pixel is difficult with Landsat images alone. To overcome this difficulty, an output signature was created using the training set together with the source image and the preprocessing file. During this process,

multiple signatures were derived representing different types of impervious surfaces (light, medium, and dark) to accommodate for impervious surfaces that were of different materials. In the last procedure of MOI classification, three different signatures were used to classify light, medium and dark impervious surfaces separately. The three outputs were combined together to form one final image that represents the total percent of impervious surface for each pixel.

Classified impervious surface pixels were visually compared with high resolution air photos of the same period to ensure consistency throughout the mapping process. Based on visual interpretation, bare soils of different color were found to be mixed with sub-pixel classified impervious surfaces. The best way to reduce the confusion of soil with impervious surface is to use a soil mask. Since new developments usually occurred within certain distances to road networks, buffers were created from TIGER/Line data and used as a mask to reduce the error in rural areas (Esch et al. 2009). Because only 1992 and 2000 TIGER/Line data is available in good quality, 1992 TIGER/Line data was used on both 1980 and 1990 Landsat images.

A series of buffer distances were compared by overlaying onto air photos and 90m was selected as the final buffer distance. Ninety meters was chosen because it generated the best balance between covering most rural impervious surface and excluding most bare soil confusion. Urban masks were also created by combining city boundaries of all Missouri cities in 1994 (MSDIS, 2010). A buffer was generated with a distance of 900 m where most of the new growths of impervious surface from 2000 were within the buffer distance. This urban mask was used to correct the confusion between impervious

surface and soil for the mapping results of year 2000. The original city boundaries were used to reduce the soil confusion for mapping results of years 1980 and 1990.

2.4. Accuracy assessment

Accuracy assessment was performed by comparing impervious surface estimated from sub-pixel classifier with ground-truth information from high resolution air photos that covered state of Missouri. Although previous research on large area sample design includes multi-level stratification and random sampling (Stehman et al., 2003; Wulder et al. 2006), we found that the traditional geographic stratification does not work well due to the uneven distribution of impervious surfaces in Missouri. Thus, a different sampling approach based on population density was used with the rationale that impervious surface usually coincides with human population (Lu et al. 2006). This design ensured no bias toward pixels of different percent of impervious surface and greater number of samples was allocated to places where more impervious surface was detected.

The actual sampling design was set up by dividing the state into five sub-regions: high, medium high, medium, medium low and low population density. Forty random points were generated in each sub-region and a total of 200 sampling points were used statewide (Congalton, 1991). To ensure correct evaluation of mapping results, each sample point was converted to pixel blocks of 3 by 3 with 30 m resolution pixel with a total area of 8100 m² (Fig. 1) (Xian and Homer, 2009). A total of 1800 pixels were used in the accuracy assessment. Corresponding to the sampling blocks, air photos were used as ground truth reference for assessing the accuracy of sub-pixel classifier. In each sample block, total amount of impervious surface was measured. Percent of impervious surface for the same block was then calculated by taking the total amount of impervious

surface and dividing by the total area of the block (900 m²) and rounded to the closest 10th percentile to ensure the same format with the sub-pixel classifier output. The ground-truth results were then compared with sub-pixel classifier mapped results. Three statistical measures were used to describe the error: 1) RMSE (Eq. (1), 2) standard error (SE) (Eq. (2), and 3) mean absolute error (MAE) (Eq. (3), and defined by the following equations, respectively,

$$RMSE = \left[\frac{1}{n} \sum_{i=1}^n (P_i - P_i)^2 \right]^{\frac{1}{2}} \quad (1)$$

$$SE = \frac{1}{n} \sum_{i=1}^n (P_i - P_i) \quad (2)$$

$$MAE = \frac{1}{n} \sum_{i=1}^n |P_i - P_i| \quad (3)$$

Where P_i is the true PIS for pixel i, and P_i is the SPC classified PIS for pixel i, and n is the total number of pixels being assessed. Mean RMSE, SE and MAE were calculated for all sample pixels.

2.5. Impervious surface growth analysis

Impervious surface growth (ISG) was determined through the subtraction of impervious surfaces mapped from each date. ISG was used to describe urban and rural sprawl because most of the growth in the last two decades fall within areas of very low density. Urban sprawl was defined as growth inside corresponding urban mask whereas rural sprawl was defined as growth outside the urban mask.

ISG was derived by subtracting the impervious surface maps of 1990 by 1980, and 2000 by 1990. Binary maps were derived from the ISG maps where PIS=0 indicated

pixels with no ISG and $PIS > 0$ indicated pixels with ISG. ISG maps were then used to calculate the area of absolute impervious surface by multiplying the total number of pixels in each PIS category of impervious surface with the PIS value. Resulting binary maps geographically depict pixels affected by new growth of impervious surface and with approximate area affected by sprawl.

Sixteen class LULC maps of 1993 and 2005 were acquired from Missouri Spatial Data Information Service (MSDIS, 2010) and used in conjunction with impervious surface binary maps of 1980s and 1990s to identify land cover that had been converted due to sprawl. Spatial pattern of land cover affected by sprawl can be mapped by class where total area of land cover affected by sprawl was estimated. To determine the effects of sprawl on Missouri landscapes, land type association (LTA) derived from Missouri ecological classification system (Nigh and Schroeder 2002) was used. Due to the heterogeneity between sizes of LTAs, the ISG maps were weighted by LTA area and ISG. Each LTA was then calculated as a percent increase. Similar analyses were conducted for 10-digit watershed and county boundaries to study the degree affected by impervious surface growth at watershed and county levels, respectively.

3. Results

3.1. Accuracy assessment

To illustrate the accuracy of impervious surface mapping, average values of overall RMSE, SE, and MAE were calculated for 1980, 1990 and 2000, respectively. The averaged RMSE for the whole study area was approximately 25 percent, with a SE of 7%, and MAE approximately 14 percent for all three time periods (Table 3). The mean values for air photo-derived PIS (PIS-t) are consistently smaller than the mean values for

satellite image-derived PIS (PIS-m) for all three time periods, which indicates that the sub-pixel classifier overestimates impervious surface by about 8% (Table 3). Results also indicate that all statistical measures are very consistent over the three time periods.

Although the averaged RMSEs, SEs and MAEs are higher for three time periods than previous research at smaller scales (Xian and Homer, 2009), the mapping accuracy is acceptable considering the size of the study area.

3.2. Statewide statistics of impervious surface growth

Within the decade of 1980, a total of 58,855 ha of land were converted to impervious surface, whereas the total affected area by sprawl was 131,202 ha. Among the conversions, more land was consumed in rural areas representing about 60% of the total converted land with an urban/rural ratio of 67.3%. Most impervious surface growth in urban areas occurred as a mixture of (approximately 30% to 40%) of impervious surface with other land cover classes, such as vegetation, bare soil, and water. Most impervious surface growth in rural areas was characterized with 20% to 30% impervious surface mixed with other land cover classes. Lower impervious surface percentages in rural areas suggest that rural sprawl has lower density of development than urban sprawl (Table 4).

In the decade of 1990s, a total of 70,998 ha of land were converted to impervious surface, whereas the total affected area was 160,377 ha. Among the conversions, about 68% of land was consumed in rural areas with an urban/rural ratio of 47.7%. Most development in urban area occurs in 30% to 40% of impervious surface per pixel. For rural areas, the most development occurs in 20% to 30% of impervious surface per pixel. The greatest difference between impervious surface growth from the 1980s and 1990s was the shift of sprawl from urban to rural areas, where more land was consumed in the

latter decade (Table 4). Further, high density developments were more likely to occur within urban areas than in rural areas. This phenomenon was confirmed by the increasing trend of urban/rural ratio in both 1980s and 1990s (Table 4).

The small area represented by impervious surface class of 0 to 10% and 10 to 20% was caused by limitations of the sub-pixel classifier where pixels with less than 20% of impervious surface cannot be identified. The abrupt increase of impervious surface between 90 to 100% could be attributed to high density developments within urban areas such as shopping centers, plazas, and parking lots or impervious structures (warehouses) found within rural areas. Further, the three signatures approach used for mapping impervious surface could also lead to a certain degree of overestimation.

3.3. Spatial patterns of impervious surface growth

Mapped impervious surfaces show diverse patterns across the state and multiple instances of these patterns are described below; however, due to the large spatial extent of the state, not all are listed. A uniform pattern occurred within residential blocks where developments appeared homogenous within each block; however, this type of distribution did not hold true across neighboring residential blocks. The uniform pattern was best illustrated by the historical impervious surface growth found in the city of Springfield where within block residential developments were similar in density and spatial arrangement (Fig. 2a, b, and c). A radial pattern of urban sprawl existed where residential developments illustrated growth trends that sprawled away from urban centers in various directions and with various speed and density, which was less organized than the uniform pattern seen within individual residential blocks. A good example was illustrated by patterns found around Jefferson City, which has various residential densities scattering

around its vicinity over time (Fig. 2d, e, and f). Leapfrog development was prevalent where new residences are constructed at various distances away from existing urban areas; bypassing vacant locations nearby. A good example was illustrated by the city of Blue Springs, which has a lower density development than Kansas City but higher density development than leap frog development displayed along highway (I-470) (Fig. 3a-c). An infill development pattern was prevalent where big undeveloped space was encompassed by highways. A good example was illustrated by St. Charles which was in the St. Louis metro area where the triangle formed by three sections of highways was filled with developments in the last two decades (B and C on Fig. 3d-f). Finally, rural sprawl pattern where developments were scattered in open space outside cities and towns and usually occurred in a random fashion unlike urban sprawl. Thus, a specific example of rural sprawl was not provided.

3.4. Sprawl affected area in relation to land cover, terrain, and road network

The most affected land cover types by sprawl in terms of total area were grassland and cropland, where both land cover types were close to 1% being affected by impervious surface growth in both decades (Table 5). Between the two type of forests evergreen seemed to be much less affected by sprawl than deciduous in terms of total area, but when we look at the per land cover class percentage the difference was not as pronounced and it was very clear that both type of forests were affected to a similar degree in two decades. There were also some significant developments happening close to water (Table 5) which suggests people's preference on housing locations close to water body for recreational purposes with the development intensity increased slightly during 1990s.

Histograms were generated for area of total sprawl and summarized by percent of road cover. Histograms depicted the occurrence of sprawl within 0.2-3.5% range of percent road cover (Fig. 4). Open land with less than 0.2% of road cover was not suitable for sprawl because of travel limitations, whereas land with over 3.5% road cover has already been filled with developments and has no space for further sprawl. The road cover effect on sprawl was very similar for the last two decades where 80% was in a range of 0.5 to 1.0 percent (Fig. 4). Sprawl in the 1990s was claiming more land than in the 1980s in the same road density range.

3.5. Impervious surface growth in relation to LTA, watershed, and county boundaries

Results from analyzing impervious surface growth by LTA show a shifting pattern from 1980s to 1990s. In the 1980s, sprawl only affected LTAs that were close to large metropolitan areas (i.e St. Louis and Kansas City). A shifting pattern was less apparent in most LTAs within the Till Plains (TP) and Mississippi Basin (MB) ecological sections, which were the state's primary agricultural regions (Fig. 5a). Also, LTAs at the core of Ozark Highlands (OZ) ecological section, the primary forest region of the state, were not affected in 1980s (Fig. 5a). In 1990s, noticeable increases in impervious surface growth were shown within LTAs of TP, MB, and OZ sections (Fig. 5b).

It was very obvious that in 1990s more LTAs were being affected by ISG (Fig. 5b). While most LTAs have experienced less than 1% ISG in both decades, only few LTAs stand out to show that they were under constant pressure. The LTAs were St. Charles Co. Prairie, Chesterfield Loess Woodland, Manchester Oak Savanna, Lower Meramec Oak/Mixed Hardwood/Forest Hills, Jackson Co. Prairie, and, Platte River Loess Prairie. Most of these LTAs were very close to St. Louis and Kansas City metro

regions. Despite the fact that ISG has started to affect more eco-regions during the 1990s, the most dominant growth hotspots were still close to metropolitan cities. The LTAs being affected most were predominantly nearby metros. The most vulnerable ecological land type was identified as prairie, which may be attributed to economic or political complexities when clearing forests for development.

The overall impervious surface growth patterns by watershed show that watersheds adjacent to metropolitan area were mostly affected (Fig. 5c and d). More watersheds were affected by ISG during 1990s than during the 1980s. The unique feature illustrated by this result was that the watersheds close to the Lake of the Ozarks were affected more by ISG during the decade of the 1980s than 1990s (A on Fig. 5c).

Sprawl was expressed in terms of change per capita share of impervious surface (PCIS). The PCIS increases from 0.133 ha/person in 1980s, to 0.139 ha/person in 1990s, and to 0.140 ha/person in 2000s at the state level. Although PCIS increased more in the 1980s than the 1990s, there was more ISG in the 1990s than the 1980s. The slight increase of PCIS for 1990s was due to faster population increase in the 1990s. Most counties have an increase in PCIS but the rate often varies (Fig. 6). A few counties show slight decreases in PCIS with the exception of Stoddard County, which had a dramatic decrease during 1980s.

The spatial pattern of impervious surface growth during the 1980s suggests that counties with the highest ISG were those that have metropolitan or small metropolitan cities inside or adjacent to the metropolitan counties (Fig. 7a). The counties with the largest increase of PCIS were mostly rural counties which have very little or even no increase in ISG. Such increases were due to loss of population in those rural counties (Fig.

7c). Among them, Worth, Mercer, and Pike counties have the highest loss of population; thus highest increase in PCIS. Counties with a slight decrease in PCIS were usually metropolitan counties or those nearby, which have some significant increase of ISG (Fig. 7a). In this case, the cause of decrease in PCIS was due to the increase of population. Among them, Stoddard County has the highest increase of population. The spatial pattern of ISG during the 1990s shows an expansion pattern of ISG. Many rural counties that do not show ISG in the 1980s have significant ISG in 1990s (Fig. 7b). The other very distinctive pattern was a collection of adjacent counties, which have significant decreases in PCIS (Fig. 7d). These counties share the Lake of the Ozarks and were a hotspot that attracted large population of retirees in the 1990s (Swanson, 1993).

4. Discussion

4.1. Approach implications

This paper shows that sub-pixel classifier was able to extract impervious surface at sub-pixel level for Landsat images for the entire state of Missouri. Sub-pixel classification of impervious surface provided more information than traditional land cover classification by providing both spatially explicit distribution of impervious surface and accurate quantification of impervious surface area at pixel level. Previous assessment of impervious surface mapping has concluded that sub-pixel classifier only has a slight disadvantage compared to other more complicated approaches, but it does have the advantage of being spatially explicit. Impervious surface density is reported at a per pixel level and is very useful for future impervious surface growth modeling (Civco, 2002).

In this research, three impervious surface signatures were used; however, there is a potential issue of overestimation with this approach due to the overlap of impervious surface classified by the three signatures. To resolve this issue, we experimented with two solutions: i) reduce the classification tolerance of sub-pixel classifier so that few pixels in the final image have density over 100%, and ii) increase the classification tolerance of sub-pixel classifier and use only one medium impervious surface signature. Results indicated that the first approach is superior, indicated by severe underestimation of impervious surface in the second solution as compared to overestimation of impervious surface in the first solution. Thus, the first solution was used in this research, where we forced the remaining pixels with over 100% impervious surface density to 100%.

Sub-pixel classifier has difficulty distinguishing between impervious surfaces and bare soil because of their innate similarity, which is compounded by the heterogeneity of mixed pixels. There are several ways to address the confusion between impervious surface and bare soil. The ideal approach is to use exposed soil maps as masks to reduce the confusion with impervious surfaces. However, such datasets are not available for the three time periods when impervious surfaces were mapped. Furthermore, it is not cost effective to produce such datasets for such a large study area. A second effective approach is to derive accurate urban boundaries from high resolution air photos (Yang et al., 2003). This approach is not practical for the same reason as the first approach. A third approach is to use multi-date imagery to minimize the effects of exposed soil confusion (Yang et al. 2003), but additional errors could be introduced due to the amount of satellite images used. Urban and road network masks were used in this research as a compromise

to the discussed approaches. Although drawbacks and confusions associated with this approach exist inside the buffer zones, the accuracy assessment results suggest that the mapping results are satisfactory.

Sub-pixel classifier is not effective in identifying pixels with less than 20% of impervious surface, which is the range of impervious surface density that lakes and streams are also sensitive to (Bauer et al., 2007). Impervious surface at this density range have some impact on water quality. Thus, the mapping result of this research may not be suitable for water quality studies in rural areas where the density of impervious surface per pixel are generally very low. The sub-pixel resolution of 20% of a Landsat pixel (around 180 m²) is sufficient in identifying new housing development and infrastructure development associated with impervious surface.

Sub-pixel classifier has the ability to classify the state mosaic with a universal signature to reduce human interaction and processing time. High quality images and good preprocessing to develop high quality mosaic of the whole study area are necessary components for modeling. In this study, an issue was discovered that there are differences inside the mosaic caused by image acquisition time and condition. Since only pure impervious surface pixels were used as PIFs for radiometric correction, vegetation cover on images obtained during different time periods have different reflectance (color) and texture (density). Water bodies also have different reflectance in different conditions along with bare soils, which have different reflectance due to differences in moisture content. When these materials mix with impervious surface over a large geographic area, the mixed pixel problem becomes complicated. Previous impervious surface mapping research mostly focused in metropolitan cities with only one or few frames of images

involved and these issues were not pronounced (Lu and Weng, 2006; Wu and Murray, 2003). Even with one image frame, the classification results can become problematic if the study uses images from different dates (Clapham, 2003). Such findings contributed to the selection of sub-pixel classifier over other approaches that focus on the interactions between different ground materials such as the V-I-S model (Ridd, 1995). The advantage with Sub-pixel classifier is the ability to focus the material of interest, such as impervious surface.

The temporal inconsistency between satellite imagery and air photos is a big source of potential error in this research. It is very difficult to acquire images on the desired date and time especially when dealing with large study areas. Previous research suggests that this issue can be resolved by using estimated conditions on the desired date based on available images for earlier or later dates (Foody, 2010). Such an approach would only be accurate if the two dates were very close in order to assume no change or that the change is linear and can be extrapolated or interpolated. Air photos have random acquisition dates for accuracy assessment in 1980 and 1990, for the 2000 accuracy assessment, the acquisition date of air photos is 2004. Thus, accuracy assessment compromises were made based on the available air photos.

4.2. Result implications

The statewide assessment of impervious surface growth for 1980s and 1990s were provided in this research. The amount of land converted to impervious surface and estimates of the area of land affected by impervious surface growth was reported. Compared to the number reported by the Brookings report (Brookings Institution, 2002), the estimated total sprawl affected area in this research was larger although the area of

pure impervious surface was smaller. The cause of the difference was from the different assessment approaches between the two studies. This approach used impervious surface per pixel to calculate both impervious surface growth and total area affected. The Brookings' approach used zoning and planning data to estimate only total area affected by impervious surface growth. The advantage of this approach is the ability to pick up new developments that were not zoned or planned, which leads to a more complete estimate of new developments for the last two decades.

Other advantages exhibited by the mapping results were the ability to estimate affected areas and determining the spatial extent as a per pixel density estimate of impervious surface. Such results can be overlaid with municipal, political, or natural units such as LTA and watershed for more magnified causal-effect studies. For example, 74 water bodies in Missouri have been identified as impaired or limited for a variety of beneficial uses as listed on the 2004/2006 303(d) list (MoDNR 2007). Using the amount of impervious surface quantified in this study can be used to explore potential correlations with water quality indicators for urban areas and subsequently, create more focused management policies.

Our results also show that fundamental relationships exist between sprawl and road infrastructure requirements for 1980s to 1990s. This suggests that people do not move to areas with very high road cover (such as city center) or areas with very low road cover. Thus, limiting sprawl by avoiding construction of road networks in the sprawl prone range (e.g., 0.5-1.0%) should be considered as a way to control sprawl. Cervero (2003) argued that the expansion of road networks will induce more sprawl and building our way out of sprawl was not a guaranteed solution. More innovation approaches, such

as investing in public transportations such as light rail, or adopting in new urbanism design to reduce automobile use should be considered with the ultimate goal of increasing residential density and reducing sprawl (Handy, 2005).

Impervious surface impact analysis at the watershed level shows most of the affected watersheds were either inside a city or close to a city where both population density and impervious surface density were high. This was reinforced by the low per capita impervious surface at metropolitan counties and contributed to the inevitable high concentrations of water pollutants confirmed by previous research (Tu et al., 2007). Policies devised for watershed protection should focus on reducing water quality degradation (brabec, 2002) in urban watersheds. The focus of policy implementation should not prevent development, but to avoid low density sprawl and reduce the possible impact of sprawl on our natural resources. Possible solutions may include emphasizing green development that incorporates watershed protection as priority goals. This type of innovation can be accomplished by increasing development density in residential areas or using more a scientific design that reduces the impact of runoff to surrounding waterways. Other solutions may include encouraging redevelopment of brown-fields or limiting total area of impervious surface construction to reduce the collective negative effects of impervious surfaces at the concentrated urban watersheds (Berke et al., 2003).

Impervious surface impact analysis at county level provides a broad comparison of all counties in Missouri. This type of distribution indicates very uneven area of impervious surface growth throughout the state. This may be caused by the uneven distribution of cities and associated socio-economic status within the state. Results suggest that county wide or city wide sprawl management plans should be comprehensive

at broad scales, but rather more local, focused policies that reflect the needs of individual counties and cities with the greatest sprawl record or those with the greatest sprawl potential. For rural counties and small cities experiencing very little sprawl, implementing any anti-sprawl policy may hurt local development and the economy (Anthony, 2004). To prevent the fast consumption of flat open land for development at individual city levels, policy tools should be implemented that include urban growth boundaries (UGB) and tax or impact fees to contain sprawl (Brueckner, 2000).

4.3. Conclusions

Impervious surface for 1980, 1990 and 2000 were mapped in this research. Accuracy of the impervious surface mapping is conducted by comparing the sub-pixel classifier derived percent of impervious versus the ground-truth percent of impervious surface derived with air photos. For the whole state of Missouri over three time periods, the assessed RMSE is between 24.89 to 25.75%, SE is between 5.89 to 8.22%, and MAE is between 14.28 to 14.64%. Considering the size of the study area, the obtained accuracy is satisfactory. Our results show that during 1980–2000, 129,853 ha of land were converted to impervious surface. While sprawl was prominent on urban fringe during 1980s with 23,674 ha of land converted to impervious surface, there was a temporal shift in the rural landscapes in the 1990s with 48,079 ha of land converted to impervious surface. Future research could focus on, but not limited to, 1) more efficient and accurate large scale impervious surface mapping, 2) associating impervious surface with population data to explore the correlation relationship (Lu et al., 2006, Zhou et al. in review) for cities of various size, and 3) modeling efforts on prediction of possible future impervious surface growth including spatial pattern and density. With the help of prediction models, the

effect of the aforementioned policy tools could be tested in the developing stage and validated after the implementation stage.

References

- ALBERTI, M. (2008) *Advances in urban ecology: integrating humans and ecological processes into urban ecosystems*. New York, NY, USA, Springer Science.
- ANDERSON, D. R. (2008) *Model based inference in the life sciences: A primer on evidence*. Springer-Verlag. New York, NY.
- ANTHONY, J. (2004) Do state growth management regulations reduce sprawl? *Urban Affairs Review*, 39, 376-397.
- ARNOLD JR, C. L. & GIBBONS, C. J. (1996) Impervious surface coverage: The emergence of a key environmental indicator. *Journal of the American Planning Association*, 62, 243-258.
- BARTLETT, J. G., MAGEEAN, D. M. & O'CONNOR, R. J. (2000) Residential expansion as a continental threat to U.S. coastal ecosystems. *Population and Environment*, 21, 429-468.
- BAUER, M. E., LOEFFELHOLZ, B. C. & WILSON, B. (2007) Estimating and mapping impervious surface by regression analysis of Landsat imagery. IN WENG, Q. (Ed.) *Remote Sensing of Impervious Surface*. Boca Raton, FL, CRC press.
- BEHAN, K., MAOH, H. & KANAROGLOU, P. (2008) Smart growth strategies, transportation and urban sprawl: Simulated futures for Hamilton, Ontario. *Canadian Geographer*, 52, 291-308.
- BERKE, P. R., MACDONALD, J., WHITE, N., HOLMES, M., LINE, D., OURY, K. & RYZNAR, R. (2003) Greening development to protect watersheds: Does new urbanism make a difference? *Journal of the American Planning Association*, 69, 397-413.
- BRABEC, E., SCHULTE, S. & RICHARDS, P. L. (2002) Impervious surfaces and water quality: A review of current literature and its implications for watershed planning. *Journal of Planning Literature*, 16, 499-514.
- BROOKINGS, I. (2002) *Growth in the heartland: challenges and opportunities for Missouri*. Washington, D. C., USA, Brookings Institution, Center on Urban and Metropolitan Policy.
- BRUECKNER, J. K. (2000) Urban sprawl: Diagnosis and remedies. *International Regional Science Review*, 23, 160-171.
- CARLSON, T. N. & TRACI ARTHUR, S. (2000) The impact of land use - Land cover changes due to urbanization on surface microclimate and hydrology: A satellite perspective. *Global and Planetary Change*, 25, 49-65.

- CARRUTHERS, J. I. (2003) Growth at the fringe: The influence of political fragmentation in United States metropolitan areas. *Papers in Regional Science*, 82, 475-499.
- CERVERO, R. (2003) Road expansion, urban growth, and induced travel: A path analysis. *Journal of the American Planning Association*, 69, 145-164.
- CHEN, S., ZENG, S. & XIE, C. (2000) Remote sensing and GIS for urban growth analysis in China. *Photogrammetric Engineering and Remote Sensing*, 66, 593-598.
- CIVCO, D. L., HURD, J. D., ARNOLD, C. L. & PRISLOE, S. (2002) Characterization of suburban sprawl and forest fragmentation through remote sensing applications. *Proceedings, Annual Conference of the American Society for Photogrammetry and Remote Sensing (ASPRS)*. Washington, D.C.
- CIVCO, D. L., HURD, J. D., ARNOLD JR, C. L. & PRISLOE, S. (1997) Impervious surface mapping for the state of Connecticut. *ASPRS 2001 Annual Convention*. Seattle, Washington.
- CLAPHAM JR, W. B. (2003) Continuum-based classification of remotely sensed imagery to describe urban sprawl on a watershed scale. *Remote Sensing of Environment*, 86, 322-340.
- CONGALTON, R. G. (1991) A review of assessing the accuracy of classifications of remotely sensed data. *Remote Sensing of Environment*, 37, 35-46.
- CRONON, W. (1991) *Nature's metropolis: Chicago and the Great West*.
- EPSTEIN, J., PAYNE, K. & KRAMER, E. (2002) Techniques for mapping suburban sprawl. *Photogrammetric Engineering and Remote Sensing*, 68, 913-918.
- ESCH, T., HIMMLER, V., SCHORCHT, G., THIEL, M., WEHRMANN, T., BACHOFER, F., CONRAD, C., SCHMIDT, M. & DECH, S. (2009) Large-area assessment of impervious surface based on integrated analysis of single-date Landsat-7 images and geospatial vector data. *Remote Sensing of Environment*, 113, 1678-1690.
- FOODY, G. M. (2010) Assessing the accuracy of land cover change with imperfect ground reference data. *Remote Sensing of Environment*, 114, 2271-2285.
- FREILICH, R. H. (2003) Smart growth in western metro areas. *Natural Resources Journal*, 43, 687-702.

- FUGUITT, G. V. (1985) The nonmetropolitan population turnaround. *Annual review of sociology*, 11, 259-280.
- HAASE, A. T., CUDABACK, C. N. & CARLSON, T. N. (2007) Development of the watershed evaluation tool using remotely sensed data. *Pennsylvania Geographer*, 45, 3-20.
- HAMMER, R. B., STEWART, S. I., WINKLER, R. L., RADELOFF, V. C. & VOSS, P. R. (2004) Characterizing dynamic spatial and temporal residential density patterns from 1940-1990 across the North Central United States. *Landscape and Urban Planning*, 69, 183-199.
- HANDY, S. (2005) Smart growth and the transportation-land use connection: What does the research tell us? *International Regional Science Review*, 28, 146-167.
- HANSEN, A. J., RASKER, R., MAXWELL, B., ROTELLA, J. J., JOHNSON, J. D., WRIGHT PARMENTER, A., LANGNER, U., COHEN, W. B., LAWRENCE, R. L. & KRASKA, M. P. V. (2002) Ecological causes and consequences of demographic change in the new west. *BioScience*, 52, 151-162.
- HARRIS, R. & LONGLEY, P. (2000) Data-rich models of the urban environment: RS, GIS and 'lifestyles'. GISRUK. York, England.
- HEIMLICH, R. E. & ANDERSON, W. D. (2001) Development at the urban fringe and beyond: Impacts on agriculture and rural land. Washington, D.C, Economic Research Service, U.S. Department of Agriculture.
- HOMER, C. G., HUANG, C., YANG, L. & WYLIE, B. K. (2002) Development of a circa 2000 land cover database for the United States. Proceedings of the ASPRS 2002 Annual Convention. Washington, D. C.
- JENSEN, J. R. (1996) *Introductory digital image processing: a remote sensing perspective*. Second edition.
- JI, C. Y., LIU, Q., SUN, D., WANG, S., LIN, P. & LI, X. (2001) Monitoring urban expansion with remote sensing in China. *International Journal of Remote Sensing*, 22, 1441-1455.
- JOHNSON, K. M. & BEALE, C. L. (2002) Nonmetro recreation counties: Their identification and rapid growth. *Rural America*, 17, 12-19.
- JOHNSON, K. M. & FUGUITT, G. V. (2000) Continuity and change in rural migration patterns, 1950-1995. *Rural Sociology*, 65, 27-49.
- KNIGHT, R. L., WALLACE, G. N. & RIEBSAME, W. E. (1995) Ranching the view: Subdivisions versus agriculture. *Conservation Biology*, 9, 459-461.

- LAW, N. L., FRALEY-MCNEAL, L., CAPPIELLA, K. & PITT, R. (2008) Monitoring to demonstrate environmental results: guidance to develop local stormwater monitoring studies using six example study designs. Ellicott City, MD USA, Center for Watershed Protection.
- LIU, J., DAILY, G. C., EHRLICHT, P. R. & LUCK, G. W. (2003) Effects of household dynamics on resource consumption and biodiversity. *Nature*, 421, 530-533.
- LO, C. P. & YANG, X. (2002) Drivers of land-use/land-cover changes and dynamic modeling for the Atlanta, Georgia metropolitan area. *Photogrammetric Engineering and Remote Sensing*, 68, 1073-1082.
- LU, D. & WENG, Q. (2006) Use of impervious surface in urban land-use classification. *Remote Sensing of Environment*, 102, 146-160.
- LU, D., WENG, Q. & LI, G. (2006) Residential population estimation using a remote sensing derived impervious surface approach. *International Journal of Remote Sensing*, 27, 3553-3570.
- MCKINNEY, M. L. (2002) Urbanization, biodiversity, and conservation. *BioScience*, 52, 883-890.
- NIGH, T. A. & SCHROEDER, W. A. (2002) Atlas of Missouri ecoregions. Jefferson City, Missouri, Missouri Conservation Commission.
- PEISER, R. (2001) Decomposing urban sprawl. *Town Planning Review*, 72, 275-298.
- PLANE, D. A. & ROGERSON, P. A. (1994) Migration: Analyzing the geographic patterns. *The Geographical Analysis of Population with Applications to Planning and Business*. New York, USA, John Wiley & Sons.
- POWELL, S. L., COHEN, W. B., YANG, Z., PIERCE, J. D. & ALBERTI, M. (2008) Quantification of impervious surface in the Snohomish Water Resources Inventory Area of Western Washington from 1972-2006. *Remote Sensing of Environment*, 112, 1895-1908.
- RADELOFF, V. C., HAMMER, R. B. & STEWART, S. I. (2005) Rural and suburban sprawl in the U.S. Midwest from 1940 to 2000 and its relation to forest fragmentation. *Conservation Biology*, 19, 793-805.
- RAUP, P. M. (1982) An agriculture critique of the national agricultural lands study. *Land Economics*, 58, 260-274.
- REISNER, M. (1993) Cadillac desert: The American west and its disappearing water, New York, NY, Penguin USA (Paper), Revised Edition.

- RIDD, M. K. (1995) Exploring a V-I-S (vegetation-impervious surface-soil) model for urban ecosystem analysis through remote sensing: comparative anatomy for cities. *International Journal of Remote Sensing*, 16, 2165-2185.
- SCHNAIBERG, J., RIERA, J., TURNER, M. G. & VOSS, P. R. (2002) Explaining human settlement patterns in a recreational lake district: Vilas County, Wisconsin, USA. *Environmental Management*, 30, 24-34.
- STEHMAN, S. V., WICKHAM, J. D., SMITH, J. H. & YANG, L. (2003) Thematic accuracy of the 1992 National Land-Cover Data for the eastern United States: Statistical methodology and regional results. *Remote Sensing of Environment*, 86, 500-516.
- SUTTON, P. C. (2003) A scale-adjusted measure of "Urban Sprawl" using nighttime satellite imagery. *Remote Sensing of Environment*, 86, 353-369.
- THEOBALD, D. M. (2001) Land-use dynamics beyond the American urban fringe. *Geographical Review*, 91, 544-564.
- TU, J., XIA, Z. G., CLARKE, K. C. & FREI, A. (2007) Impact of urban sprawl on water quality in eastern Massachusetts, USA. *Environmental Management*, 40, 183-200.
- VOGELMANN, J. E., D., H., T., M., J., C. M., W., M. J. & H., B. (2001) Effects of Landsat 5 Thematic Mapper and Landsat 7 Enhanced Thematic Mapper Plus radiometric and geometric calibrations and corrections on landscape characterization. *Remote Sensing of Environment*, 78, 55-70.
- VOGELMANN, J. E., HOWARD, S. M., YANG, L., LARSON, C. R., WYLIE, B. K. & VAN DRIEL, J. N. (2001) Completion of the 1990's National Land Cover Data Set for the conterminous United States. *Photogrammetric Engineering and Remote Sensing*, 67, 650-662.
- WALKER, B. & SALT, D. (2006) *Resilience thinking: sustaining ecosystems and people in a changing world*, Washington D. C., USA, Island Press.
- WARD, D., PHINN, S. R. & MURRAY, A. T. (2000) Monitoring growth in rapidly urbanizing areas using remotely sensed data. *Professional Geographer*, 52, 371-386.
- WENG, Q. & LU, D. (2009) Landscape as a continuum: An examination of the urban landscape structures and dynamics of Indianapolis City, 1991-2000, by using satellite images. *International Journal of Remote Sensing*, 30, 2547-2577.
- WU, C. & MURRAY, A. T. (2003) Estimating impervious surface distribution by spectral mixture analysis. *Remote Sensing of Environment*, 84, 493-505.

- WULDER, M. A., FRANKLIN, S. E., WHITE, J. C., LINKE, J. & MAGNUSSEN, S. (2006) An accuracy assessment framework for large-area land cover classification products derived from medium-resolution satellite data. *International Journal of Remote Sensing*, 27, 663-683.
- XIAN, G. & HOMER, C. (2009) Monitoring urban land cover change by updating the national land cover database impervious surface products. 2009 Joint Urban Remote Sensing Event.
- YANG, L., HUANG, C., HOMER, C. G., WYLIE, B. K. & COAN, M. J. (2003) An approach for mapping large-area impervious surfaces: Synergistic use of Landsat-7 ETM+ and high spatial resolution imagery. *Canadian Journal of Remote Sensing*, 29, 230-240.
- YEH, A. G. O. & LI, X. (2001) Measurement and monitoring of urban sprawl in a rapidly growing region using entropy. *Photogrammetric Engineering and Remote Sensing*, 67, 83-90.

Tables

Table 1. Landsat imagery utilized for impervious surface mapping

Path	Row	Date		
		TM	TM	ETM+
23	34	12 Dec. 1982	29 Nov. 1992	14 Nov. 2001
23	35	13 Jan. 1983	12 Oct. 1992	22 Mar. 2002
24	33	17 Nov. 1982	17 Nov. 1991	9 Feb. 2002
24	34	4 Jan. 1983	27 Feb. 1988	8 Nov. 2002
24	35	19 Dec. 1982	4 Dec. 1991	8 Nov. 2002
25	32	5 Nov. 1984	23 Apr. 1994	12 Nov. 2001
25	33	5 Nov. 1984	24 Sept. 1992	12 Nov. 2001
25	34	5 Nov. 1984	21 Mar. 1988	12 Nov. 2001
25	35	5 Nov. 1984	6 Apr. 1988	27 Oct. 2001
26	32	15 Nov. 1982	23 Mar 1992	19 Nov. 2001
26	33	15 Nov. 1982	6 Apr. 1991	24 Mar. 2001
26	34	15 Nov. 1982	23 Mar. 1992	14 Nov. 1999
26	35	15 Nov. 1982	23 Mar. 1992	23 Feb. 2002
27	32	6 Nov. 1982	28 Mar. 1991	10 Nov. 2001
27	33	6 Nov. 1982	14 Mar. 1992	28 Mar. 2000

Table 2. Coefficients for conversion of Landsat 5 TM DN to Landsat 7 ETM+ DN

Band	Slope	Intercept
1	0.9398	4.2934
2	1.7731	4.7289
3	1.5348	3.9796
4	1.4239	7.032
5	0.9828	7.0185
7	1.3017	7.6568

Table 3. Accuracy assessment

Date	Mean PIS-t	Mean PIS-m	RMSE	SE	MAE
1980	30	38	25.75	8.08	14.28
1990	31	40	25.57	8.22	14.48
2000	35	41	24.89	5.89	14.64

Mean PIS-t is the true percent of impervious surface measured from airphotos and averaged for all the sampled pixels. Mean PIS-m is the SPC classified percent of impervious surface averaged for all the sampled pixels. RMSE is root-mean squared error, SE is systematic error, and MAE is mean absolute error.

Table 4. Impervious surface growth (ISG) and total area of pixels with ISG in hectare

PIS (%)	Urban areas (ha)		Rural areas (ha)		Urban + Rural (ha)		U/R (%)
	Pure	Pixels with	Pure	Pixels with	Pure	Pixels with	
1980 - 1990							
0-10	1	5	239	2,388	239	2,393	0.2
10-20	1	2	170	849	170	851	0.3
20-30	3,461	11,535	9,972	33,239	13,432	44,774	34.7
30-40	4,341	10,852	9,527	23,816	13,867	34,669	45.6
40-50	4,118	8,235	6,587	13,174	10,705	21,409	62.5
50-60	3,284	5,473	3,146	5,244	6,430	10,716	104.4
60-70	2,356	3,366	1,513	2,162	3,869	5,528	155.7
70-80	1,534	1,918	769	962	2,303	2,879	199.4
80-90	876	973	415	461	1,291	1,434	211.3
90-100	3,705	3,705	2,844	2,844	6,549	6,549	130.3
Total	23,675	46,064	35,181	85,138	58,855	131,202	67.3
1990 - 2000							
0-10	1	4	258	2,584	259	2,588	0.2
10-20	1	2	175	877	176	879	0.2
20-30	3,675	12,249	13,206	44,020	16,881	56,269	27.8
30-40	4,287	10,718	13,421	33,551	17,708	44,269	31.9
40-50	3,744	7,488	9,295	18,590	13,039	26,078	40.3
50-60	2,931	4,885	4,559	7,597	7,489	12,482	64.3
60-70	2,023	2,890	2,002	2,860	4,025	5,750	101.0
70-80	1,231	1,539	850	1,062	2,081	2,601	144.9
80-90	686	763	404	448	1,090	1,211	170.1
90-100	4,340	4,340	3,911	3,911	8,251	8,251	111.0
Total	22,918	44,877	48,080	115,500	70,998	160,377	47.7

Urban and rural area was distinguished by the two urban boundaries for the state of Missouri. Total areas of pixels with impervious surface growth were calculated by adding up pixels that have impervious surface by the categories of PIS and converted to hectare.

Pure impervious surface area was calculated by the Pixels with impervious area multiplied by the corresponding PIS, in this case 10% to 100% with 10% increment. The column total was the sum of all 10 categories of PIS. U/R stands for urban ISG versus rural ISG ratio and was calculated by urban and rural sprawl in each category of PIS as well as the total value.

Table 5. The amount of land affected by impervious surface growth (ISG) by land cover in hectare

Land cover	1980-1990 (%)	1990-2000 (%)
Grassland	69564 (1.0)	59673 (0.8)
Cropland	23229 (0.6)	40816 (1.0)
Deciduous forest	27728 (0.5)	26281 (0.4)
Open water	2251 (0.8)	2478 (0.9)
Barren or sparsely vegetated	579 (2.5)	1811 (7.9)
Evergreen forest	253 (0.1)	610 (0.2)

% in this table stands for percent of each class being affected compared to the total of that class

Figures

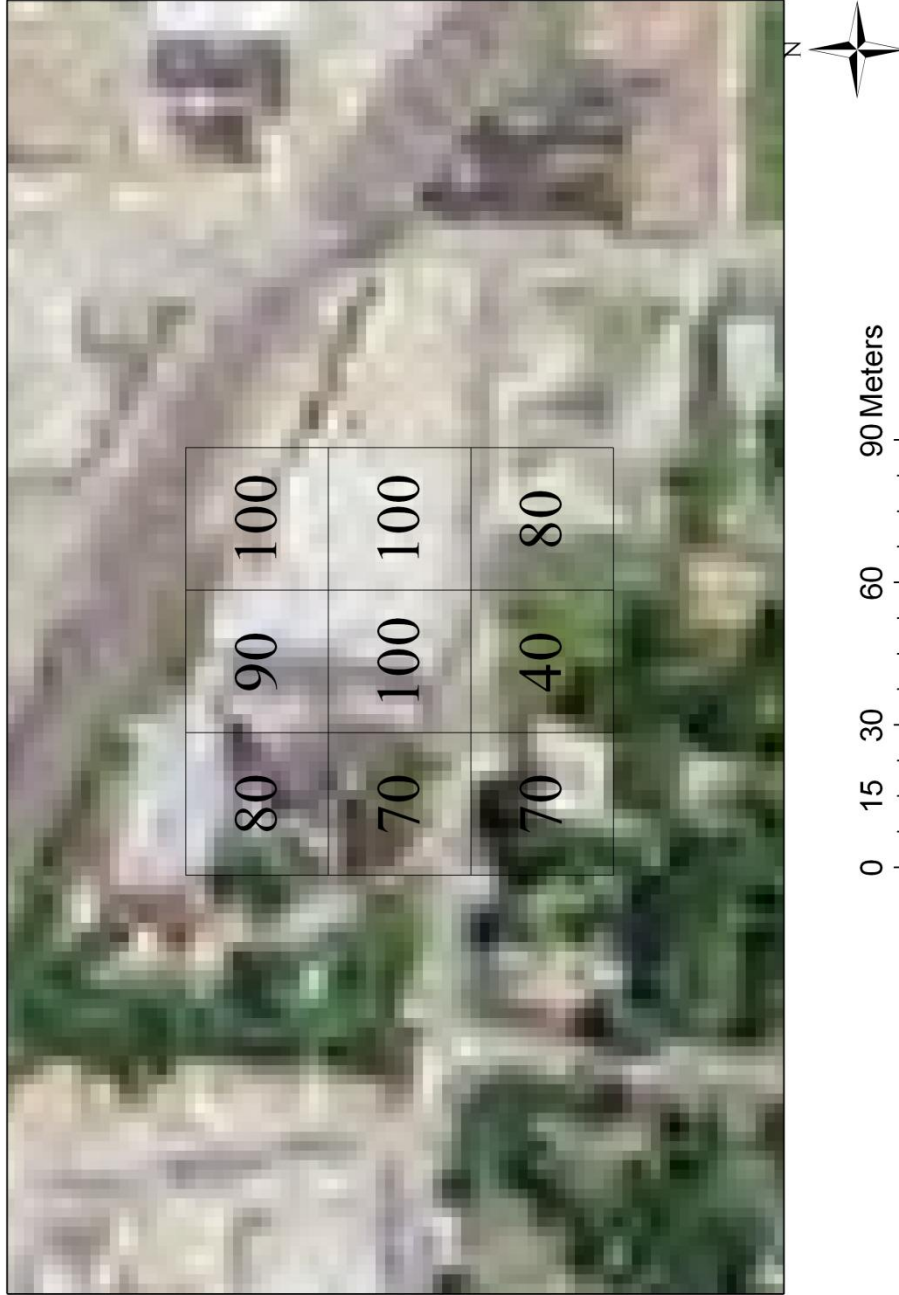


Figure 1. The 2 m NAIP image overlapped with a validation block inside the study area. Each outlined small box represents a 30 m pixel corresponding to the Landsat pixel. The numbers inside each box is corresponding to the digitized and measured PIS inside each box.

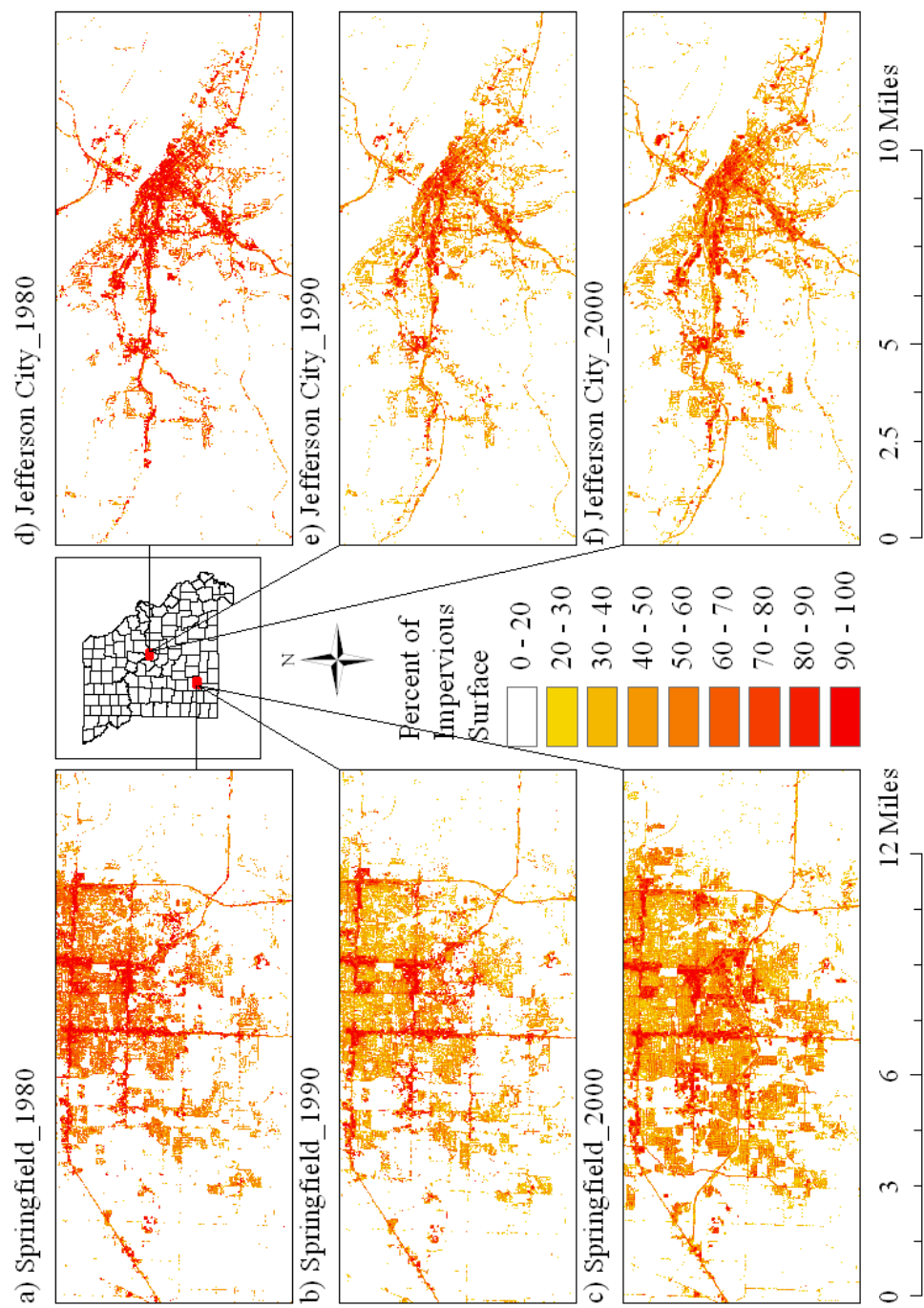


Figure 2. Sub-pixel classifier (SPC) for percent of impervious surface (PIS) for the state of Missouri: a portion of Springfield in (a) 1980; (b) 1990; (c) 2000; and Jefferson City in (d) 1980; (e) 1990; (f) 2000.

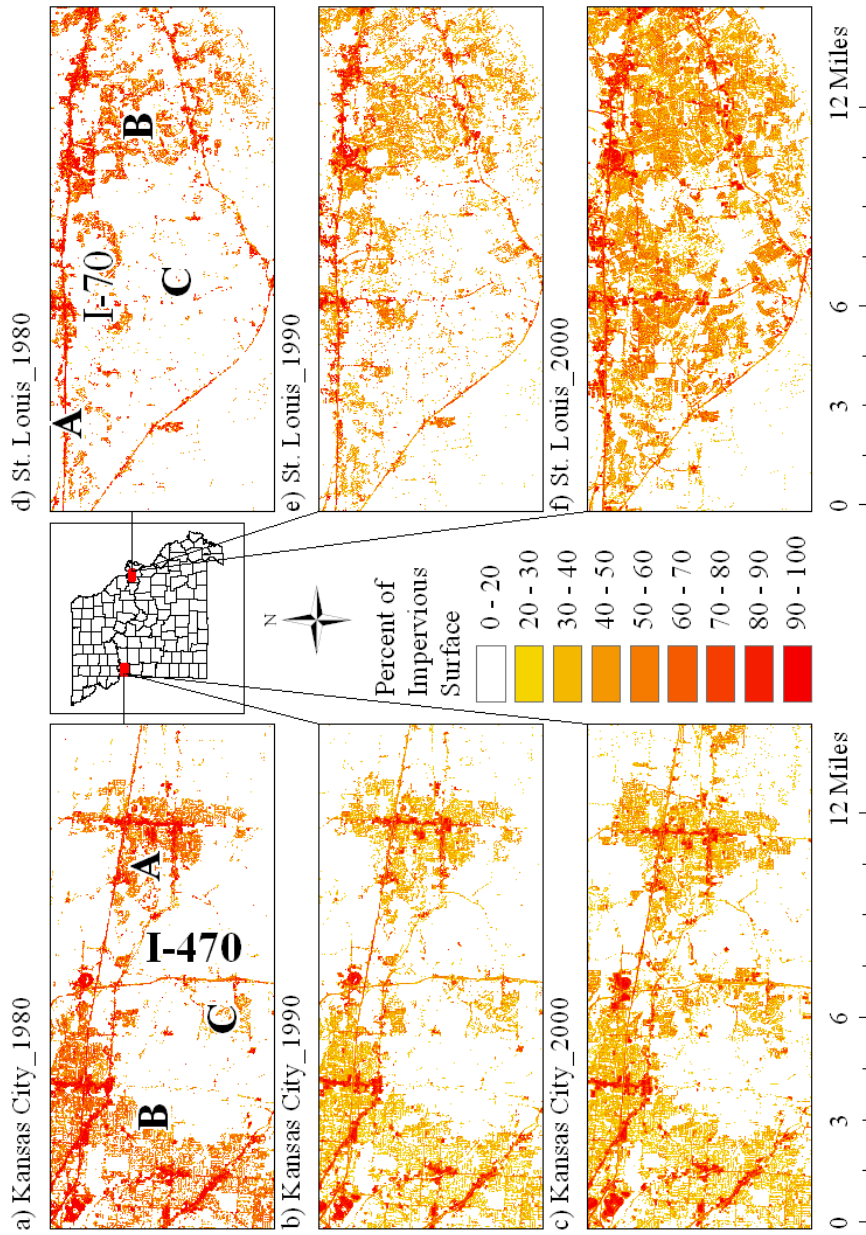


Figure 3. Sub-pixel classifier (SPC) for percent of impervious surface (PIS) for the state of Missouri: a portion of Kansas City in (a) 1980; (b) 1990; (c) 2000 with A indicating leap frog, B indicating low density development on urban fringe of Kansas City, and C indicating low density development along the highway I-470; and a portion of St. Louis metro in (d) 1980; (e) 1990; (f) 2000 with A indicating development along highway I-70, B indicating infilling pattern, and C indicating rural sprawl.

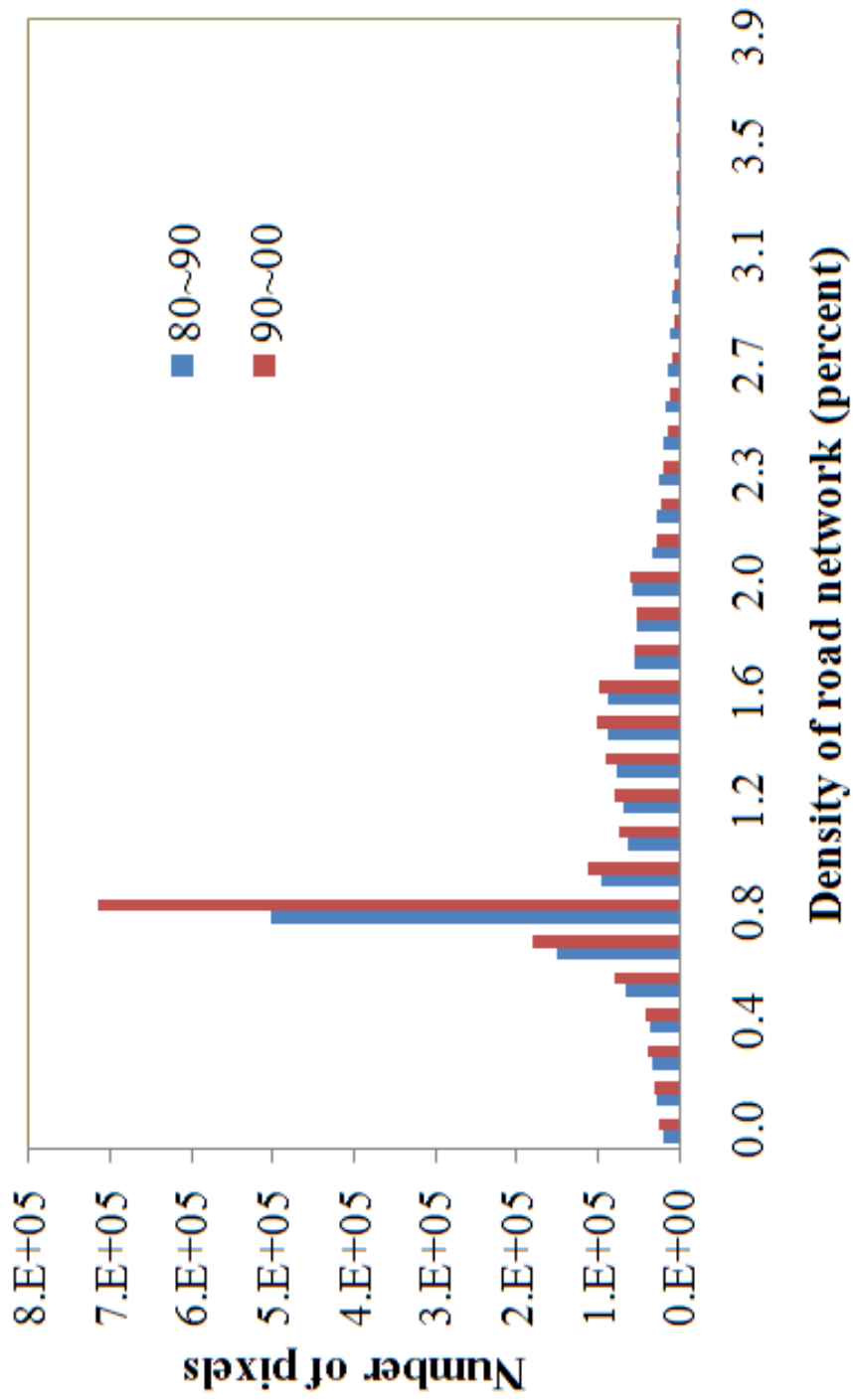


Figure 4. Impervious surface growth (ISG) in the state of Missouri versus density of road networks for 1980s, and 1990s.

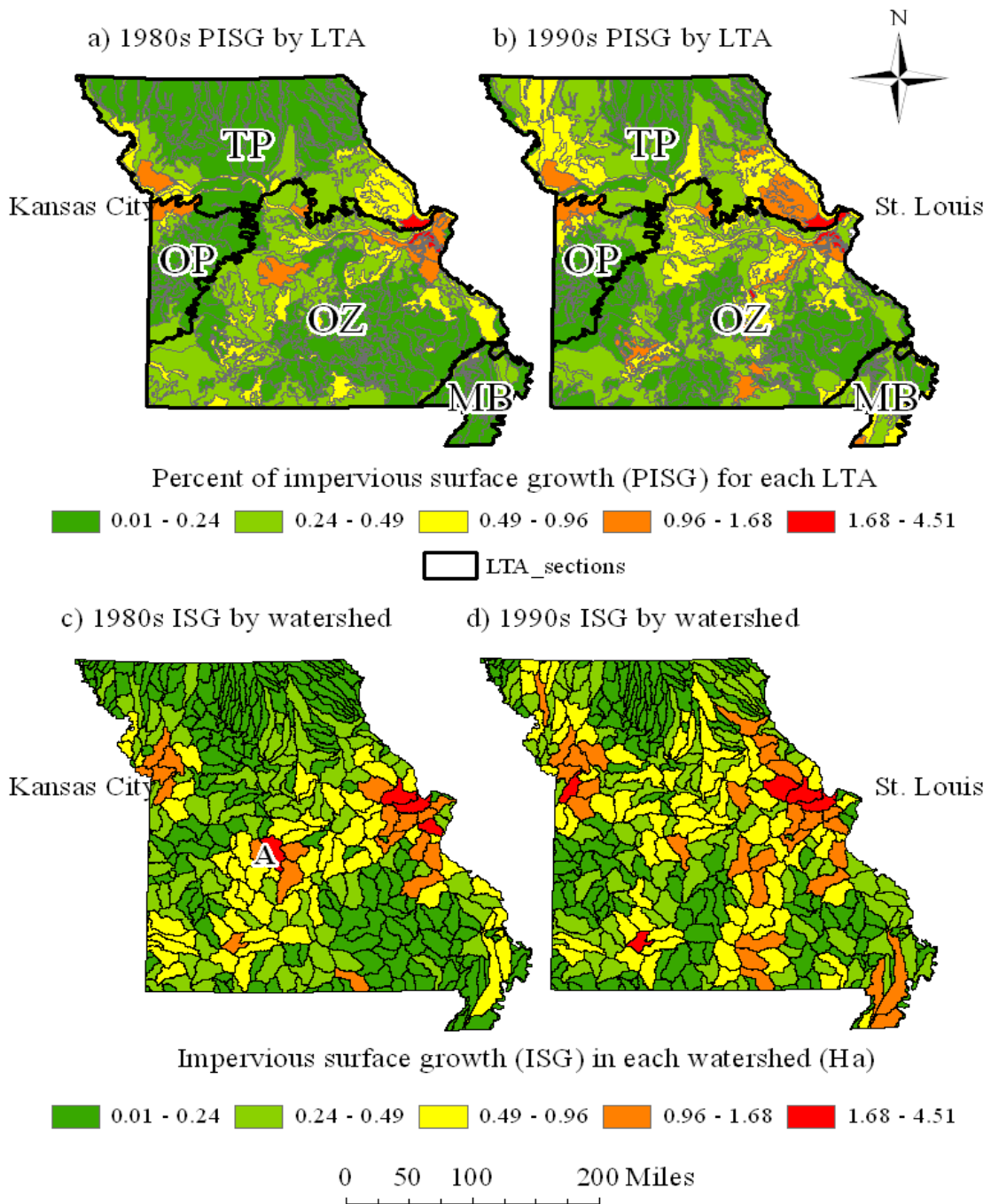


Figure 5. Percent of Impervious surface growth (ISG) summarized by Land type association (LTA) in the state of Missouri: a) 1980s; b) 1990s. ISG summarized by 10 digit watershed of the state of Missouri: c) 1980s; d) 1990s.

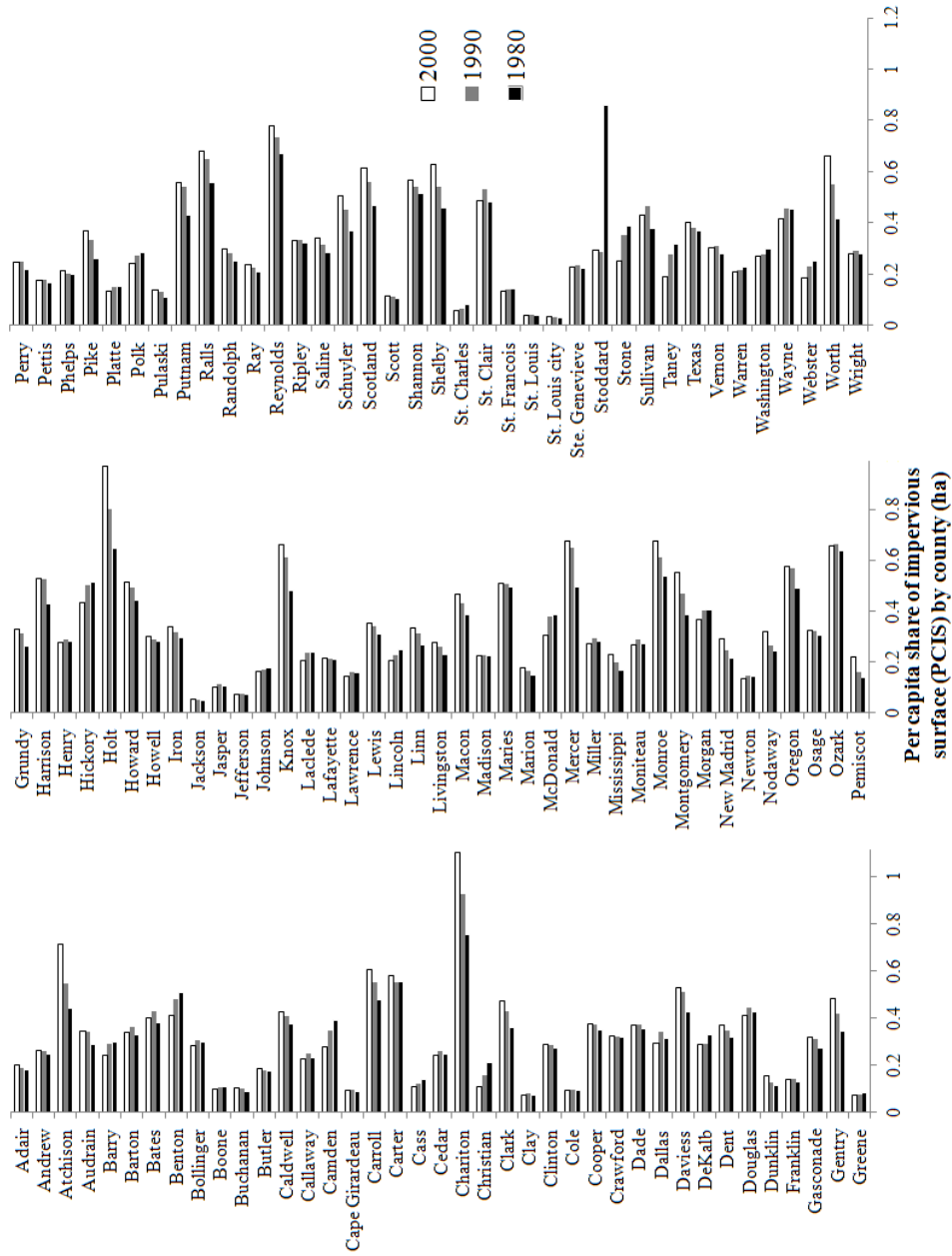


Figure 6. Per capita share of impervious surface (PCIS) summarized by county for 1980, 1990 and 2000 in the state of Missouri.

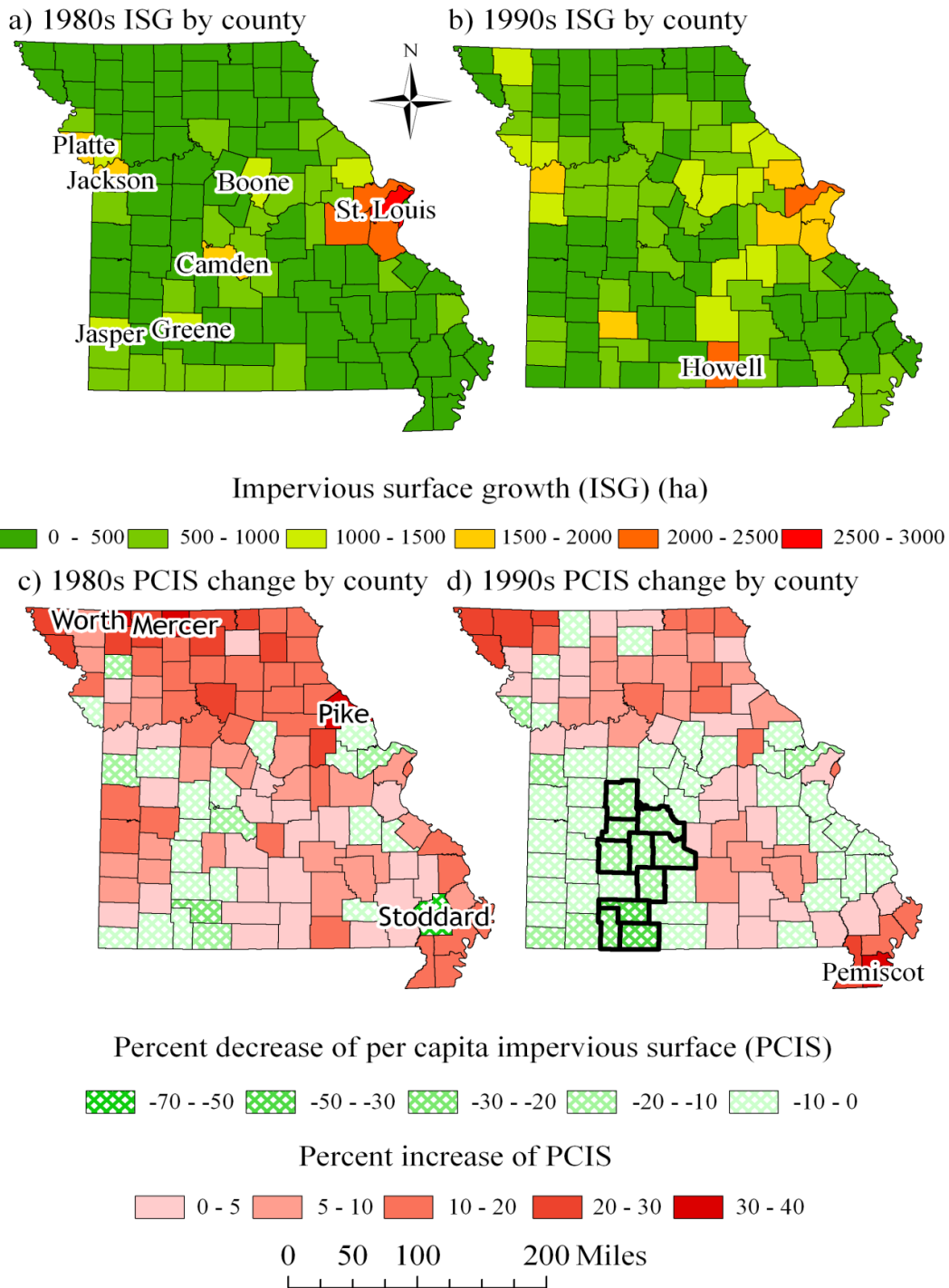


Figure 7. Impervious surface growth (ISG) by county in hectare: (a) 1980s; (b) 1990s. Percent change of per capita share of impervious surface (PCIS) by county: (c) 1980s; (d) 2000s.

Chapter II. A pixel level approach of population estimation from Landsat derived impervious surface and Census data for the state of Missouri

Abstract

Land use and planning decisions, typically made at the municipal level, can be aided by the use of high resolution population information. In this study pixel-level population was derived for the state of Missouri using a combined approach that included dasymetric mapping and regression analysis. The predictor variables used to map population included Census population and imperviousness, which are strongly correlated. Mapping accuracy was assessed by comparing mapped pixel-level population, aggregated by Census block, with the corresponding Census block population. The level of accuracy achieved in this research is comparable to other studies conducted in smaller study areas, because its approach combined the benefits of both dasymetric mapping and regression analysis. The resulting pixel-level population data exhibited a realistic spatial pattern that was strongly correlated with the distribution of impervious surface. Results from this work can be aggregated to any geographic unit (e.g. hydrologic boundaries, administrative boundaries), thus making it possible to incorporate high resolution population data in a variety of studies. The methodology developed in this study can also be used to map pixel-level population in other statewide mapping efforts.

Keywords: Impervious surface; population; pixel-level; GIS

1. Introduction

The fast growing population and rapid expansion of urbanized area has huge impact on natural resource conservation, environmental protection and economic growth. Most of the urban sprawl occurred right on the edges of cities and towns in various speed, shape, density and direction. Thus, it is crucial to have accurate spatial information of the extent of urbanized area and population density for decision making in natural resource management and environmental protection. Missouri is a Midwestern state containing a mixture of highly urbanized metropolitan areas, mid-sized cities, rural communities, and considerable agricultural and forested landscapes. During the 1980s, the Kansas City and St. Louis metropolitan areas led the state in terms of population growth, while mid-sized cities such as St. Joseph, Joplin, Columbia, and Springfield grew fastest in the 1990s (Brookings Institution, 2002). Decentralized growth, or sprawl, can impair the ability of local governments to provide essential services to the general public. Thus, planning at municipal, county, watershed, regional, or statewide scales is critical to ensure that future growth not only provides economic benefits but is accompanied by effective use of natural resources (Verbesselt et al., 2010). For planners to make informed decision, spatial information of urbanized area and population density are necessary at local, regional and state level.

In U.S., decadal population information is usually disseminated at census block level and subsequently aggregated to each ascending geographic census reporting unit (e.g. block group, census tract, and county). Such polygon-based reporting units are often insufficient in representing the true spatial distribution of population density inside each unit because their population values are assumed to be uniformly distributed, thus

failing to account for within unit population variation (Moon and Farmer, 2001). An additional shortcoming of census reporting units is that they are often arbitrary (i.e. having irregular shape) especially in rural areas. Oftentimes, spatial datasets such as hydrologic units and administrative boundaries have different areal units that may not conform to census reporting units, rendering integrating census data with other spatial data difficult. Moreover, when the boundaries and/or scale of data aggregation are modified during the data integration process, the result of spatial data analysis will be greatly affected which is commonly known as the modifiable areal unit problem (MAUP) (Openshaw, 1983). Because of the problems with polygon-based population data, efforts to map population as a continuous raster surface are being made (Langford and Unwin, 1994; Mennis, 2003). By modeling population as a continuous raster surface, the spatial aggregation of population to any predefined boundaries will become a simple process of addition, thus alleviating the MAUP problem.

Previous population modeling can be categorized into areal interpolation and statistical modeling (Wu et al. 2005). Areal interpolation is the transformation of geographic data from one set of boundaries to another. Areal interpolation can be further divided into interpolation based on mathematical functions and ancillary information (Wu et al., 2005). Mathematically based interpolation methods include areal based repartitioning (Tobler 1979) and point based interpolation (Martin 1989). The benefit of areal based repartitioning is the mass preserving, or pycnophylactic, property as coined by Tobler (1979). Areal repartitioning is usually based upon areal weighting. This approach requires the assumption that population is evenly distributed inside each census reporting unit at which areal repartitioning is performed. Point based areal interpolation

was developed in part to solve the problem of assuming uniform population distribution introduced by areal repartitioning. In point based interpolation, the population of each census reporting unit is assigned to centroids, and distance based functions (e.g. inverse distance weighting) are used to assign population to pixels (Martin, 1989). Unlike areal based interpolation, point based interpolation assumes that population density decreases away from the centroid. However, in many cases, centroids are not the population center in a census reporting unit (Wu and Murray, 2005) and population decay functions are not necessarily accurate in describing the actual spatial pattern of population (Martin, 1989). Thus, both areal repartitioning and point-based interpolation are not ideal for precise population modeling.

Areal interpolation based on ancillary information is usually known as dasymetric mapping. The earliest reference to dasymetric mapping is the population map of European Russia in 1992 by Russian cartographer Semenov Tian-Shansky (Mennis and Hultgren, 2006). The origin of the method also explains the Russian heritage of the term “dasymetric” (Wright, 1936). Modern cartography textbooks define a dasymetric map as one that illustrates the statistical surface of data by partitioning space into zones exhaustively which reflect the underlying statistical variation of the data (Dent, 1999; Slocum et al., 2003; Mennis and Hultgren, 2006). The most widely used dasymetric mapping variables are derived from remote sensing. Among all the ancillary datasets used for dasymetric mapping of population, remote sensing derived variables such as land use/land cover (LULC) data (Mennis, 2003) and statistics such as image spectral and textural statistics (Harvey, 2002) are the most widely studied. The mathematical relationship between population data and ancillary datasets can be derived using

regression analysis (Wu, 2007 and Mennis, 2003) to support population mapping. The advantage of dasymetric mapping (e.g. LULC based) over areal interpolation is that it assumes equal population density within the same LULC classes. However, dasymetric mapping is not without flaws. For example, Langford et al. (1991) used dasymetric mapping with LULC data to redistribute polygon-based population to raster cells based on population density. Langford et al. (1991) later discovered that their approach underestimated urban population while overestimating rural population, due to the fact that it assumed equal population density for land use classes without differentiation for location (e.g. urban vs rural). To address this shortcoming, Langford and Unwin (1994) improved their previous work by classifying satellite images to residential and nonresidential areas and assigning census reporting unit population only to residential pixels inside each census reporting unit. The most recent application of dasymetric mapping utilized address points as ancillary data (Zandbergen, 2011). However, this application requires high resolution address point datasets which might not be readily available.

Unlike areal interpolation, statistical modeling infers a regression relationship between population and other physical and socioeconomic variables. There are two advantages with statistical modeling: the first is the ability to include multiple variables in the regression analysis. For instance, previous studies have used urban areas (Tobler, 1969), dwelling units (Lo, 1989), land use classes (Lo, 2003), physical and socioeconomic characteristics such as slope and road density (Dobson, 2000), and spectral features such as greenness and surface temperature (Li and Weng, 2005) as predictor variables. The second advantage of statistical modeling is the ability to estimate

population without census population data as input, which makes it possible to estimate population in regions without census data or to estimate intercensal population (Wu and Murray, 2007). However, statistical modeling approaches may have disadvantages. For instance, by including multiple predictor variables in the regression analysis, the model can become overcomplicated and may result in problems of collinearity. Moreover, such regression models do not use census population data as input, thus making it difficult to transfer them to other study areas. Furthermore, the pycnophylactic property of areal interpolation is not warranted even within the study area where the regression models are developed. Thus, rescaling of the population mapping result is required (Wu and Murray, 2005).

The choice of ancillary datasets and predictor variables for dasymetric mapping and statistical modeling is also very important. Recent researches suggest that imperviousness derived from remotely sensed images can be a promising candidate for dasymetric mapping (Wu and Murray, 2005; Morton and Yuan, 2009). Density, distribution, areal extent, and temporal change of impervious surfaces, are representative of anthropogenic effects in urban and rural areas (Arnold and Gibbons, 1996; Powell et al., 2008). Impervious surfaces have distinct man-made features that can be detected and quantified using remote sensing to reflect anthropogenic development over time (Cronon, 1991; Reisner, 1993; Alberti et al., 2008; Anderson, 2007). In residential areas impervious surfaces are generally associated with housing, which is a strong indicator of population (Theobald, 2001). Impervious surface also provides information on urban morphology (Ji and Jensen, 1999), which can be used to evaluate zoning and planning

outcomes. Imperviousness and population are so strongly correlated that one can be used to predict the other (Wu and Murray, 2005) (Chabaeva et al., 2004).

Wu and Murry (2005) used a cokriging method and spatial autocorrelation between imperviousness and Census population to map pixel level population. Morton and Yuan (2009) used regression analysis to derive a relationship between imperviousness and population density to map population at the pixel level. In a comparison study, Wu and Murray (2007) found that imperviousness estimated population considerably better than both spectral radiance and LULC by achieving 7% less relative error for the entire study area and 30–31% less mean average percentage error at the Census block group level.

Despite recent successes of using imperviousness in population estimation, there are still critical issues that need to be resolved. For example, a limitation of the regression approach is that the relationship between population and imperviousness developed in one study area is generally not applicable in another study area. Morton and Yuan (2009) suggested that a single regression relationship is insufficient when the study area contains both metropolitan and rural areas. The insufficiency is due to the varying population density pattern that differs by region (Pozzi and Small, 2005). A limitation with the cokriging approach is its assumption that the mapped population raster resembles a continuous surface. In reality, however, population exists primarily in developed areas which are represented by impervious surfaces. The spatial distribution of population is not continuous, because urbanized areas such as commercial, industrial and infrastructural areas have no population. Consequently, high density impervious surfaces may have low or no population. Previous researches have shown that excluding

high density imperviousness values improves population mapping (Morton and Yuan, 2009; Zandbergen and Ignizio, 2010). Morton and Yuan (2009) found impervious surface with density smaller than 60% and 75% performed better than impervious surface with high density retained. However, the appropriate thresholds of impervious surface density for population mapping may vary by location and study area.

The current research will utilize dasymetric mapping and regression analysis to map per pixel population using imperviousness and census population for the state of Missouri. Specifically, we intended to: (1) identify the best range of imperviousness for statewide population mapping, (2) develop a per pixel population model using dasymetrically mapped block population and imperviousness, (3) develop regression relationships between population and imperviousness at the census block level, and (4) combine dasymetric and regression approaches to map population at the pixel level for the entire state. The benefit of this hybrid model is to combine the benefit of both dasymetric mapping and statistical modeling while alleviating the drawbacks introduced by both approaches when used separately.

2. Method

2.1. Data

According to the 2000 US Census, Missouri has an area of 180,472.6 km² and consists of 4,545 block groups and 241,655 blocks with average sizes of 39.7 km² and 6.8 km², respectively. Geographic census data were acquired from the Missouri Spatial Data Information Service (MSDIS). These datasets contained population data at multiple spatial scales (tracts, blocks, and block groups). Fifteen Landsat ETM+ scenes were obtained in 2000 from the USGS to perform impervious surface mapping. ERDAS

IMAGINE's Subpixel Classifier (SPC) was used to derive the per-pixel (30m resolution) proportion of imperviousness for the entire state. The mapping of impervious surface included a procedure specifically tailored for sub-pixel classification, a procedure for signature derivation, and finally the procedure for material of interest classification. The first procedure was automated by SPC software. The second procedure was conducted semi-automatically using areas-of-interest (AOIs) derived to represent pixels with 100% pure impervious surface. This procedure was assisted by overlaying aerial photos with Landsat imageries to better identify Landsat pixels with impervious surface only. During this process, multiple signatures were derived representing different type of impervious surfaces: light, medium, and dark. The three different signatures were then used to classify light, medium and dark impervious surfaces separately. The three outputs were combined together to form one final image that represented the total percentage of imperviousness for each pixel. The classification scheme for imperviousness consisted of 9 classes and preserved a 10% increment between classes, except from the 0 to 20% range, which was classified as 0%. The difference in increment at the beginning of the range was due to the limitation of the SPC software that materials covering less than 20% of a pixel are unidentifiable. The remaining imperviousness values were classified with 10% increments as follows: 30%, 40%... 90%, and 100%. Since 20% of a pixel is equivalent to 180 m², the median and average floor area in new single-family houses are 183 m² and 202 m² for the Midwest region of U.S. (U.S. Census, 2000). The floor areas together with driveway will most likely have a footprint larger than 180 m². Thus, such a limitation of the software is not going to hurt the accurate mapping of population based on impervious surface.

To avoid assigning population values where roads were present, vector based TIGER/Line road network data (U.S. Census, 2000) was used to mask out coincident impervious surface pixels (Morton and Yuan, 2009). The preprocessed imperviousness per pixel data was then overlaid onto census block group boundaries to 1) illustrate the distribution of impervious surface pixels, and 2) define spatial relationships between census block group boundaries and impervious surface pixels for Missouri (Fig. 1).

2.2. Identify the best range of imperviousness for population mapping

Since the relationship between population and imperviousness varies by location, it was necessary to identify the range of imperviousness most directly correlated with population for the state of Missouri. We also want to gain a more comprehensive understanding of the performance of various types of imperviousness in population estimation accuracy. To accomplish this, four datasets with varying ranges of imperviousness were prepared (Figure 2) to identify the most accurate candidate for population mapping. First, total imperviousness was used to illustrate the overall spatial pattern of impervious surface (Fig. 2A). Second, cells with imperviousness greater than 80 percent removed (Fig. 2B). Third, cells with imperviousness greater than 70 percent removed (Fig. 2C). Fourth, cells with imperviousness greater than 60 percent removed (Fig. 2D). The performance of each dataset was determined by using block group level populations to estimate block level populations so that they could be directly compared with Census block level population data. Since statewide accuracy assessments are excessively time-consuming, subsets were taken from each of the four datasets in order to determine the optimal threshold range of imperviousness for population mapping. We randomly picked 1,500 out of the 4,545 block groups in the state of Missouri which

contained 21,145 blocks. After both dasymetric mapping and regression analysis were applied to estimate block population based on the selected block group population and the four types of imperviousness. The estimated values were compared with the known block population. An error analysis was performed based on similar studies (Zandbergen and Ignizio, 2010; Zandbergen, 2011). For each block, the following error metrics were determined: (1) the number of people placed incorrectly determined by the sum of the absolute values of the difference between estimated and known population counts for each block, divided by two, (2) the median of the absolute value of the percent error for each block group, using the known population for each block as the denominator, (3) the R-squared value of the correlation between estimated and known population counts for each block. These error metrics were determined for each of the approach and ancillary datasets combination (Table 1). Based on Table 1, it is apparent that pixels with imperviousness values greater than 70% removed performed the best across the board regardless of the approach used. Between the two approaches, dasymetric mapping performed consistently better than regression. Thus, it is appropriate to use dasymetric approach using pixels with imperviousness values greater than 70% removed to estimate block population from block group population in the state of Missouri. We have also calculated the percent area of the removed impervious surface pixels which turned out to be 0.27% of the total study area. Thus, the removal of imperviousness greater than 70% will have very little impact on the final population mapping.

2.3. Regression relationship between population and imperviousness

The imperviousness raster with values greater than 70% removed was used to estimate the total amount of impervious area for each block group and block. To redistribute the

population from block group to block, the total amount of imperviousness for each block were used as weight factors to assign portions of the block group population to each block. In order to further disseminate the block population to finer spatial units such as a raster grid with resolution equivalent to the imperviousness raster, we need to study the relationship between population and imperviousness at the pixel level. Since there is no raster population data with resolution comparable to the imperviousness raster used in this research, validating the mapping result is difficult. However, strong relationships between imperviousness and population exist, and utilizing these relationships for population assignment is warranted because the true spatial distribution of population is not uniform. Since the relationship between imperviousness and population can vary among Census blocks, multiple scenarios should be considered when mapping population based on imperviousness. Common scenarios include: 1) Census block polygons containing only single-family residential units, where the spatial distribution of population coincides with each housing unit and is also spatially correlated with low density impervious surface, 2) Census block polygons containing both single-family residential units and apartment complexes, where the spatial distribution of population coincides with both types of structures and is spatially correlated with low to medium density impervious surface, 3) Census block polygons containing both residential and commercial areas, where the spatial distribution of population coincides only with the residential areas although the commercial areas might have higher density impervious surface.

With the aforementioned scenarios in mind, three assumptions were made in order to study the relationship between imperviousness and population. The first assumption

was that population was entirely associated with pixel level imperviousness (i.e. 0% imperviousness corresponds to 0 population). The second assumption was that pixels with low density impervious surfaces have low population. That is, pixels in rural areas and low density residential neighborhoods with low densities of imperviousness will have low population values. The third assumption was that high density imperviousness can be associated with either low or high population values, a problem partially ameliorated by removing imperviousness values greater than 70%. However, this approach does risk excluding high density residential areas (e.g. high-rise) which contain large populations and are typically located in large urban centers.

Based on the three assumptions, it is appropriate to assign population only to pixels that spatially coincide with imperviousness greater than zero inside each census block. This census block based average population per pixel can be used together with an error term to model the actual population for each pixel. The average population for each impervious surface pixel was determined from the following formula (Eq. [1]):

$$PPP_i = \frac{POP_i}{N_i}, N_i = \sum_{j=0}^m n_{ij} \quad (1)$$

Where PPP_i is population per pixel in block i , POP_i is population for block i , N_i is the number of impervious surface pixels in block i , and n_{ij} is the number of impervious surface pixels with percent of impervious surface j , where $j = 0, 20, 30 \dots 100$, in block i .

A GIS model was created to calculate the average population estimation (Fig. 3). The following equation was used to quantify the actual population for each pixel inside block i (Eq. [2]):

$$PPP_{ij}^* = PPP_i + \varepsilon_{ij}, \sum_{i=0}^n \sum_{j=0}^m n_{ij} \varepsilon_{ij} = 0 \quad (2)$$

Where PPP_{ij}^* is the actual population per pixel in block i with percent of impervious surface j and ε_{ij} as the error term with percent of impervious surface j in block i . Similar to population for each pixel, percent of impervious surface for each pixel also has estimation errors and was expressed using the following formula (Eq. [3]):

$$PIS_j^* = PIS_j + pis, PIS_j = j \text{ and } pis = [-5\%, 5\%] \quad (3)$$

Where PIS_j^* is the actual percent of impervious surface for pixels classified j percent of impervious surface. Since both the predictor variable PIS_j^* and dependent variable PPP_{ij}^* are modeled with an asymptotic value plus an error term. Thus, the regression problem between PPP_{ij}^* and PIS_j^* per pixel for all blocks i or any subsets of all the blocks belong to the errors-in-variables regression problem.

Before running the regression analysis between population and impervious surface at the pixel level, it is necessary to solve the spatial autocorrelation problem which violates the independence assumption in standard regression models (Wu et al., 2006). Every city inside the state can be viewed at as a cluster of population. The best way to resolve the spatial autocorrelation problem is to break the clusters into several subsets by classifying them into various population density (PD) categories (Morton and Yuan, 2009). In this study, however, clustering is not alleviated after classifying the census blocks into five evenly distributed PD classes (Fig. 4). Thus, in this investigation, a different density measurement of population called adjusted population density (APD) was proposed. Instead of using the total area for each Census block, the total area of impervious surface inside each Census block was used as the denominator in the density measurement. The following equation was used to calculate the APD of the corresponding Census block (Eq. [4]):

$$APD_i = \frac{POP_i}{\sum_{j=0}^J A * PIS_j * n_{ij} * 10^{-6}} \quad (4)$$

Where APD_i is adjusted population density per square kilometer for block i , POP_i is population for block i , A is the area of each pixel (900 m^2), PIS_j is percent of impervious surface, and n_{ij} is the number of pixels for percent of impervious surface j in block i .

The APD was used because the traditional PD can introduce bias at the pixel scale, particularly in rural areas. This is due to the fact that the majority of land cover in rural Census blocks was classified as non-urban (i.e. forest, agriculture, pasture, bare soil, and water), consequently diluting the PD for areas with population. Therefore using the adjusted density equation helped to avoid underestimating the actual PD within areas that were considered developed land within rural Census blocks.

To reduce the problem of spatial clustering of population, the blocks were classified into five categories based on quantile rules using APD per square kilometer: (1) low density (≤ 1500), (2) medium – low (1501 – 4000), (3) medium (4001 – 8000), (4) medium – high (8001 – 13500), and (5) high (> 13500). The reclassified census blocks significantly reduced spatial clustering compared to the classification based on PD (Fig. 5). Moran's I statistics were also calculated to quantify the degree of clustering of Census block level population. A Moran's I value near +1.0 indicates clustering, a value near -1.0 indicates dispersion, and a value close to zero indicates a random pattern. The Moran's I values were summarized for both the five PD categories as well as for the five APD categories in Table 2. The overall Moran's I for all the census blocks based on PD is 0.153, indicating classifying census blocks based on APD instead of PD is more effective in reducing spatial autocorrelation between census block PD.

The sample sizes for each adjusted population density categories were very large (about 50,000 census blocks for each density category) and the estimation errors for all population pixels summed to zero (Eq. [2]). That is, the sample size was large enough to assume that the average of independent observations will be approximately normally distributed, as described by the Central Limit Theorem (Billingsley, 1995). Thus, it is reasonable to assume that the summarized mean population would be the same based on either the actual population for each pixel PPP_{ij}^* or the averaged population for each pixel PPP_i . For the sake of simplicity, PPP_i values are summarized for each percent of impervious surface category as well as for the five density categories of Census blocks with mean and standard deviations (Table 3). Raster cells with population values equal to zero can be associated with either zero percent impervious surface pixels (undeveloped) or very high percent impervious surface pixels (industrial and commercial areas). Thus, only non-zero population and impervious surface pixels are included in the analysis to reduce confusion.

We plotted the distributions of population against imperviousness classes in each APD category based on the mean and standard deviation of population in Table 3 (Fig. 6). We noticed the mean values of population indicated by the hollowed dots have linear increasing trends (Fig. 6). Thus, we ran regression analysis between sampled population and percent of impervious surface based on the mean values for the five APD categories. Accordingly, five regression lines are generated based on the five APD categories (Fig. 7). The R^2 statistics were not reported with the regression equations because these regression lines were based on mean population values for percent of impervious surface categories instead of actual populations for each pixel.

The slopes of the five regression relationships follow an increasing trend with the increase of APD (Fig. 7). Thus, it is reasonable to believe that the slope of the regression relationship is correlated with the adjusted population density. In order to find out if such an assumption is valid, the average adjusted population density is calculated for each APD category. After comparing the five slopes of the regression relationships with the average APD of each category, we were able to confirm the positive correlation.

2.4. Estimating per pixel population

A population mapping model can be established based on the regression relationships derived between population and imperviousness together with the two correlation relationships with APD. The first regression relationship takes the form (Eq. [5]):

$$POP_{Ij} = \alpha_I * PIS_j \quad (5)$$

Where POP_{Ij} is the population for pixel with density j in subset of Census blocks I , coefficient α_I is the slope of the regression relationship between population and percent of impervious surface per pixel for subsets of Census blocks I , PIS_j is the percent of impervious surface density. There is no intercept for this regression relationship due to the assumption that zero population is associated with zero imperviousness. The regression relationship between the slope of the first regression relationship and the adjusted population density takes the form (Eq. [6]):

$$\alpha_I = \gamma * APD_I + \theta \quad (6)$$

Where coefficient γ is the slope of this relationship between the slope of the first regression relationship α_I and APD_I which is the adjusted population density for subset of Census blocks I . Coefficient θ is the intercept of this relationship.

By substituting α_I into the first regression relationship, the following equation results (Eq. [7]):

$$POP_{Ij} = (\gamma * APD_I + \theta) * PIS_j \quad (7)$$

Note that the subset of Census blocks I can be any subset of all Census blocks. Thus, i may be substituted for I , which corresponds to the subset of each individual Census block and gives the following equation (Eq. [8]):

$$POP_{ij} = (\gamma * APD_i + \theta) * PIS_j \quad (8)$$

The above equation is the regression relationship between populations and percent of impervious surfaces at the pixel level where APD_i is the dasymetric component (or geographically weighted component) and PIS_j is the regression component. This regression relationship may be applied to study areas of various sizes and in different locations to calculate population per pixel based on any Census population units and the percent of impervious surface information therein.

Unlike areal interpolation, this regression approach does not have the pycnophylactic property. Thus, a rescaling approach is used to preserve the total number of population for each Census polygon (Wu and Murray, 2005). The equation used for rescaling takes the form (Eq. [9]):

$$POP_{ij}^* = POP_{ij} \frac{POP_i}{\sum_{j=0}^m POP_{ij}} \quad (9)$$

Where POP_{ij}^* is the rescaled mass preserved population for pixels with percent of impervious surface j in Census polygon i , POP_{ij} is the population estimation obtained through the regression equation (Eq. [8]), and POP_i is the dasymetricly mapped population for Census polygon i and $\sum_{j=0}^m POP_{ij}$, which is the sum of POP_{ij} for Census polygon i .

A GIS model was developed to implement the aforementioned procedures and to map populations at pixel level (Fig. 8). The required inputs for this GIS model include the following: Census population, percent of impervious surface, and two regression relationship coefficients: γ , θ , which are site specific and need to be derived for each individual study area. To address the problem of associating high density imperviousness with either high density or low density population, a procedure was added to remove Census blocks that overlapped areas with high density impervious surface. For simplicity, we assigned uniform population based on the estimated block population and the presence of impervious surface pixels. It is not feasible to assess pixel level accuracy because there was no accurate pre-existing population information available at the pixel level for the state of Missouri.

3. Results

3.1. Results validation

The block population estimation based on block group population is summarized in Table 1. The best performance combination is dasymetric mapping using imperviousness with road network data and pixels with imperviousness values less than 70%. The percent of people placed incorrectly is 19.5% with a median absolute percent error of 27.7 and R-squared value of 0.787 using the actual block population for comparison. This result is consistent with previous research. If we subject the per pixel population estimation to the block level population validation, the accuracy will be very similar to the best accuracy reported in Table 1. However, without the availability of statewide population at pixel level, we are not capable of reporting the pixel level population estimation accuracy.

3.2. Pixel-based regression model

This study has derived unique deterministic relationships for each census block based on their adjusted population density. Thus, the errors are minimized in the modeling process.

The model used for the state of Missouri takes the following form (Eq. [10]):

$$POP_{ij} = 5 \times 10^{-6} * APD_i * PIS_j + 0.0092 * PIS_j \quad (10)$$

Where POP_{ij} is the population per pixel in block i for percent of impervious density j .

This regression model was specifically derived for the state of Missouri. Thus, to implement this approach in study areas other than Missouri, it is necessary to derive model coefficients specific to the study area in question.

3.3. Map results

Due to the large extent of the study area, not all areas can be presented and described.

Figure 9 shows the mapped population density for each pixel in four panels representing four different cities in Missouri. Results show the spatial distribution, actual location, and spatial variations of population in detail unattainable with Census population data alone (Fig. 9). For example, it is shown that residential neighborhoods in Springfield have relatively uniform population densities within each neighborhood but large variances among different neighborhoods. The downtown core areas are generally without population (A on Springfield panel in Fig. 9). The railway hub is also without population (B on Springfield panel in Fig. 9). In the park or forested area, there is low and scattered population (C on Springfield panel in Fig. 9). The general population distribution pattern outside the downtown core area is an increase followed by a decrease in population radiating out from the city center.

The city of Columbia has a gradual trend in decreasing population radiating out from the inner city. In the inner city of Columbia, there is a concentration of population near the University Hospital Center (A on Columbia panel in Fig. 9). In the outer city of Columbia, there exists a scattered pattern in spatial distribution of residential neighborhood (B and C on Columbia panel in Fig. 9). Kansas City exhibits both the patchy relationships of Springfield and the gradual decreasing trend of the city of Columbia. Plus, there is many rural population scattering between Kansas City and the leapfrog developments (A on Kansas City panel in Fig. 9). St. Louis, on the other hand, is more uniform in distribution of population density in residential areas of various densities. The core of downtown area (A on St. Louis panel in Fig. 9) as well as the Forest Park area (B on St. Louis Panel in Fig. 9) is without any population. In general, the per-pixel population map has a very similar spatial pattern to the imperviousness map, which is due to the assumption that population will coincide with the presence of impervious surface. Moreover, the map result ensures a reasonable estimate of population density, which is highly correlated to impervious surface. The mapping results also ensure that spatial allocation of population is consistent with block level Census population data.

A histogram showing the frequency of pixel level population values for the entire study area can be seen in Figure 10; pixels with no population values were not included in the analysis. Results indicate that for pixels with population over 99% will contain 6 or less persons (Fig. 10).

4. Discussion

4.1. Approach implications

This approach avoided several problems at the data preprocessing stage encountered by previous studies. For example, the cokriging approach (Wu and Murray, 2005) where point population is necessary, assumptions must be made to convert U.S. Census population data to point population data. In this study, block population was first estimated by a well-established dasymetric mapping technique and then disseminated to each pixel based on the presence of impervious surface, which is more accurate than assigning the entire population to an arbitrary or geometrically derived point. Instead of using a single linear regression relationship for the entire study area (Morton and Yuan, 2009), five initial regression relationships were derived between adjusted population density and imperviousness per pixel, a concept unique to this research. Since the five regression relationships derived from the five subsets of data were not spatially clustered, it can be concluded that they were independent of one another. Thus, it was possible to expand these regression relationships to ensure that each Census block has its own regression relationship based on the locally calculated adjusted population density. Another example is the approach by Wu and Murray (2005) where residential area was derived with conventional image classification. This approach requires separate procedures to derive residential area which might introduce more errors due to issues of error propagation. Moreover, this type of approach might risk the exclusion of areas with low density population (e.g. exurban areas and some high density urban centers). In this study, the assignment of population to non-residential area is reduced by excluding areas such as census blocks with no population, pixels with no impervious surface, and

impervious surface overlapped with all road networks. Last but not least, previous studies generate continuous surfaces of population density (Wu and Murray, 2005). In reality, population distribution is not always continuous over the landscape. Although GIS masks were used to filter unrealistic population pixels, the use of masks after assigning population to each pixel will reduce the total predicted population, thereby requiring further adjustment (Wu and Murray, 2005).

There are two advantages associated with the methodology presented in this study. First, this approach assumes a strong correlative relationship between imperviousness and population at the pixel level. The strong relationships ensure the use of different deterministic relationships tailored to each census unit. These relationships are then used to map population at the pixel level rather than using a single universal regression model for the entire study area (Morton and Yuan, 2009). By modeling population versus impervious surface at each census block, population variation due to location is considered and incorporated into the mapping model by introducing the local population density measure of adjusted population density. The second advantage of using this approach is only impervious surface mapped population is strongly associated with the presence of impervious surface. This is different from interpolation models used in other studies where population is assigned to the entire study area with varying densities (Wu and Murray, 2005).

4.2. Data implications

There are three major limitations with the dataset used in this study. First, per pixel population information is not available for error checking. The only population information available was aggregated population for each Census block. For the same

reason, the relationship between imperviousness and population at the pixel level cannot be established directly. Several assumptions have to be made in order to study the relationship between population and imperviousness. Second, population in Missouri has a high degree of spatial variability. Thus, it is necessary to analyze population at smaller scales, such as by Census block or block group. Third, imperviousness, which is obtained from subpixel classification of Landsat images, is subject to mapping accuracy which can lead to error propagation in the population mapping process.

4.3. Result implications

We have presented a method for mapping statewide pixel level population that achieved similar or better accuracy compared to previous population estimates based on Census block group data (Wu and Murray, 2005 and 2007; Wu et al., 2005 and 2006; Morton and Yuan, 2009; Zandbergen and Ignizio, 2010). More importantly, this study showed that it was possible to map pixel level population for the entire state of Missouri. Using pixel level population data has many advantages relative to U.S. Census population data. For example, pixel based population data can be easily associated with all other spatial datasets (e.g. watershed boundaries, ecological units, and elevation data), avoids problems with boundary discrepancies caused by the irregular shape and size of Census polygons, and can be easily plugged into raster based models with minimal adjustment. Moreover, traditional estimations of population density only give a per area average of population distribution, whereas pixel based population data provides a more detailed illustration of the spatial distribution of population. The results of this study also confirm Sutton's (2009) theory regarding the population holding capacity (~ 6 persons/900 m² in this study) of a given area of impervious surface and establish a correlation between

imperviousness and population, thus suggesting that pixel based population estimates are possible when predicated on coincident areas of imperviousness (Fig. 10). The population estimation method presented here also makes it possible to infer population based on imperviousness derived from remotely sensed imagery or model predictions without relying on decadal Census population data (Fig. 10). Pixel based population data is also useful in numerous ways, such as: location analyses for health-care centers and public libraries, integration of demographic and socioeconomic characteristics for risk and impact assessments, and emergency planning and management, consequence assessment, mitigation planning, and implementation.

5. Conclusions

A dasymetric mapping with localized regression approach was presented here to model per pixel population using per-pixel imperviousness and Census population at Census unit level for the state of Missouri. Unique relationships were discovered between population and imperviousness at the pixel level for each census block. These relationships were used to assign Census block level population values to each pixel in accordance with the presence of imperviousness. The findings inferred from the mapping result indicated that over 99% of the pixel population values in Missouri contained between one and six people. This population mapping approach improves upon previous methods because it allows for the use of Census data at various scales (e.g. block, block group, tract) and is insensitive to the size and location of the study area. The mapping result is an improvement over the uniform distribution of population as defined by U.S. Census geographic data. This approach also manages to map per pixel population for a large geographic area at a high spatial resolution.

The major limitation of the approach reported in this study includes the inability of the procedure to perform accuracy assessment at the pixel level due to lack of accurate high resolution raster population data. This issue could be alleviated by acquiring ground-truth data, which was beyond the scope of this investigation, but provides impetus for future investigations. Another limitation is the somewhat diminished model efficiency resulting from the large size of the study area. Future studies using large spatial extents will need to be separated into several subsets in order for the model to more accurately produce population at the pixel level without exceeding the limit of the computer's physical memory. An additional limitation is associated with the use of imperviousness data in this study, due to the fact that high density imperviousness may imply either high density population or no population. The removal of high density imperviousness values may improve the overall accuracy of population estimation; however, it should again be noted that this approach operates on the assumption that areas with high density imperviousness (e.g. >70%) are considered to have no population. This assumption was made due to the fact that the occurrence of both high density imperviousness and high density population is extremely rare compared to the coincidence of high density imperviousness with little or no population. Thus, it would be beneficial to more deeply explore the relationship between very high density imperviousness and population in future studies.

References

- ALBERTI, M. (2008) *Advances in urban ecology: integrating humans and ecological processes into urban ecosystems*. New York, NY, USA, Springer Science.
- ANDERSON, D. R. (2008) *Model based inference in the life sciences: A primer on evidence*. Springer-Verlag. New York, NY.
- ARNOLD JR, C. L. & GIBBONS, C. J. (1996) Impervious surface coverage: The emergence of a key environmental indicator. *Journal of the American Planning Association*, 62, 243–258.
- BILLINGSLEY, P. (1995) *Probability and Measure*, Wiley-Interscience.
- BROOKING, I. (2002) *Growth in the heartland: challenges and opportunities for Missouri*. Washington, D.C., USA, Brookings Institution, Center on Urban and Metropolitan Policy.
- CHABAEVA, A., CIVCO, D. L. & PRISLOE, S. (2004) Development of a population density and land use based regression model to calculate the amount of imperviousness. Denver, CO: Proceedings 2004 ASPRS Annual Convention.
- CRONON, W. (1991) *Nature's metropolis: Chicago and the Great West*.
- DOBSON, J. E., BRIGHT, E. A., COLEMAN, P. R., DURFEE, R. C. & WORLEY, B. A. (2000) LandScan: A global population database for estimating populations at risk. *Photogrammetric Engineering and Remote Sensing*, 66, 849-857.
- EICHER, C. L. & BREWER, C. A. (2001) Dasymetric mapping and areal interpolation: Implementation and evaluation. *Cartography and Geographic Information Science*, 28, 125–138.
- HARVEY, J. T. (2002) Estimating census district populations from satellite imagery: Some approaches and limitations. *International Journal of Remote Sensing*, 23, 2071-2095.
- JI, M. & JENSEN, J. R. (1999) Effectiveness of subpixel analysis in detecting and quantifying urban imperviousness from landsat thematic mapper imagery. *Geocarto International*, 14, 31-39.
- LANGFORD, M., MAGUIRE, D. J. & UNWIN, D. J. (1991) The areal interpolation problem: estimating population using remote sensing in a GIS framework. *Handling geographical information*, 55-77.

- LANGFORD, M. & UNWIN, D. J. (1994) Generating and mapping population density surfaces within a geographical information system. *Cartographic Journal*, 31, 21-26.
- LI, G. & WENG, Q. (2005) Using Landsat ETM+ imagery to measure population density in Indianapolis, Indiana, USA. *Photogrammetric Engineering and Remote Sensing*, 71, 947–958.
- LO, C. P. (1989) A raster approach to population estimation using high-altitude aerial and space photographs. *Remote Sensing of Environment*, 27, 59-71.
- LO, C. P. (2003) Zone-based estimation of population and housing units from satellite-generated land use/land cover maps. *Remotely Sensed Cities*, 157-180.
- LU, D., WENG, Q. & LI, G. (2006) Residential population estimation using a remote sensing derived impervious surface approach. *International Journal of Remote Sensing*, 27, 3553-3570.
- MARTIN, D. (1989) Mapping population data from zone centroid locations. *Transactions - Institute of British Geographers*, 14, 90-97.
- MENNIS, J. (2003) Generating surface models of population using dasymetric mapping. *Professional Geographer*, 55, 31-42.
- MOON, Z. K. & FARMER, F. L. (2001) Population density surface: A new approach to an old problem. *Society and Natural Resources*, 14, 39–49.
- MORTON, T. A. & YUAN, F. (2009) Analysis of population dynamics using satellite remote sensing and US census data. *Geocarto International*, 24, 143–163.
- OPENSHAW, S. (1983) The modifiable areal unit problem. *CATMOG (Concepts & Techniques in Modern Geography)*, 38.
- POWELL, S. L., COHEN, W. B., YANG, Z., PIERCE, J. D. & ALBERTI, M. (2008) Quantification of impervious surface in the Snohomish Water Resources Inventory Area of Western Washington from 1972-2006. *Remote Sensing of Environment*, 112, 1895–1908.
- POZZI, F. & SMALL, C. (2005) Analysis of urban land cover and population density in the United States. *Photogrammetric Engineering and Remote Sensing*, 71, 719–726.
- REISNER, M. (1993) *Cadillac desert: The American west and its disappearing water*, New York, NY, Penguin USA (Paper), Revised Edition.

- SATTERTHWAITE, D. (2005) "The scale of urban change worldwide 1950-2000 and its underpinnings". Human Settlements Discussion Paper Series.
- STEHMAN, S. V. & CZAPLEWSKI, R. L. (1998) Design and analysis for thematic map accuracy assessment: Fundamental principles. *Remote Sensing of Environment*, 64, 331–344.
- SUTTON, P. C., ANDERSON, S. J., ELVIDGE, C. D., TUTTLE, B. T. & GHOSH, T. (2009) Paving the planet: Impervious surface as proxy measure of the human ecological footprint. *Progress in Physical Geography*, 33, 510–527.
- THEOBALD, D. M. (2001) Land-use dynamics beyond the American urban fringe. *Geographical Review*, 91, 544–564.
- TOBLER, W. R. (1969) Satellite confirmation of settlement size coefficients. *Area*, 1, 30-34.
- TOBLER, W. R. (1979) Smooth pycnophylactic interpolation for geographical regions. *Journal of the American Statistical Association*, 74, 519-530.
- VERBESSELT, J., HYNDMAN, R., NEWNHAM, G. & CULVENOR, D. (2010) Detecting trend and seasonal changes in satellite image time series. *Remote Sensing of Environment*, 114, 106–115.
- WU, C. & MURRAY, A. T. (2005) A cokriging method for estimating population density in urban areas. *Computers, Environment and Urban Systems*, 29, 558–579.
- WU, C. & MURRAY, A. T. (2007) Population estimation using landsat enhanced thematic mapper imagery. *Geographical Analysis*, 39, 26–43.
- WU, S. S., QIU, X. & WANG, L. (2005) Population estimation methods in GIS and remote sensing: A review. *GIScience and Remote Sensing*, 42, 80-96.
- WU, S. S., QIU, X. & WANG, L. (2006) Using semi-variance image texture statistics to model population densities. *Cartography and Geographic Information Science*, 33, 127-140.
- ZANDBERGEN, P. A. & IGNIZIO, D. A. (2010) Comparison of dasymetric mapping techniques for small-area population estimates. *Cartography and Geographic Information Science*, 37, 199-214.
- ZANDBERGEN, P. A. (2011) Dasymetric Mapping Using High Resolution Address Point Datasets. *Transactions in GIS*, 15, 5-27.

Tables

Table 1. Performance metrics of regression analysis versus dasymetric mapping, comparison is made upon four different types of imperviousness datasets all of which have road network imperviousness removed.

Imperviousness	People Placed Incorrectly			Median Abs. % Error	R-squared
	Count	Percentage	Rank		
Regression					
Imperviousness	1074783	29.8	4	35.1	0.470
Imperviousness < 80%	946892	26.2	2	34.8	0.599
Imperviousness < 70%	930774	25.8	1	35.9	0.641
Imperviousness < 60%	962284	26.7	3	38.7	0.628
Dasymetric					
Imperviousness	820982	22.8	4	32.2	0.716
Imperviousness < 80%	728489	20.2	3	28.5	0.772
Imperviousness < 70%	703457	19.5	1	27.7	0.787
Imperviousness < 60%	709271	19.7	2	28.2	0.786

Table 2. Moran's I values calculated for the census blocks population density classified based on the five population density categories and the five adjusted population density categories.

Moran's I	Population density categories	Adjusted population density categories
Low	0.546	0.029
Med-Low	0.985	0.028
Medium	0.770	0.017
Med-Hi	0.743	0.019
High	0.497	0.021

Table 3. Average and standard deviation of population for the pixels classified by both percent of impervious surfaces and adjusted population density (APD). Pixels with either zero population or zero percent impervious surfaces are not included to reduce confusion between the population and imperviousness relationship.

Imperviousness	Low APD		Med-low APD		Medium APD		Med-Hi APD		High APD	
	Mean	STD	Mean	STD	Mean	STD	Mean	STD	Mean	STD
20	0.12	0.19	0.51	0.50	1.29	1.29	2.30	3.81	4.46	5.21
30	0.15	0.27	0.68	1.45	1.59	1.14	2.78	1.05	5.50	4.71
40	0.18	0.38	0.84	1.12	1.83	1.14	3.24	2.22	6.58	5.56
50	0.20	0.52	0.94	0.57	2.02	1.06	3.68	3.24	7.98	7.32
60	0.22	0.45	1.00	0.66	2.17	0.83	4.18	1.41	9.46	7.69
70	0.23	0.35	1.06	0.88	2.29	0.91	4.60	1.68	10.57	7.04

Figures

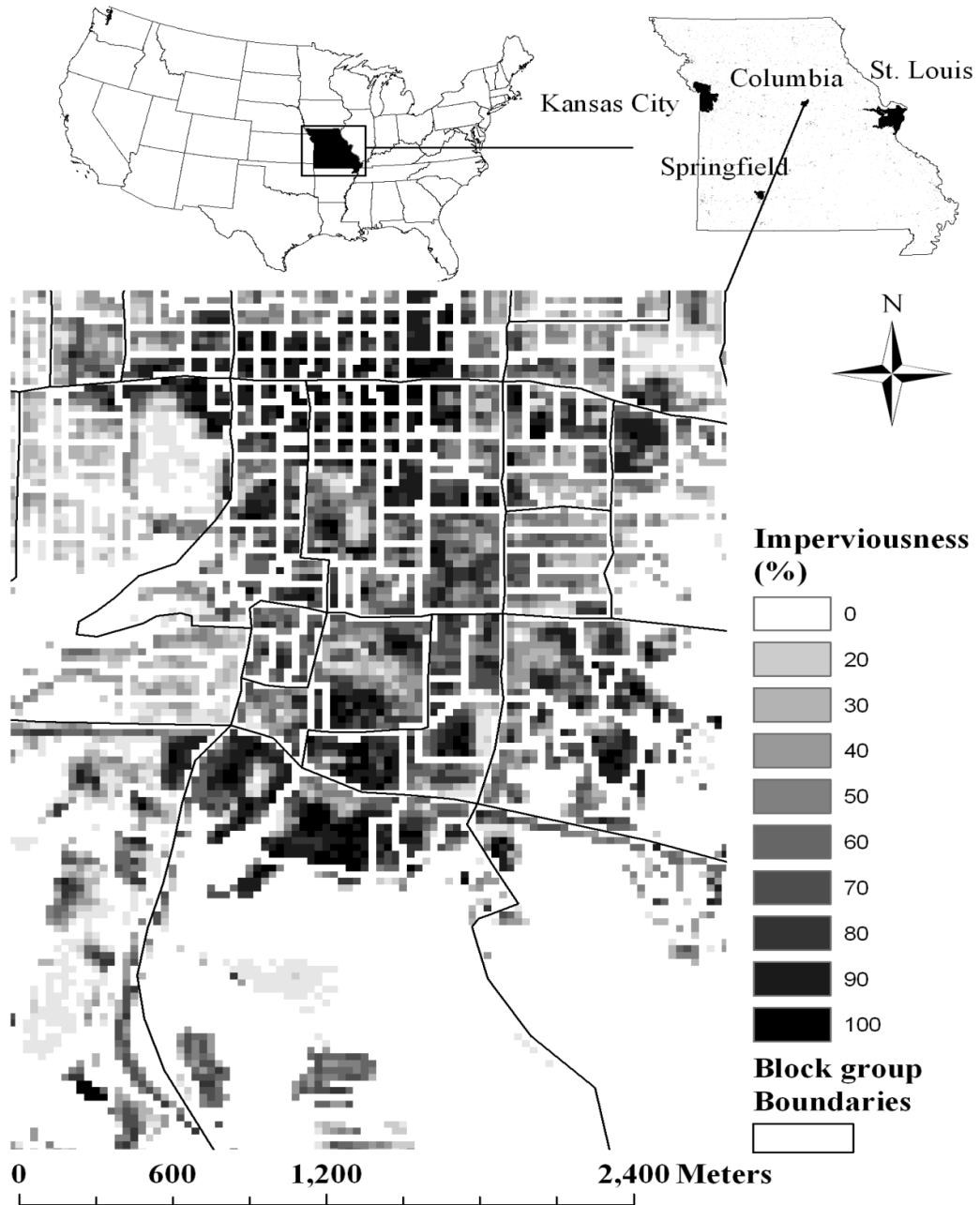


Figure 1. Study area in Missouri, USA with preprocessed impervious surface data overlaid with Census block boundaries. A small area is magnified to show details.

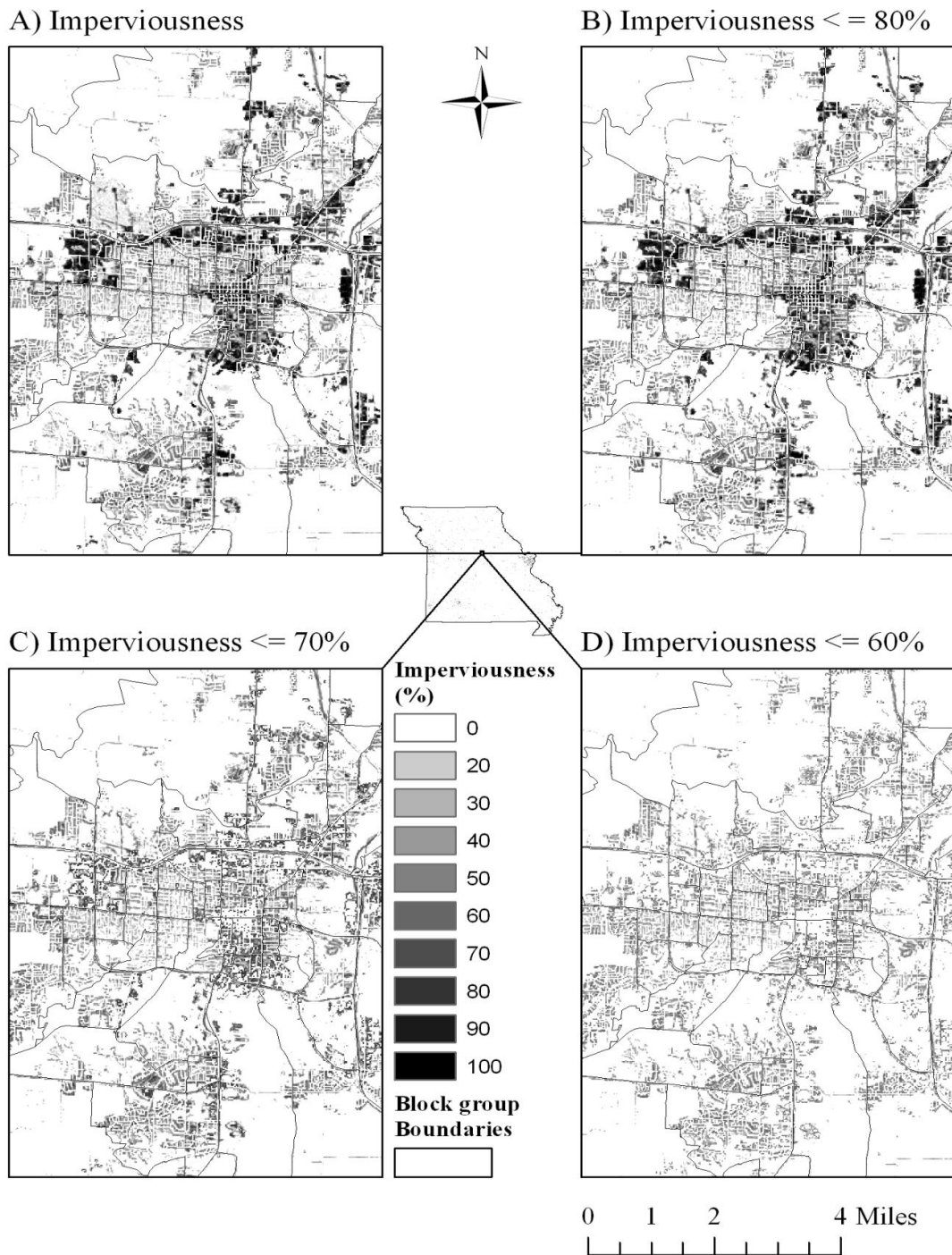


Figure 2. Four different versions of preprocessed imperviousness: a) imperviousness with road network removed; b) imperviousness with road network and values larger than 80% removed; c) imperviousness with road network and values larger than 70% removed; d) imperviousness with road network and values larger than 60% removed.

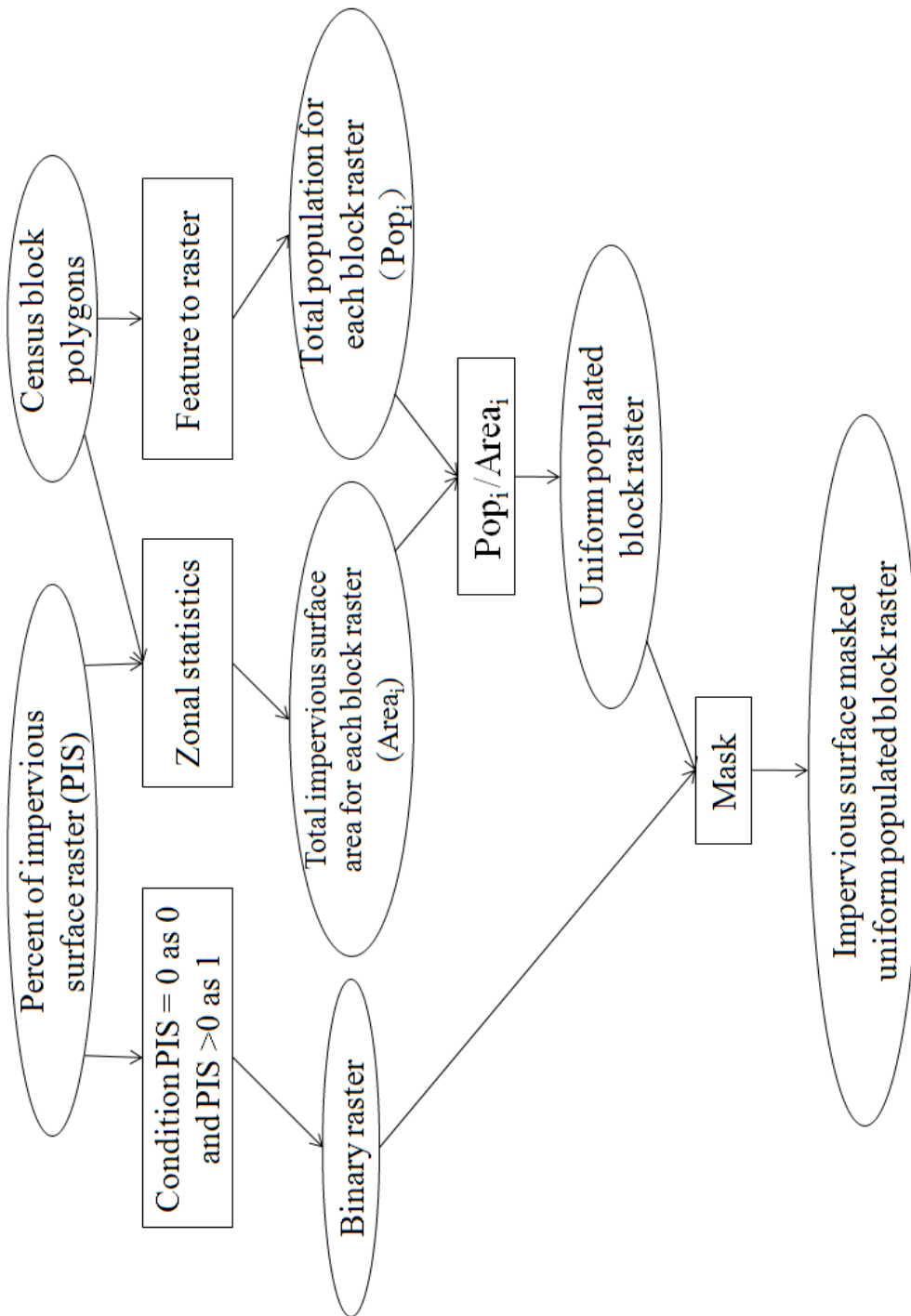


Figure 3. GIS model diagram for attaching census population to each pixel inside based on the assumption that uniform population for each impervious surface pixel.



Figure 4. Census blocks classified into five categories based on population density with percent of impervious surface as background.



Figure 5. Census blocks classified into five categories based on adjusted population density with percent of impervious surface as background.

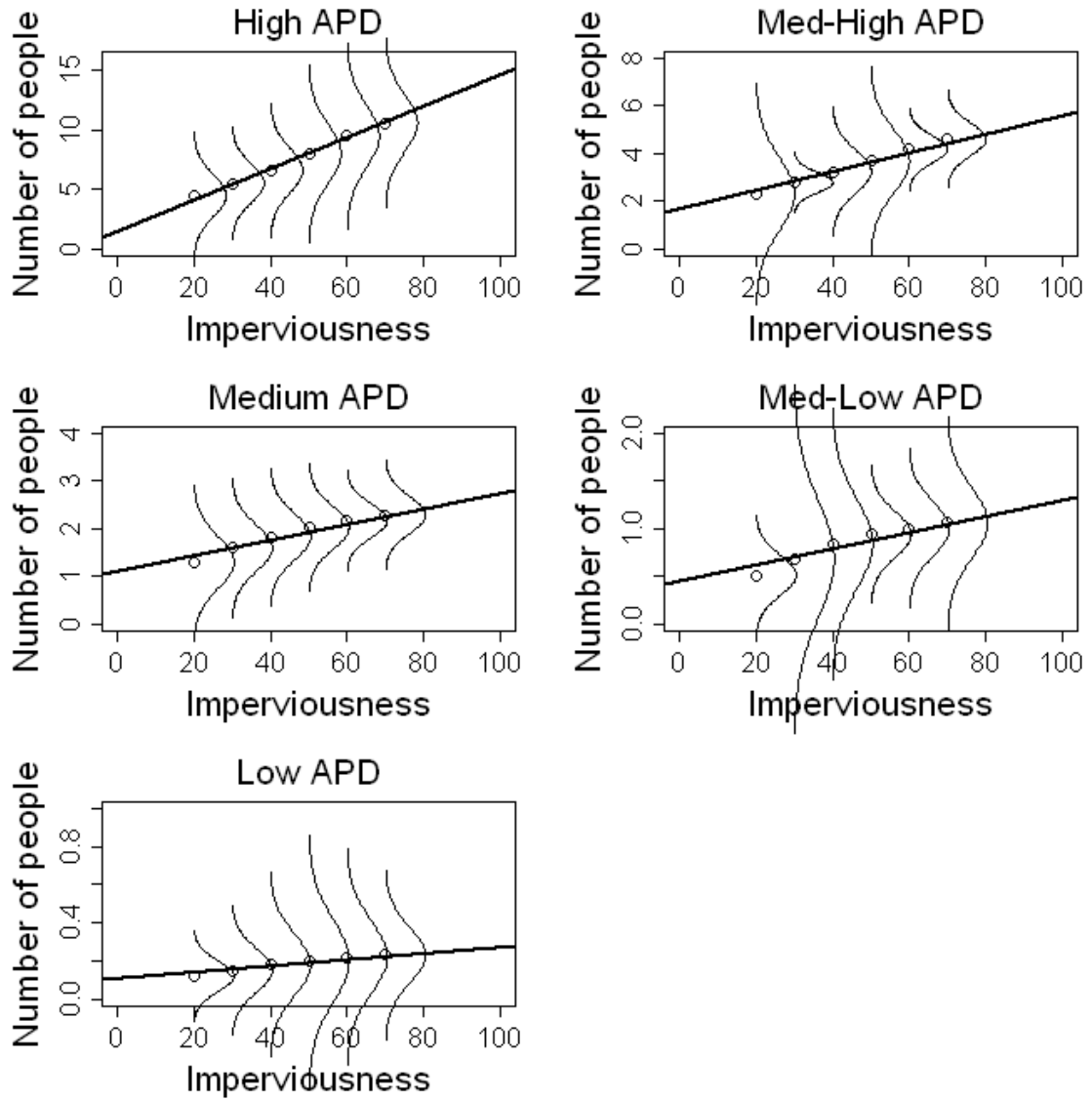


Figure 6. The distributions of population against percent of impervious surface class in each adjusted population density category based on the mean and standard deviation of population in Table 1.

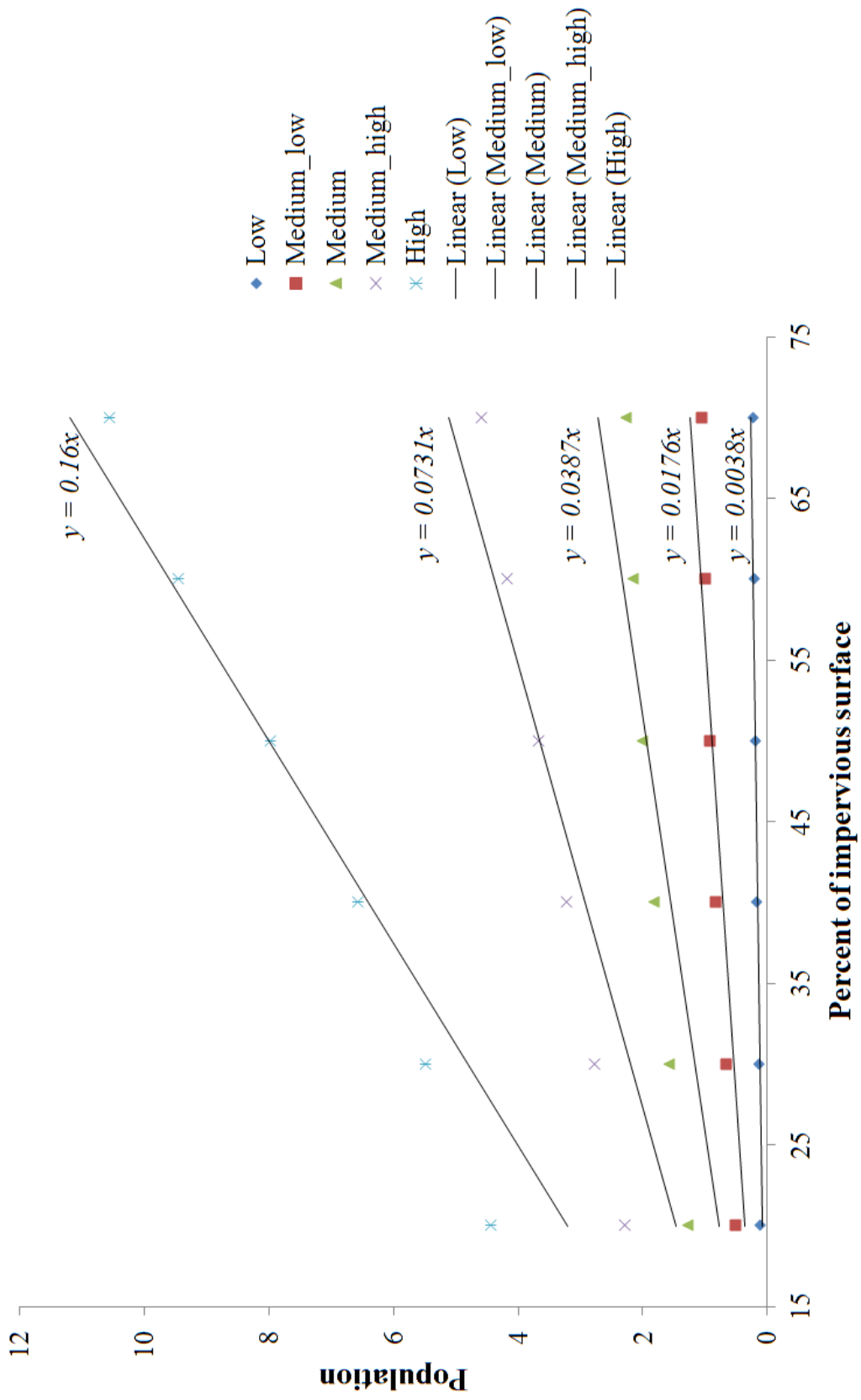


Figure 7. Regression relationships between population and impervious surface for blocks of different adjusted population density.

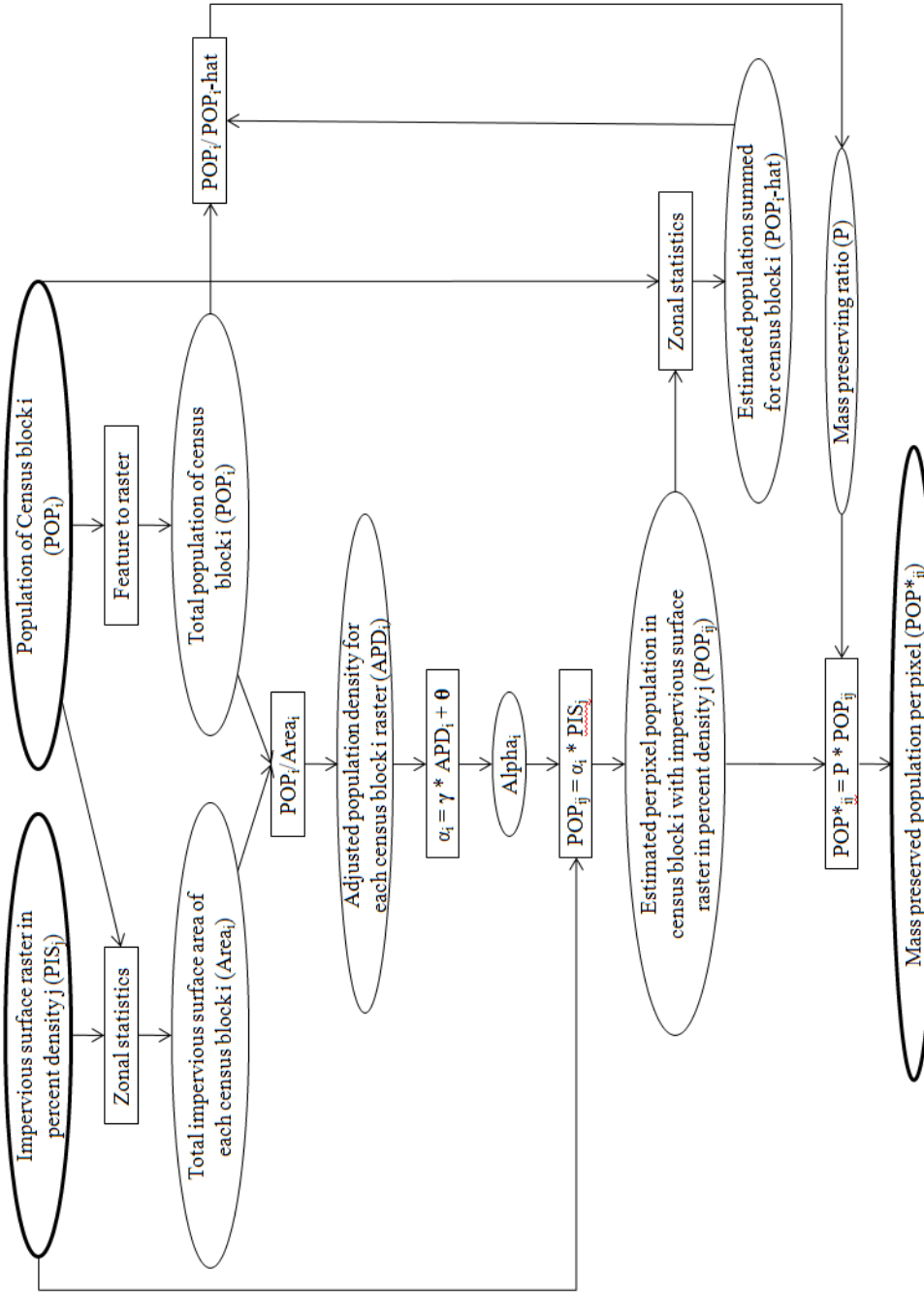


Figure 8. GIS model diagram for calculating population estimates based Census population and percent of impervious surface plus four unique coefficients of γ , θ , κ , and λ derived from Missouri, USA.

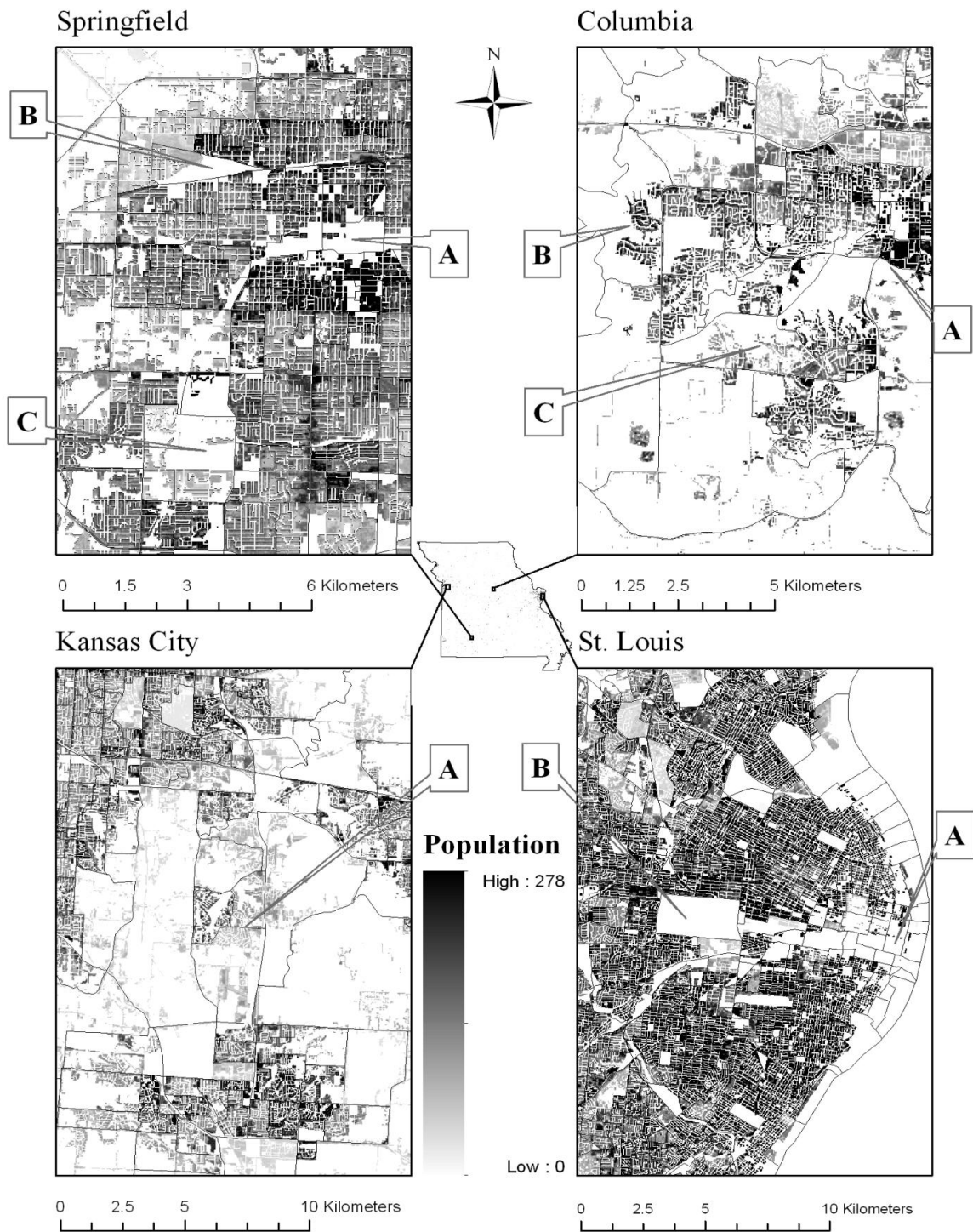


Figure 9. Per-pixel population for Missouri, USA with four panels magnified for detail with the open space indicating no population and darker color indicating more population.

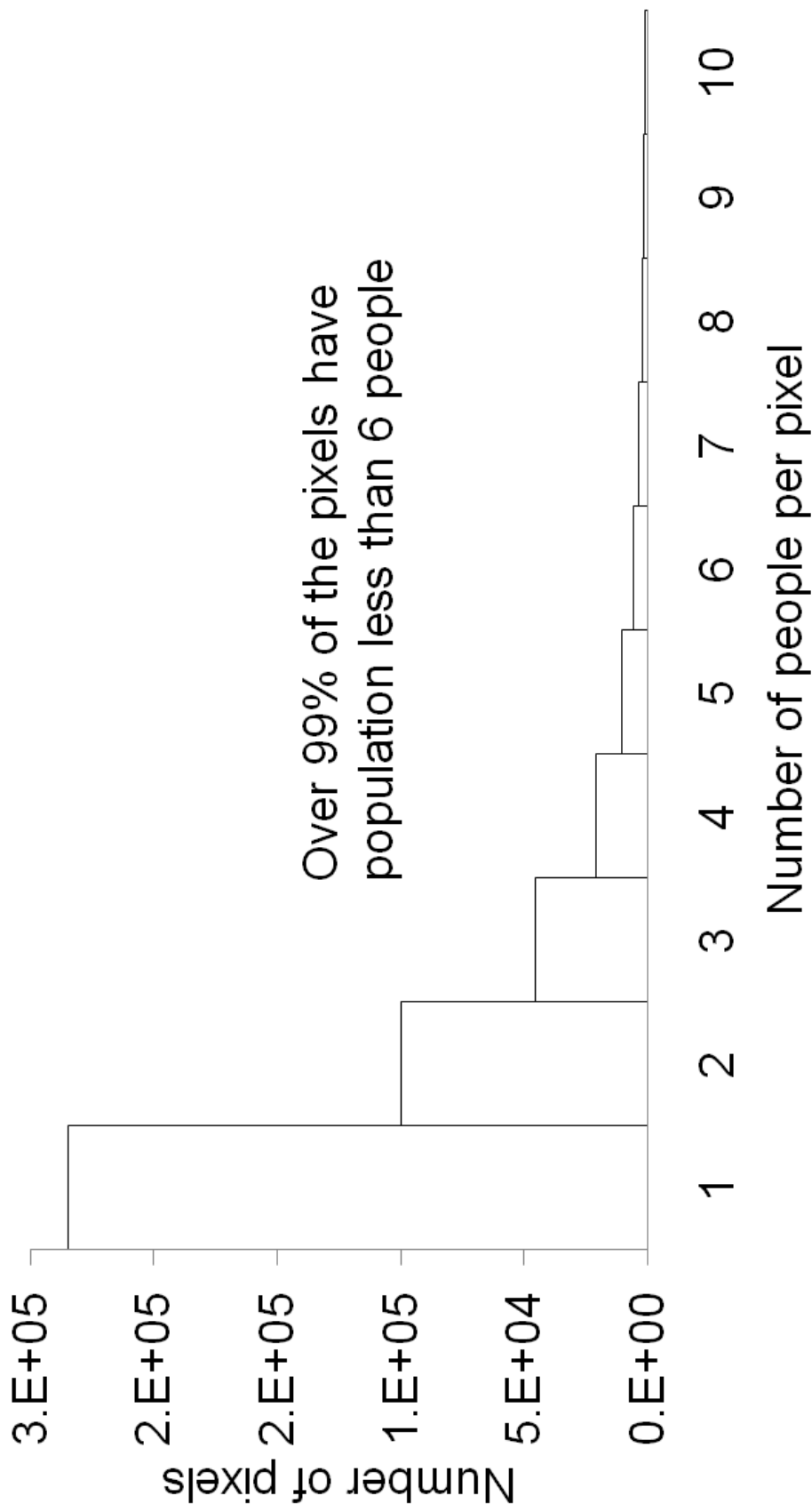


Figure 10. Histogram of number of people per pixel for the whole state of Missouri, USA excluding pixels with zero population.

Chapter III. A pixel-level approach of GIS simulation of urban growth from historical impervious surface and population in Jackson County, Missouri

Abstract

This research analyzes the historical urban growth for the two decades of 1980s and 1990s in three Missouri counties: Jackson, Greene and Boone. Historical urban growth was coupled with various predictor variables to investigate their influences on urban growth processes. The knowledge derived from the analysis was then used to design a GIS-based urban growth model. A holistic modeling approach is often inadequate for characterizing the complex nature of urban systems. To address this issue, a flexible modeling approach was developed using modules to represent different components of urban growth processes. The model's structure ensured that each individual module could be updated and modified independently, and allowed for the addition of new modules. The model's primary module for urban growth simulation was built using a rule-based framework that incorporated multi-criteria evaluation (MCE). This module was designed to be calibrated using historical urban growth in order to simulate future urban growth which is represented by pixel level imperviousness. After analyzing historical urban growth in the selected counties, the model was used to simulate pixel level imperviousness for the years 2010, 2020 and 2030. The modeling framework presented in this study is not reliant on long term historical datasets, and is thus transferrable to other study areas.

Keywords: Impervious surface; urban growth simulation; GIS

1. Introduction

Urban development in the United States since the 1950s has been dominated by the shift of residential, commercial, and industrial land uses to the urban fringe which stimulates the conversion of rural landscape near major metropolitan areas into low-density residential subdivisions together with strip commercial developments (Radeloff, 2005). Situated in the Midwestern portion of the United States, Missouri reflects a full range of urban and rural sprawl characteristics that include large metropolitan centers (Kansas City, St. Louis) and numerous small to mid-sized cities and towns (Zhou et al., 2012). The rapid pace, broad scope, and complex spatial dynamics of urban growth challenge city planners, resource managers and decision makers to address the cumulative effect of ecosystem degradation (Fang et al., 2005; Lathop et al., 2007). Common questions researchers and decision-makers face are: How quickly will urbanization occur? What will be the spatial extent and density of future urban growth? Unfortunately, there are no definitive answers to these questions. Without the ability to simulate urban growth with reasonable accuracy, developing future urban growth and land use policies is difficult. By making robust urban growth predictions available to decision makers, they can better understand the dynamics of urban systems to make informed policy decisions.

Land use change modeling and urban growth prediction dates back to 1950s, however the utility of early models was limited. It was not until the advent of modern computers in the 1990s and advances in geographic information systems (GIS) that urban growth modeling was rigorously revived (Wegener 1994). During recent years, land use change and urban growth models have become a very important tool for city planners, economists, ecologists and resource managers to support decision making. There are two

approaches towards land use change studies. The first approach focuses on the specific mechanisms that drive land use change and urban growth in a particular city or region. The site specific approach often uses statistical methods such as logistic regression, with coefficients derived for a given study area (Huang et al., 2009). In the second approach transferrable land use change models that can be calibrated in a variety of study areas are developed. Examples of transferrable land use change models include: Land Use Change Analysis System (LUCAS) (Berry et al., 1996), Land Transformation Model (LTM) (Pijanowski et al., 1997; Pijanowski et al., 2000, Pijanowski et al., 2002), Urban SIMulation (UrbanSIM) (Waddell, 1998), Slope, Land use, Exclusion, Urban extent, Transportation, Hillside (SLEUTH) model (Clarke and Gaydos, 1998), and California Urban Future (CUF) (Landis 1995). While these approaches differ in terms of transferability, both may contain aspects of certain widely used model algorithms such as: multi-criteria evaluation (MCE) (Jiang and Eastman, 1999), cellular automata (Wu, 1996; Clarke et al., 1997), and Markov Chain (Zhang, 2011).

Many land use change models emphasize on rigorous model calibration, are heavily study area and data dependent, and may require deep mathematical and statistical understanding in order to be used. Such a high technical threshold is impractical for city planners, resource managers and decision makers to overcome. Thus, these approaches are still mostly restricted to academia (Allen and Lu, 2003). The MCE approach, on the other hand, is much easier to understand and implement; it simply evaluates the influence of each predictor variable independently and assesses their impact on urban growth. Predictor variables can then be weighted accordingly to predict future urban growth.

Such an approach can fit different study areas easily which ensures the transferability of the model.

Each of the land use change models mentioned above has its own merits, but they also have drawbacks that precluded their applicability in this research. The LUCAS model is very desirable due to its modular structure and the fact it uses open source GIS software (GRASS). The modular structure ensures that different physical processes related to land use change and urban growth are modeled separately, thus making the processes easier for users to understand. Another benefit of the modular structure is expandability; new modules can be added as better understanding of the system is achieved. However, LUCAS employs a patch-based simulation which is not realistic compared to actual land use change and urban growth. The LTM model is GIS based and relies on artificial neural network (ANN) routines and a MCE approach to identify influential land use change factors and weight them accordingly. However, the demand on specific datasets such as high-quality vantage points is difficult to acquire especially for model applications in large areas (Agarwal, 2002). The UrbanSIM model excels in the incorporation of public policies in the modeling process which considers the human aspects, the behavior of policy makers, planners and the general public. However, this model relies on vector-based datasets, which can be difficult to obtain for certain study areas. The SLEUTH model is unique in that it captures urban patterns through the application of four urban land use change types: spontaneous growth, new spreading center growth, edge growth, and road-influenced growth. These four growth types are applied sequentially during each growth cycle, and are controlled by the interactions of five growth coefficients: dispersion, breed, spread, road gravity and slope. However,

SLEUTH lacks drivers of urban growth such as population and economic growth. The CUF model utilizes population projections for new parcel allocation and incorporates incentives for adjacent development by annexation. However, this model is also vector based which has the similar drawbacks with census data such as change of boundaries over time and the modifiable areal unit problem (Openshaw, 1983). Last but not least, the aforementioned models use a black-box approach which prevents the user from making changes to the model other than parameter modifications. Since decision makers require higher model flexibility for practical application purposes, a more open model framework is desired. Moreover, most land use change models cannot be executed on standard GIS platforms (e.g. ArcGIS) which are widely used in academia, government, and industry. Thus, it would be beneficial to develop land use change and urban growth models that can be deployed on widely used geospatial platforms, such as ArcGIS.

When majority of the attention was paid to the test of different approach and land use change model development, relatively less was done to polish the datasets used for land use change and urban growth studies. One of the problems with model inputs is the lack of consistent methodology to measure sprawl due to the differences in defining this phenomenon (Batisani and Yarnal, 2009). This lack of understanding in the pattern and processes of urban growth in a landscape is stemmed from the inconsistent definition of urbanized areas (Tsai, 2005). Census bureau has four different definitions related to urbanized areas: Census Designated Place, Consolidated City, Incorporated Place, and Urbanized Areas. All of them are vector datasets delineating urbanized areas with polygon based on different criteria. They are all representing cities with different spatial extent for different research purpose. However, none of them is capable of describing the

spatial distribution and density of urbanized areas. A very important feature of urban sprawl is the low density growth of residential areas. However, most urban models are not capable of illustrating the density of growth. Without the density information, the urban model is not getting detailed urbanization information as input. Thus, the outputs of the urban models are going to be less useful for decision makers who are more interested with the density rather than the extent of urban growth. In light of this problem, a more consistent measure of urbanized area is necessary. Recently, impervious surface derived from Landsat ETM+ imageries emerged to be a promising candidate. The density, distribution, areal extent and temporal change of impervious surface, is considered emblematic of human-related effects in both urban and rural areas (Arnold and Gibbons, 1996; Powell et al., 2008). Impervious surface has distinct man-made features and can be detected and quantified by remote sensing to reflect anthropogenic development over time (Alberti et al., 2008, Zhou et al. 2012). Impervious surface also provides information on urban morphology (Ji and Jensen, 1999) and urban morphology information assists with evaluating outcomes of zoning and planning.

This research builds upon previous research to develop a new land use change and urban growth model that is open, modulated, and GIS based. This model platform utilizes pixels as basic modeling unit suitable for universal application in vastly different areas. The driver identified in this model is population growth induced impervious surface growth. Other predictor variables used are commonly available pixel based datasets (e.g. elevation, slope, road network, and water body). There are four major objectives in this research. The first objective is to build several GIS analysis modules (terrain analysis, distance analysis, demand analysis, suitability analysis and urban

growth). The second objective is to study the relationship between the explanatory drivers of urban growth with historical urban growth through MCE to determine the influence of each explanatory driver. The third objective is to calibrate the urban growth model using weights derived from MCE as well as human interaction until the simulated historical growth is consistent with actual historical growth. The fourth objective is to generate future urban growth with the calibrated model.

2. Methodology

2.1. Study area

This study utilized three counties: Jackson, Greene and Boone each contained a large metropolitan, medium metropolitan and a small city respectively to proof the effectiveness of the model on cities of various sizes. Jackson County encompasses the majority of Kansas City metropolitan area in the Missouri part of the city. Jackson County has a total area of 1595.77 km², inside which Kansas City was ranked high among the sprawl-threatened metropolitan areas in the United States (Ewing et al., 2002). Jackson County has witnessed significant urban growth in the last few decades mostly from the growth of Kansas City. Impervious surface has increase 6.99 km² with an impact area of 14.59 km² in the 1980s and 18.53 km² with an impact area of 38.51 km² in the 1990s (Zhou et al., 2012). In the mean time the total population for Jackson County has decreased from 668,893 in 1980 to 633,151 in 1990 and recovered to 654,856 in 2000 (U.S. Census Bureau). As a very typical county of the state of Missouri, Jackson County is generally characterized by rolling hills and open plains. Because of the suburbanization, the county has experienced significant alteration of its natural landscape into urban buildup in the form of impervious surface. Greene County encompassed the

city of Springfield which is identified as one of the four medium metropolitan cities in the state of Missouri that fueled the rapid urban growth in the 1990s (Brookings Institution, 2002). Greene County has a total area of 1,754.13 km². Impervious surface has increased 3.41 km² with an impact area of 6.37 km² in the 1980s and 18.94 km² with an impact area of 35.25 km² in the 1990s (Zhou et al., 2012). In the mean time the total population for Greene County has maintained an increasing trend from 185,302 in 1980 to 207,949 in 1990 and to 240,391 in 2000 (U.S. Census Bureau). Situated on the Springfield plateau, Greene County is generally very flat with no significant resistance towards urban growth. Thus, we have witnessed some tremendous growth in the last two decades. Boone County encompassed the city of Columbia which is one of the fastest growing small cities in the state of Missouri (Brookings Institution, 2002). Boone County has a total area of 1789.22 km². Impervious surface has increased 3.19 km² with an impact area of 6.13 km² in the 1980s and 4.30 km² with an impact area of 8.14 km² in the 1990s (Zhou et al., 2012). In the mean time the total population for Boone County also maintained a growing trend from 100,376 in 1980 to 112,379 in 1990 and to 135,454 in 2000 (U.S. Census Bureau). The study of these three counties may provide a framework for other counties in the state of Missouri to examine the interaction between the natural landscape and driving forces for urbanization.

2.2. Data preparation

Impervious surface is the primary modeling component in this research. Sub-pixel classifier (SPC) in ERDAS IMAGINE software was used to derive 30 m by 30 m resolution imperviousness per pixel using Landsat Thematic Mapper (TM) imagery. The classification scheme for imperviousness consisted of 9 classes and preserved a 10%

increment between classes except from the 0 to 20% range, where 0–20% was classified as 0%, and 90 – 100%, which was classified as 100%. The difference in increment at the beginning and end of the range was due to the software limitation of the SPC that it cannot identify material covers less than 20% of a pixel. The remaining classes followed 10% increments where 20–30% classified as 30% up to 80–90% classified as 90%. Since 20% of a pixel is equivalent to 180 m², most single family houses plus driveway will have a footprint larger than 180 m². Thus, such a limitation of the software is not going to hurt the accurate mapping of population based on impervious surface. In a preliminary research, imperviousness per pixel has been derived for the whole state of Missouri for the year 1980, 1990 and 2000 (Zhou et al., 2012).

Beside the primary modeling unit, there are many predictor (independent) variables. Since this research is precursor and foundation to a statewide study, the availability of statewide dataset is a crucial criterion in choosing the candidates. Considering the data availability and previous research, elevation, slope, waterbody, road network, urban center and historical impervious surface growth are chosen as the predictor variables in this research (Poelmans and Van Rompaey, 2009). More predictor variables can be easily added as model input once available. Elevation data is obtained from Missouri Spatial Data Information Service (MSDIS) in the format of 30m resolution raster (hereafter referred to as ‘DEM’). Slope data is calculated from the elevation data using Slope function in ArcGIS while retaining the same resolution (hereafter referred to as ‘slope’). Waterbody is obtained from MSDIS as the overall hydrology combining rivers, streams, lakes and ponds (hereafter referred to as ‘water’). An alternative

waterbody data is obtained by extracting major rivers from the hydrology dataset (hereafter referred to as ‘major water’).

Road network data from 1992 and 2000 were obtained from U.S. Census website in the topologically integrated geographic encoding and referencing (TIGER) road centerline format. The TIGER road centerline data consist of polylines at a scale of 1:100,000 with codes for road types. Each road type can be assigned a weight in the modeling process to imply their level of importance towards urban growth (Clarke and Gaydos, 1998). However, due to the empirical nature of weights for different road types, equal weights were used in one road network data (hereafter referred to as ‘road’). And major roads were extracted as another road network data to provide an alternative (hereafter referred to as ‘major road’).

Urban center is a very important variable for urban modeling, which is used in almost all urban modeling endeavors. However, it is by far the most difficult predictor variable to obtain. Because it is not readily available and the entire collection of Census defined urban boundaries are not satisfactory in generating urban centers for satellite cities and leapfrog development surrounding metropolitans. Thus, a morphological operation was used on impervious surface to achieve core urban areas through dilation and erosion. The urban cores are then subject to a geometric mean center operation which outputs the centroids of the urban core polygons which are used as a predictor variable in this research (hereafter referred to as centroid). A graphic illustration is also provided to show the derivation of core urban areas using impervious surface in the study area of Jackson County (Fig. 1). To illustrate the superiority of urban core in terms of centroids derivation, Census designated place (CDP), a very popular urban boundary

definition (Butzler et al., 2011), as well as Census designated urbanized area, another common urban boundary definition, are included for comparison. Census designated places (CDPs) are delineated for each decennial Census as the statistical counterparts of incorporated places (U.S. Census Bureau). An urbanized area (UA) consists of densely settled territory that contains 50,000 or more people (U.S. Census Bureau). According to the definitions, both urban boundaries are defined based on population but with different purposes. The urban boundaries derived by impervious surface are used in this research because not only of its association with population, but also of its actual spatial distribution and density that is geographically more accurate in defining the actual urbanized area. Figure 1 also illustrates that the centroids generated by urban core are located right in the middle of all sizable developments. On the other hand, centroids derived by both Census designated place and urbanized area are either too numerous or too clustered to show the actual growth center (Fig. 1).

Historical impervious surface growth is obtained by subtracting 1980 imperviousness by 1990 imperviousness and 1990 imperviousness by 2000 imperviousness. All the feature datasets are then converted to 30m by 30m resolution raster through feature to raster tool in ArcGIS. The use of 30m by 30m resolution for all the analysis dataset is on one hand determined by the resolution of satellite image derived imperviousness and on the other hand the recent trend of using finer grids for urban growth modeling and the availability of more powerful computers. Although previous researches have outlined the benefit of different modeling units such as parcels (Landis, 1994). The benefit of using raster based modeling approach far outweighs the use of parcels. For one thing, parcel data is not available for most States; another issue is parcel

boundaries may change overtime. Thus, more recent researches chose to use 30m by 30m raster as basic modeling unit (Deal and Schunk, 2004; Fang et al., 2005; Batisani and Yarnal, 2009; Jokar Arsanjani et al., 2012). Moreover, raster data can be easily aggregated to any geographical unit (hydrologic boundaries, administrative boundaries and even parcels) allowing higher flexibility in model output utility.

Given the fact that not all predictor variables are created for this particular study, data preprocessing is necessary to ensure they are spatially and temporally consistent. Elevation, slope and waterbody do not change dramatically over time. Thus, no further preprocessing is necessary. For source data collected in years other than the three baseline years of 1980, 1990 and 2000, a linear interpolation is necessary to estimate the values for the desired year provided the availability of multiple road network datasets (Allen and Lu, 2003). However, since the TIGER data is in vector format, thus the interpolation is not very convenient compounded by the reality that TIGER data prior to 1992 is not available. So imperfect data is still used in this research considering road network is very important predictor variable for urban growth models.

2.3. Model design

The design principle is to build a simulation model instead of a forecasting model. The simulation unit of the model is each county in the state of Missouri. In this pilot study, only a few Counties are illustrated. The rationale to have county boundaries as the basic modeling unit is that decision making is usually made at the political boundary level. City boundaries are not used because a broader extent such as county provides the spatial extent to which the urban area expands.

A rule-based model is used instead of the more popular logistic regression model, because the latter relies entirely on historical data for calibration and simulation. For example, the logistic regression approach is not capable of incorporating other factors, new growth policies such as growth boundaries, which will have a bearing on the future urban growth but are not responsible for the spatial pattern of historical urban growth. In a rule-based model, these factors can be easily incorporated. Moreover, the effectiveness of logistic regression approach is not very stable with a success rate ranging from less than 30% to more than 90% depending on the study area (Allen and Lu, 2003). Another very important feature of rule-based model is less computational intensive than a logistic regression model. Thus, it will be more accessible to decision-makers who are less familiar with the technical and statistical aspect of more complicated models such as logistic regression, cellular automata or Markov Chain models. Finally, a rule-based model is very easy and convenient to implement in the ModelBuilder environment of ArcGIS.

This study used an open and modulated modeling approach, integrating several individually developed modules to accomplish the urban growth simulation task at pixel level. The rationale to take this specific approach is to make maintenance, update, and expansion of simulation model easier than a holistic model. The justifications to use multiple modules instead of a big model include: first, limited understanding of the urban systems; second, individual processes related to urban growth may follow different mathematical or physical processes that can be analyzed more effectively individually (Landis, 1994); third, the modules can be easily modified and improved to meet future

needs, and new modules can be added to incorporate more aspect of urban systems upon acquisition of new knowledge or expert input.

As shown in figure 2, the conceptual model framework involves five sub modules. Distance Analysis Module calculates the Euclidean distance between all the undeveloped pixels on the landscape against all distance based predictor variables (in raster format) and then performs an overlay analysis between historical impervious surface growth and distance based predictor variables. Terrain Analysis Module performs an overlay analysis of historical impervious surface growth and its relationship to terrain based predictor variable. Transition Probability Module combines together the output of distance analysis and terrain analysis module to analyze the effect of various predictor variables on historical urban growth. It then assigns weight to each predictor variable and then combines them together to form the final raster transition probability surface which contains the probability of each non-impervious surface pixels being converted to impervious surface. Demand and Scenario Module determines the total urban growth demand based on historical population growth as well as specified urban growth scenarios. Urban Growth Simulation Module utilizes the output of transition probability module and demand and scenarios module to simulate urban growth through calibration and prediction. Calibration is done by comparing simulated historical growth with actual historical growth. If the calibration failed to pass the ROC criteria, the transition probability surface will be regenerated with different weights. Once the calibration is passed, the same weights will be used to generate a new transition probability surface for future urban growth prediction.

2.4. Model structure

Both distance and terrain analysis module will perform normalization to all the predictor variables changing their value range to between 0 and 100 following the formula (Eq. [2]):

$$N = \text{INT}[100(V - V_{\min})/(V_{\max} - V_{\min})] \quad (1)$$

Where N is the normalized value, V is absolute value, V_{\min} is minimum value and V_{\max} is maximum value and the function INT convert all decimal to integer. The purpose of normalization is to ensure the model outputs of different study areas can be compared in terms the underlying characteristics instead of the absolute values.

Transition probability module utilizes a rule-based modeling approach which uses MCE derived statistical results to reclassify normalized predictor variables into transition probability surface with higher value meaning more likely to transition into urbanized pixel. The transition probability surfaces are then combined with weights determined by expert inputs to determine the overall transition probability for the study area. The final transition probability surface is then generated by applying a mask of unsuitable areas for urbanization (Fig. 3).

Demand and scenario module utilizes different scenarios other than the default as specified by historical trend. Growth scenarios are very important for simulation models because the actual future urban growth is not predictable. But we could use different scenarios for decision making purpose in order to prevent the fruition of undesirable development outcomes. Growth scenarios could also be expressed as policy constraints, growth rules, growth rates, or even to set up growth boundaries (Allen and Lu, 2003). Different growth ratios will be used to determine the scenarios for future urban growth. Growth ratio is also called sprawl index or sprawl scatter index and is defined as the ratio

of urban population growth versus urban area growth measured as the total imperviousness growth. It can be defined using the following formula (Eq. [2]):

$$r = [(P_1 - P_0) / P_0] / [(I_1 - I_0) / I_0] \quad (2)$$

Where r is the growth ratio; P_0 is the starting population; P_1 is the ending population; I_0 is the starting total imperviousness; and I_1 is the ending total imperviousness. The simulated total imperviousness growth is determined by the formula (Eq. [3]):

$$\Delta I = I_1 - I_0 = I_0(A_1 - A_0) / rA_0 \quad (3)$$

Different growth ratios were chosen to implement different growth scenarios for two reasons. First, previous researches have indicated population growth to be the fundamental driving force for future urban growth (Barlett et al., 2000; Heimlich and Anderson, 2001; Johnson and Beale, 2002; Schnaiberg et al., 2002). Second, the relationship between population and imperviousness has been researched in a precedent study (Zhou et al., under review)

2.5. Model calibration

The calibration of the transition probability module is done by combining the output of the Transition probability module and historical urban growth in a model simulation run in the urban growth simulation module. The simulated historical urban growth is then compared with the actual urban growth to evaluate the output of transition probability module. There are quantification errors and locations errors for the simulated urban growth pixels. Due to the design of this simulation model, quantification errors can be ignored. So the accuracy assessment will focus on the location errors. The ROC method will be used to assess the performance of the transition probability as compared to a random decision surface (Pontius and Schneider, 2001). Two raster maps are needed to

calculate the ROC curve: (1) the suitability map that illustrate the relative likelihood of each pixel undergoing a transition from undeveloped to developed, and (2) a map of actual urban growth for the same timeframe of the simulation. The suitability map is the most appropriate candidate to calculate a ROC curve, because it is the easiest to understand that suitability map shows the priority in which pixels are selected to transition from undeveloped to developed. The ROC curves work the best with binary maps (i.e. developed and undeveloped). If more than two land-cover types are present, then a ROC curve can be created for each land-cover type (i.e. one land-type versus the rest). The first step in creating a ROC curve is to first slicing the suitability map into several percentile groups. One common slicing scheme is to assign 10% of pixels for each percentile group. Therefore, each of the 10 groups contains 10% of the pixels in the study area. An increase in number of groups increases accuracy of estimated ROC, but increases also the calculation complexity. If the evaluation result does not pass the standard established by the user, the weight factor for each predictor variables need to be changed. The default weights for each predictor variables are ones. It is preferable to have expert input on the weight factors. However, in case expert inputs are not available, a trial and error approach is used until the predetermined standard is reached. This process can be done interactively by overlaying historical urban growth with each predictor variable to find the ones with higher impact factor.

2.6. Model simulation

Urban growth simulation module serves two purposes: (1) for calibration runs, the random component is deactivated in order to have the highest validation accuracy (Fig. 4); (2) for simulation runs, the random component is turned on in order to capture the more

or less random aspect of the future urban growth. This module utilizes iterations to turn undeveloped pixel into urbanized pixel. At the end of each model iteration the module uses a Boolean logic to determine if more iteration is necessary based on the demand and scenarios module output of total urban growth. This density of each impervious surface pixel is determined by the historical relationship with elevation and slope. If only location information is desired, the final output of this module can be reclassified into a binary raster with 1 indicating urban and 0 indicating non-urban. Regardless of the format, the final output of this module and the whole model can be used for land use decision making, urban growth policy testing, public education of the negative effect of urban sprawl and etc.

All of the modules described above are capable of processing raster datasets of various resolutions. These modules were developed using ESRI's ModelBuilder, an ArcGIS application. In ModelBuilder, the model is represented by a flux diagram in a graphic user interface that facilitates the creation, visualization, editing, and execution of geoprocessing workflows which can be shared, modified and reused in different geographic areas (Allen, 2011). A flowchart is presented here to illustrate all the major procedures in a model simulation run (Fig. 5).

3. Results

3.1. Pattern of historical impervious surface growth

Figure 6 shows the distance analysis module and terrain analysis module output maps. The impervious surface growths for two decades were compared against these maps to generate the statistical results. The general pattern of impervious surface growth versus

terrain is similar between 1980s and 1990s (Fig. 7). More land was consumed in the decade of 1990s compared to the 1980s. Moreover, impervious surface growth in the 1990s has consumed more high elevation land (Fig. 7A) as well as high slope land (Fig. 7B). Although a strong trend of slope resistance is preventing impervious surface growth encroaching into even higher sloped areas (Fig. 7B). The peaks for impervious surface growth occurred at similar ranges for both elevation (Fig. 7A) and slope (Fig. 7B). Similarly, distance measures were analyzed using historical impervious surface growth. The two distance measure of normalized distance to road and water are not used because of their high density distribution which leads to the impervious surface growths concentrated in a narrow band of values. Figure 8A has the most complicated trend of distribution due to the spatially uneven distributed centroids. Figure 8B is very intuitive in that it shows new urban growth are usually very close to the road network. In other words, undeveloped pixels that are close to the major highways are more likely to turn into developments. Figure 8C is even more extreme than 8B in that it shows majority of developments are very close to the most recent developments. More explicitly speaking, impervious surface increments in the 1980s are more closely related to the impervious surface of 1980 and impervious surface increments in the 1990s are more closely related to the impervious surface of 1990. Figure 8D is showing a slow but affirmative decrease in development as distance to major water increases. In other words, although the influence of water on impervious surface growth is not as immediate as historical impervious surface or road network, the influence is still clear enough that it can't be ignored.

3.2. Model calibration

Based on the statistic results of figure 7 and 8, all of the predictor variables were reclassified using the frequency of impervious surface growth. These reclassified transition probability surfaces for the decade of 1980s (Fig. 9) and 1990s (Fig. 10) are showing areas with high impervious surface growth in red and low growth area in green. These transition probability surfaces are summed with default weight to generate the total transition probability surfaces (Fig. 11). The default weights were chosen so that each transition probability surfaces is exerting similar amount of influence towards the total transition probability surface. Two total transition probability surfaces for the decades of 1980s and 1990s with historical impervious surface removed are produced for calibration using Jackson County as example (Fig. 11). Similar steps were taken for both Greene and Boone County with two more sets of total transition probability surfaces produced for comparison purpose. For calibration purpose, the historical growth scenarios are used for the decade of 1980s and 1990s to generate the suitability maps for three counties. These suitability maps are compared with the actual urban growth for two decades in these three counties to validate the effectiveness of the simulation model. Six ROC curves are generated based on the simulated historical growth (Fig. 12). The areas under the six ROC curves are ranged from 0.68 to 0.85 with a short span. In both decades, the ROC has an increasing trend from large metropolitan county (Jackson) to medium metropolitan county (Greene) to small city county (Boone) with the decade of 1990s' ROC having slightly higher values (Fig. 12). Statistically, ROC above 50% is better than random. Similar research has reported ROCs ranging from 65 to 70% in a different study area (Pontius and Schneider, 2001) which proved the performance of the simulation

model satisfactory. Thus, the same approach can be applied to predict future urban growth under the same scenario of historical urban growth.

3.3. Future impervious surface growth prediction

For large metropolitan area (Jackson County in this study), potential urban development mostly circled around the leap-frog development from the satellite cities of Kansas City metropolitan area with a high likelihood to merge with the core Kansas City urban area to form an even bigger metro (Fig. 13). According to this simulation, the total population for Jackson County will increase by 21,705 for every time step of 10 years with a net growth of 65,115. The total population of Jackson County will reach 719,971 in the year 2030 based on historical population growth trend. Similarly, the urban growth for each decade is measured at 18.53 km² in terms of impervious surface growth with a potential impact area of 38.51 km². By 2030, the total urbanized area of Jackson County will reach 250 km² in total impervious surface with a potential to impact about 500 km² of land which is near a third of the total land area of Jackson County. If the growth rate continues, the entire area of Jackson County will be developed in less than 250 years considering areas that are not suitable for development. All of the above projections are based on the same growth rate during the decade of 1990s. In light of the fact that urban growth is considerably faster in the 1990s than the 1980s, a possible exponential growth trend will consume the open land in Jackson County even faster.

In medium sized metropolitan cities (Greene County in this study), potential urban development concentrated around the urban fringe of the city of Springfield and along the major highways (Fig. 14). According to this simulation, the total population for Greene County will increase by 32,442 for every time step of 10 years with a net growth

of 97,326. The total population of Greene County will reach 337,717 in the year 2030 based on historical population growth trend. Similarly, the urban growth for each decade is measured at 18.60 km² in terms of impervious surface growth with a potential impact area of 35.20 km². By 2030, the total urbanized area of Greene County will reach 160 km² in total impervious surface with a potential to impact about 300 km² of land which is near a sixth of the total land area of Greene County.

In small cities (Boone County), potential urban development concentrated mostly in the northwest and west region and scattered around southwest, southeast and northeast regions of the city of Columbia. Some rural urban growth can also be spotted in the northeast and southeast corner as well as west side of Boone County (Fig. 15).

According to this simulation, the total population for Boone County will increase by 23,075 for every time step of 10 years with a net growth of 69,225. The total population of Boone County will reach 204,679 in the year 2030 based on historical population growth trend. Similarly, the urban growth for each decade is measured at 4.23 km² in terms of impervious surface growth with a potential impact area of 8.10 km². By 2030, the total urbanized area of Boone County will reach 55 km² in total impervious surface with a potential to impact about 100 km² of land.

4. Discussion

The ultimate purpose of building a simulation model is to apply it towards decision making. A useful urban growth simulation model should eventually be used by urban planners and policy makers. The biggest reason that urban growth simulation models are rarely used by policy makers and urban planners and only circulated in the field of academia is because most models are too complicated to use. Take the very population

logistic regression approach as an example which was implemented in most urban growth models, the derivation of model coefficients are too time-consuming and statistically demanding. One misstep in the data collection or preprocessing stage will lead to the coefficients that are against common sense and even ridiculous in certain cases. Distance to urban centers, elevation, distance to roads and distance to streams are considered very important predictor variable as a consensus among urban growth modelers. However, the coefficients of these predictor variables, according to a recent research, are so small that the effects of these predictor variables are negligible (Jokar Arsanjani et al., 2012). Another very important reason to explain the unflattering popularity of urban growth model is that most model frameworks focused more on model structure design but neglected the importance of data preprocessing which might be more important than the model structure. As illustrated in this research the derivation of growth centroids is a very good example of outlining the procedures to prepare predictor variables that are more likely to generate more meaningful results.

It may be argued that a rule-based model is less scientific than a more rigorous deterministic model with statistics derived coefficients. However, people like policy makers and urban planners may have more “knowledge” of the urban systems than any outgoing urban growth models. Plus, knowledge from the experts could be used to guide smarter growth through a more environmental and ecological friendly way of urban development (Freilich, 2003). Moreover, humans have the tendencies to not follow the established common sense on building new urban areas. Thus, many new growths can only be linked to personal preference rather than the rules deducted from predictor variable evaluation. After all, humans are the underlying driving forces for all urban

growths and there is a certain stochastic components related to people's preference and decision making. Thus, a stochastic component is added to the urban growth simulation module to at least partly explain the stochastic nature of individual's decision making in terms of urban growth preference.

This research establishes a solid framework for future urban growth research as well as providing a preliminary tool for decision making in terms of future urban growth. However, it still has constraints and limitations. The biggest limitation is the absence of a macro-economic module that can better predict future population demographics by inferencing the supporting capacity of local economy in order to more scientifically calculate the fluctuation of population instead of using the historical trend. Another limitation of this modeling approach is the inability to link growth scenarios to actual growth policies. In this research, the historical development density is used in absence of the knowledge of future growth density. Default scenarios could be used to give a range of variability for decision making purpose. However, unless the physical meaning of development density is defined, this issue will always be a limitation for urban growth models. Other minor limitations include but are not limited to predictor variable accuracy including spatial and temporal consistencies. The most important model input in this research is the historical impervious surface which is derived by satellite image and will subject to classification accuracy. Due to the time frame chosen by this research, some predictor variables may not be available at certain fixed time steps. Either data interpolation is used to alleviate the problem, or the less than perfect data will be used when interpolation is not feasible.

Finally, it is very important to work with decision makers and urban planner such as state and city agencies in charge of growth management to further develop this model provided with their expertise stemmed from previous management experience on urban growth. At the end of the day, a model has to be used to show its value. And only through practical applications can a theoretical models be updated regularly and improved.

5. Conclusion

In this research, an open, rule-based, modulated, GIS model was developed using ModelBuilder in ArcGIS. Multiple independent variables are identified and analyzed as the predictor variables of this model. Model calibration was done using MCE of historical urban growth. A trial and error approach was used to derive weights for each predictor variable in order for the simulated urban growth to be consistent spatially with the actual urban growth. The calibrated model is used to simulate future urban growth for 2010, 2020 and 2030 under the historical growth trend during the 1990s.

Urban growth simulation is a very complicated physical process that imposes a huge challenge to researchers who are trying to model and simulate future urban growth. With the help of a GIS model, the urban growth process can be quantified, analyzed and replicated to simulate future urban growth. The model framework and analysis workflows can have a huge impact on future urban growth management. Even under the conservative historical growth trend, it is still projected that a third of the land area of Jackson County will be developed by 2030. This model simulation result can be used to education citizens the negative effects of low density urban growth through statistics reporting and visual demonstration. More importantly, the simulated results can urge the

policy makers and urban planners to take a different route in urban growth management before everything get out of control. It is very imperative for researchers and policy makers to work together to link urban growth policies with actual model simulation output in order to build a more practical model that can be used in real life application.

References

- AGARWAL, C., GREEN, G. M., GROVE, J. M., EVANS, T. P. & SCHWEIK, C. M. (2002) A review and assessment of land-use change models: Dynamics of space, time, and human choice. *A Review and Assessment of Land-Use Change Models: Dynamics of Space, Time, and Human Choice*.
- ALBERTI, M. (2008) *Advances in urban ecology: integrating humans and ecological processes into urban ecosystems*. New York, NY, USA, Springer Science.
- ALLEN, D. W. (2011) *Getting to Know ArcGIS ModelBuilder*, ESRI Press.
- ALLEN, J. & LU, K. (2003) Modeling and prediction of future urban growth in the Charleston region of South Carolina: A GIS-based integrated approach. *Ecology and Society*, 8.
- ARNOLD JR, C. L. & GIBBONS, C. J. (1996) Impervious surface coverage: The emergence of a key environmental indicator. *Journal of the American Planning Association*, 62, 243–258.
- BARTLETT, J. G., MAGEEAN, D. M. & O'CONNOR, R. J. (2000) Residential expansion as a continental threat to U.S. coastal ecosystems. *Population and Environment*, 21, 429-468.
- BATISANI, N. & YARNAL, B. (2009) Urban expansion in Centre County, Pennsylvania: Spatial dynamics and landscape transformations. *Applied Geography*, 29, 235-249.
- BERRY, M. W., HAZEN, B. C., MACINTYRE, R. L. & FLAMM, R. O. (1996) Lucas: a system for modeling land-use change. *IEEE computational science & engineering*, 3, 24-35.
- BROOKINGS, I. (2002) *Growth in the heartland: challenges and opportunities for Missouri*. Washington, D. C., USA, Brookings Institution, Center on Urban and Metropolitan Policy.
- BUTZLER, S. J., BREWER, C. A. & STROH, W. J. (2011) Establishing classification and hierarchy in populated place labeling for multiscale mapping for the National map. *Cartography and Geographic Information Science*, 38, 100-109.
- CLARKE, K. C. & GAYDOS, L. J. (1998) Loose-coupling a cellular automaton model and GIS: long-term urban growth prediction for San Francisco and Washington/Baltimore. *International Journal of Geographical Information Science*, 12, 699-714.

- CLARKE, K. C., HOPPEN, S. & GAYDOS, L. (1997) A self-modifying cellular automaton model of historical urbanization in the San Francisco Bay area. *Environment and Planning B: Planning and Design*, 24, 247-261.
- DEAL, B. & SCHUNK, D. (2004) Spatial dynamic modeling and urban land use transformation: A simulation approach to assessing the costs of urban sprawl. *Ecological Economics*, 51, 79-95.
- EICHER, C. L. & BREWER, C. A. (2001) Dasymetric mapping and areal interpolation: Implementation and evaluation. *Cartography and Geographic Information Science*, 28, 125-138.
- EWING, R. (1994) Characteristics, causes, and effects of sprawl: A literature review. *Environmental and Urban Issues*, 21, 1-15.
- FANG, S., GERTNER, G. Z., SUN, Z. & ANDERSON, A. A. (2005) The impact of interactions in spatial simulation of the dynamics of urban sprawl. *Landscape and Urban Planning*, 73, 294-306.
- FREILICH, R. H. (2003) Smart growth in western metro areas. *Natural Resources Journal*, 43, 687-702.
- HEIMLICH, R. E. & ANDERSON, W. D. (2001) Development at the urban fringe and beyond: Impacts on agriculture and rural land. *Development at the Urban Fringe and Beyond: Impacts on Agriculture and Rural Land*.
- HUANG, B., ZHANG, L. & WU, B. (2009) Spatiotemporal analysis of rural-urban land conversion. *International Journal of Geographical Information Science*, 23, 379-398.
- JI, M. & JENSEN, J. R. (1999) Effectiveness of subpixel analysis in detecting and quantifying urban imperviousness from landsat thematic mapper imagery. *Geocarto International*, 14, 31-39.
- JIANG, H. & EASTMAN, J. R. (2000) Application of fuzzy measures in multi-criteria evaluation in GIS. *International Journal of Geographical Information Science*, 14, 173-184.
- JOHNSON, K. M. & BEALE, C. L. (2002) Nonmetro recreation counties: Their identification and rapid growth. *Rural America*, 17, 12-19.
- JOKAR ARSANJANI, J., HELBICH, M., KAINZ, W. & DARVISHI BOLOORANI, A. (2012) Integration of logistic regression, Markov chain and cellular automata models to simulate urban expansion. *International Journal of Applied Earth Observation and Geoinformation*.

- LANDIS, J. D. (1994) The California Urban Futures model: a new generation of metropolitan simulation models. *Environment & Planning B: Planning & Design*, 21, 399-420.
- LANDIS, J. D. (1995) Imagining land use futures: applying the California urban futures model. *Journal - American Planning Association*, 61, 438-457.
- LATHROP, R. G., TULLOCH, D. L. & HATFIELD, C. (2007) Consequences of land use change in the New York-New Jersey Highlands, USA: Landscape indicators of forest and watershed integrity. *Landscape and Urban Planning*, 79, 150-159.
- LO, C. P. & YANG, X. (2002) Drivers of land-use/land-cover changes and dynamic modeling for the Atlanta, Georgia metropolitan area. *Photogrammetric Engineering and Remote Sensing*, 68, 1073-1082.
- OPENSHAW, S. (1983) The modifiable areal unit problem. *CATMOG (Concepts & Techniques in Modern Geography)*, 38.
- PIJANOWSKI, B. C., BROWN, D. G., SHELLITO, B. A. & MANIK, G. A. (2002) Using neural networks and GIS to forecast land use changes: A Land Transformation Model. *Computers, Environment and Urban Systems*, 26, 553-575.
- PIJANOWSKI, B. C., GAGE, S. H., LONG, D. T. & COOPER, W. C. (2000) A land transformation model: Integrating policy, socioeconomic and environmental drivers using a geographic information system. *Landscape Ecology: A Top Down Approach*, 183-198.
- PIJANOWSKI, B. C., LONG, D. T., GAGE, S. H. & COOPER, W. E. (1997) A land transformation model: Conceptual elements, spatial object class hierarchies, GIS command syntax and an application to Michigan's Saginaw Bay Watershed. *Land Use Modeling Workshop*, Sioux Falls, SD, 3-5 June, available from 203 Forestry Building.
- POELMANS, L. & VAN ROMPAEY, A. (2009) Complexity and performance of urban expansion models. *Computers, Environment and Urban Systems*, 34, 17-27.
- PONTIUS JR, R. G. & SCHNEIDER, L. C. (2001) Land-cover change model validation by an ROC method for the Ipswich watershed, Massachusetts, USA. *Agriculture, Ecosystems and Environment*, 85, 239-248.
- POWELL, S. L., COHEN, W. B., YANG, Z., PIERCE, J. D. & ALBERTI, M. (2008) Quantification of impervious surface in the Snohomish Water Resources Inventory Area of Western Washington from 1972-2006. *Remote Sensing of Environment*, 112, 1895-1908.

- RADELOFF, V. C., HAMMER, R. B. & STEWART, S. I. (2005) Rural and suburban sprawl in the U.S. Midwest from 1940 to 2000 and its relation to forest fragmentation. *Conservation Biology*, 19, 793-805.
- SCHNAIBERG, J., RIERA, J., TURNER, M. G. & VOSS, P. R. (2002) Explaining human settlement patterns in a recreational lake district: Vilas County, Wisconsin, USA. *Environmental Management*, 30, 24-34.
- TSAI, Y. H. (2005) Quantifying urban form: Compactness versus 'sprawl'. *Urban Studies*, 42, 141-161.
- WADDELL, P. (1998) Oregon Prototype Metropolitan Land Use Model. *Proceedings of the Conference on Transportation, Land Use, and Air Quality*.
- WEGENER, M. (1994) Operational urban models: state of the art. *Journal - American Planning Association*, 60, 17-29.
- WU, F. (1996) A linguistic cellular automata simulation approach for sustainable land development in a fast growing region. *Computers, Environment and Urban Systems*, 20, 367-387.
- YU, J., CHEN, Y., WU, J. & KHAN, S. (2011) Cellular automata-based spatial multi-criteria land suitability simulation for irrigated agriculture. *International Journal of Geographical Information Science*, 25, 131-148.
- ZHANG, R., TANG, C., MA, S., YUAN, H., GAO, L. & FAN, W. (2011) Using Markov chains to analyze changes in wetland trends in arid Yinchuan Plain, China. *Mathematical and Computer Modelling*, 54, 924-930.
- ZHOU, B., HE, H. S., NIGH, T. A. & SCHULZ, J. H. (2012) Mapping and analyzing change of impervious surface for two decades using multi-temporal Landsat imagery in Missouri. *International Journal of Applied Earth Observation and Geoinformation*, 18, 195-206.

Tables

Table 1. Model simulation validation for the decade of 1980s and 1990s presented as (%) error.

Model validation	1980s	1990s
<i>Omission error</i>		
Urban (simulated as non-urban)	57.55	51.23
Non-urban (simulated as urban)	0.95	2.75
<i>Commission error</i>		
Urban (simulated as non-urban)	54.96	50.61
Non-urban (simulated as urban)	1.06	2.82
<i>Overall error</i>	1.97	5.27

Figures

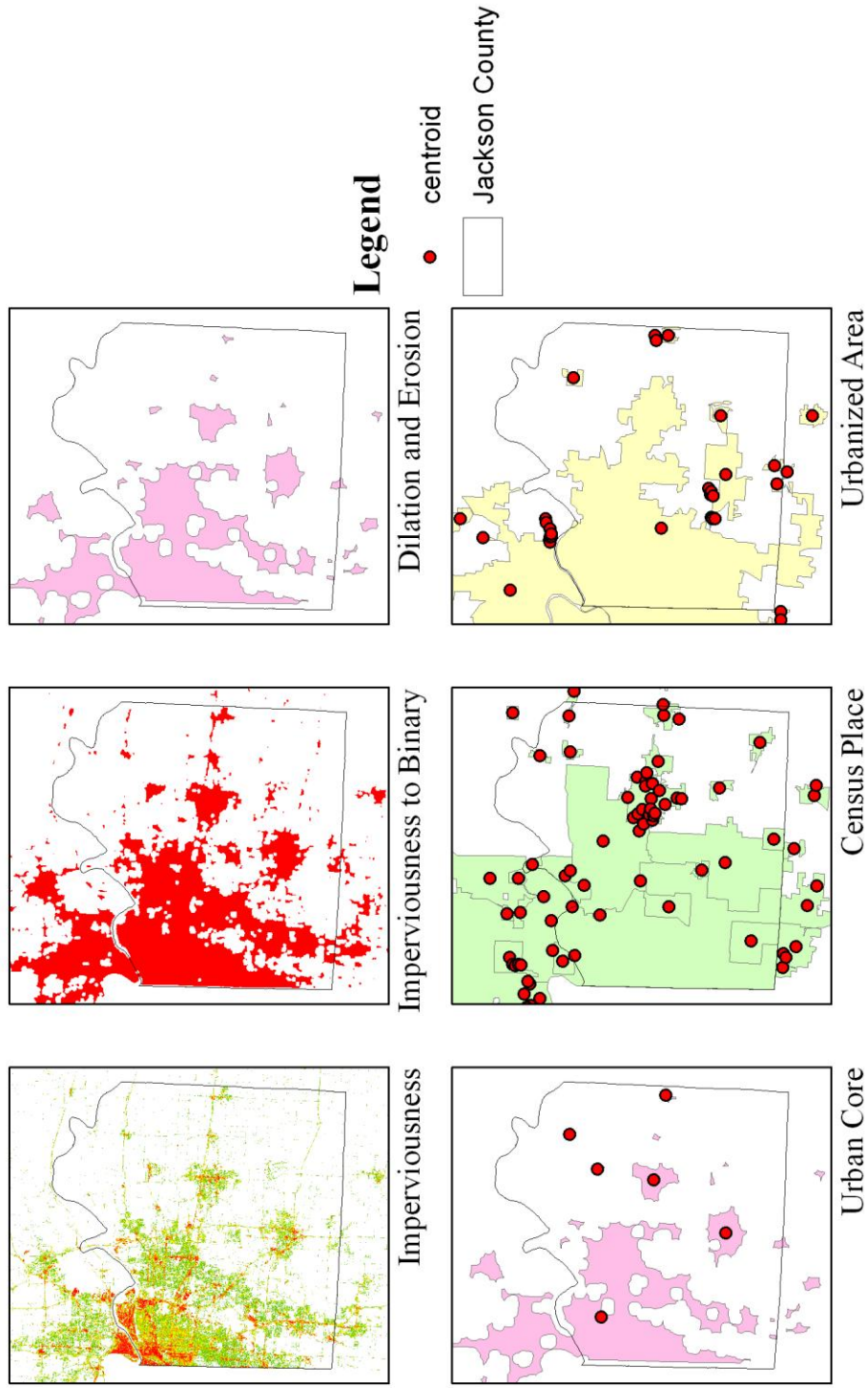


Figure 1. Graphic illustration to show the derivation of core urban areas using impervious surface generated binary urban and non-urban dataset. A morphological operation involving dilation and erosion is used to delineate the core urbanized areas. The core urban derived centroids are visibly better than the ones generated by Census designated place and urbanized areas by Census definition.

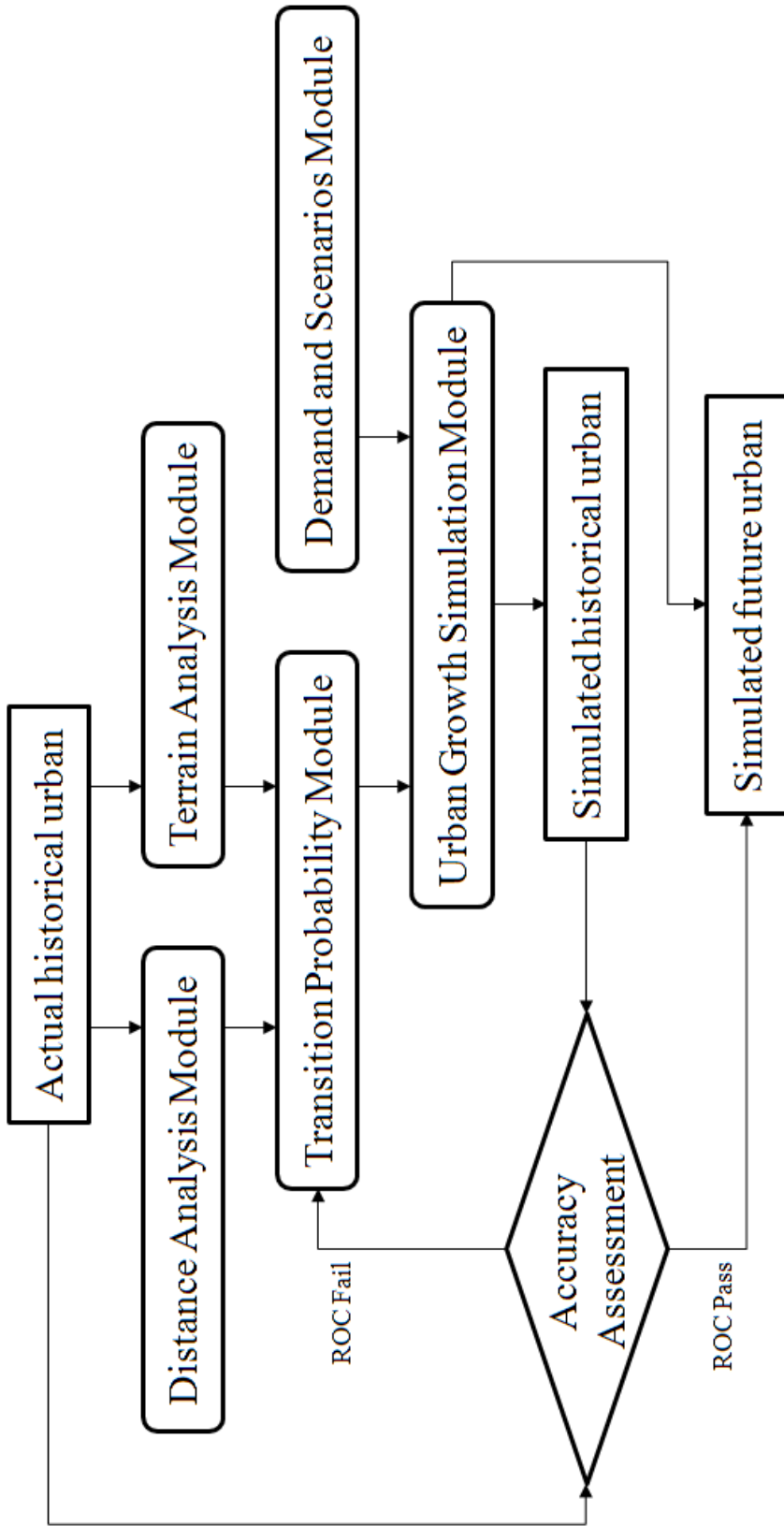


Figure 2. Overall model structure of the urban growth simulation model with a total of 6 sub-modules illustrated.

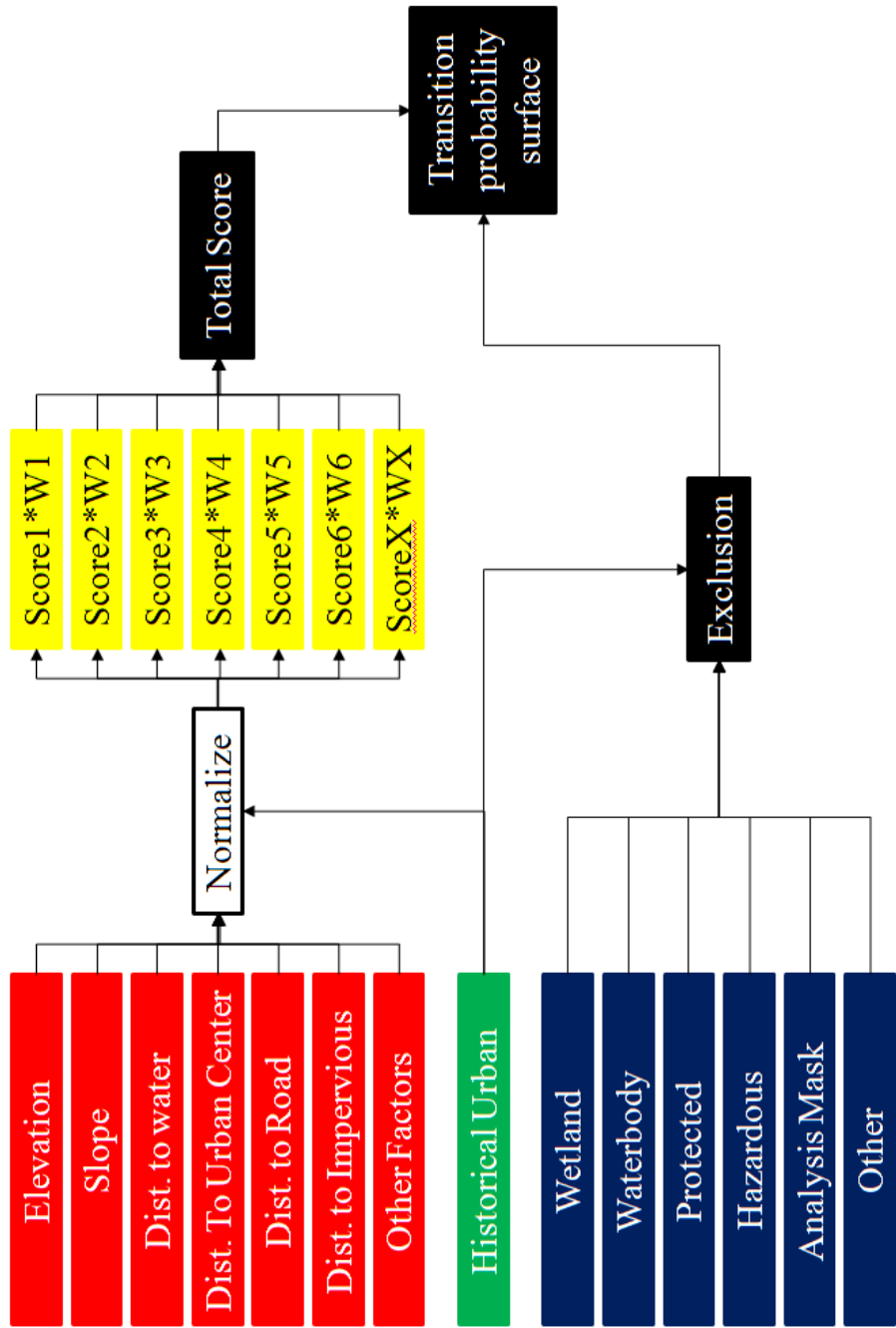


Figure 3. Diagram of the transition probability module, all the predictor variables are reclassified based on the statistical results generated from the multi-criteria evaluation of historical impervious surface coupled with default or expert input weights excluding the non-developable areas to generate the final transition probability surface output.

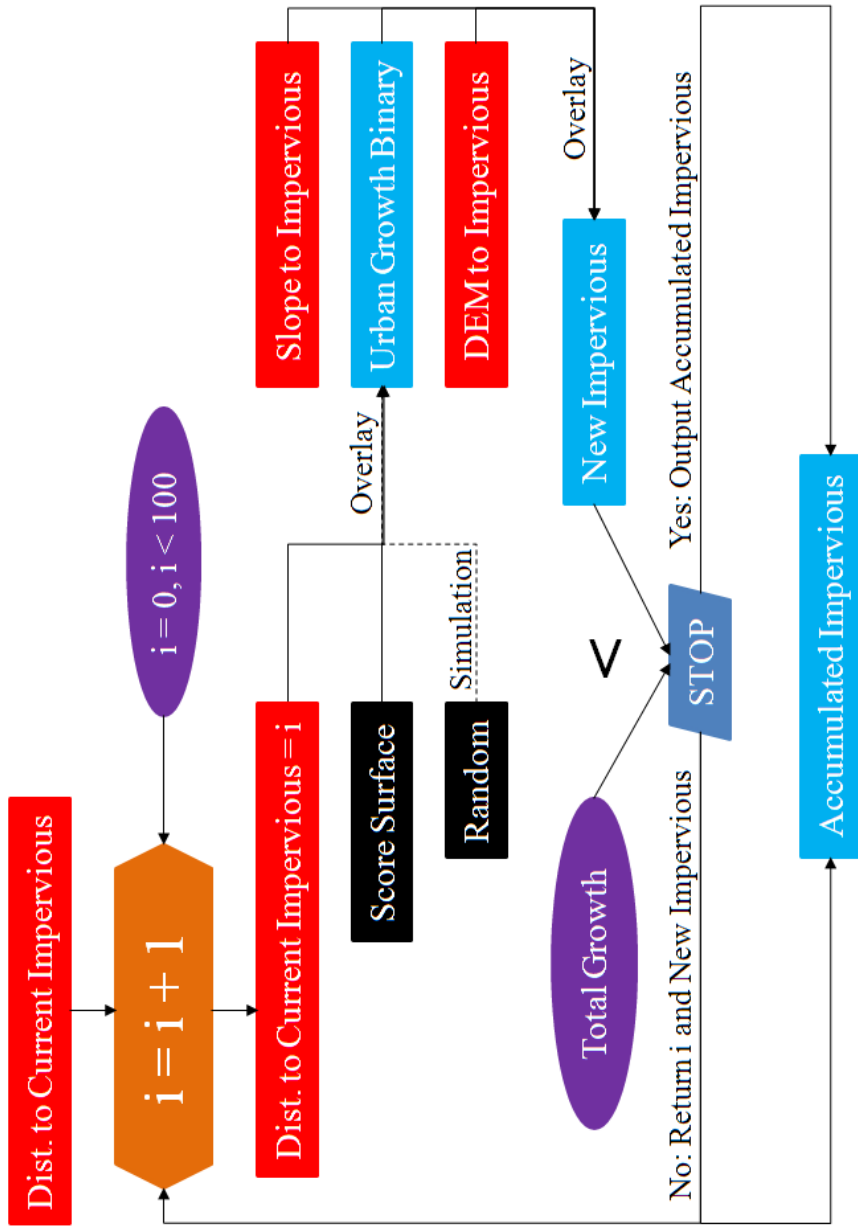


Figure 4. Diagram of the urban growth simulation module, the generation of new impervious surface pixels is based on an iteration loop controlled by the input of preset total growth. The module is stopped by a Boolean logic once the designated growth total is met. The output can be impervious surface density based on the location of new urban and historical density distribution of impervious surface or simply the location of new urban growth.

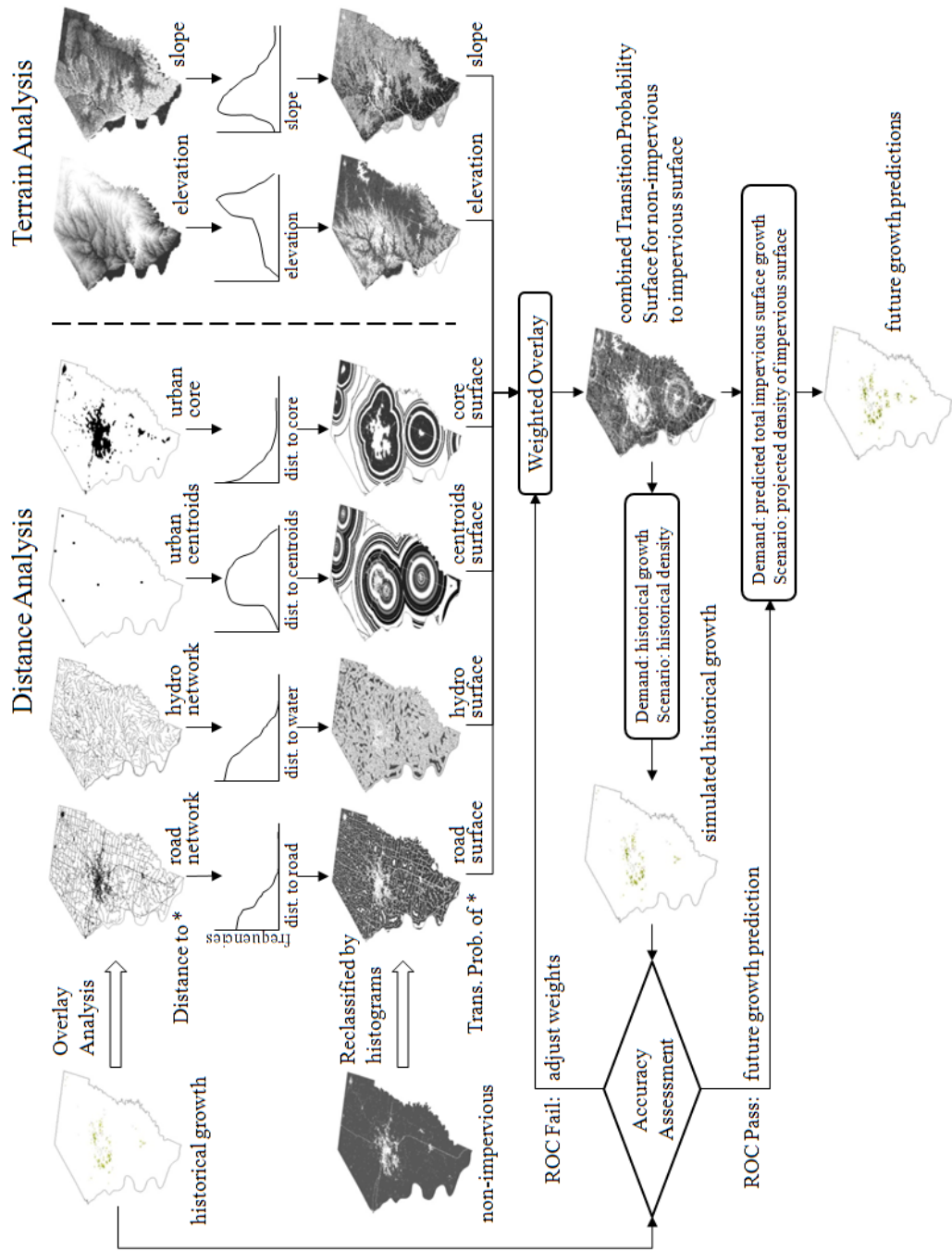


Figure 5. Flowchart of overall model simulation of future urban growth.

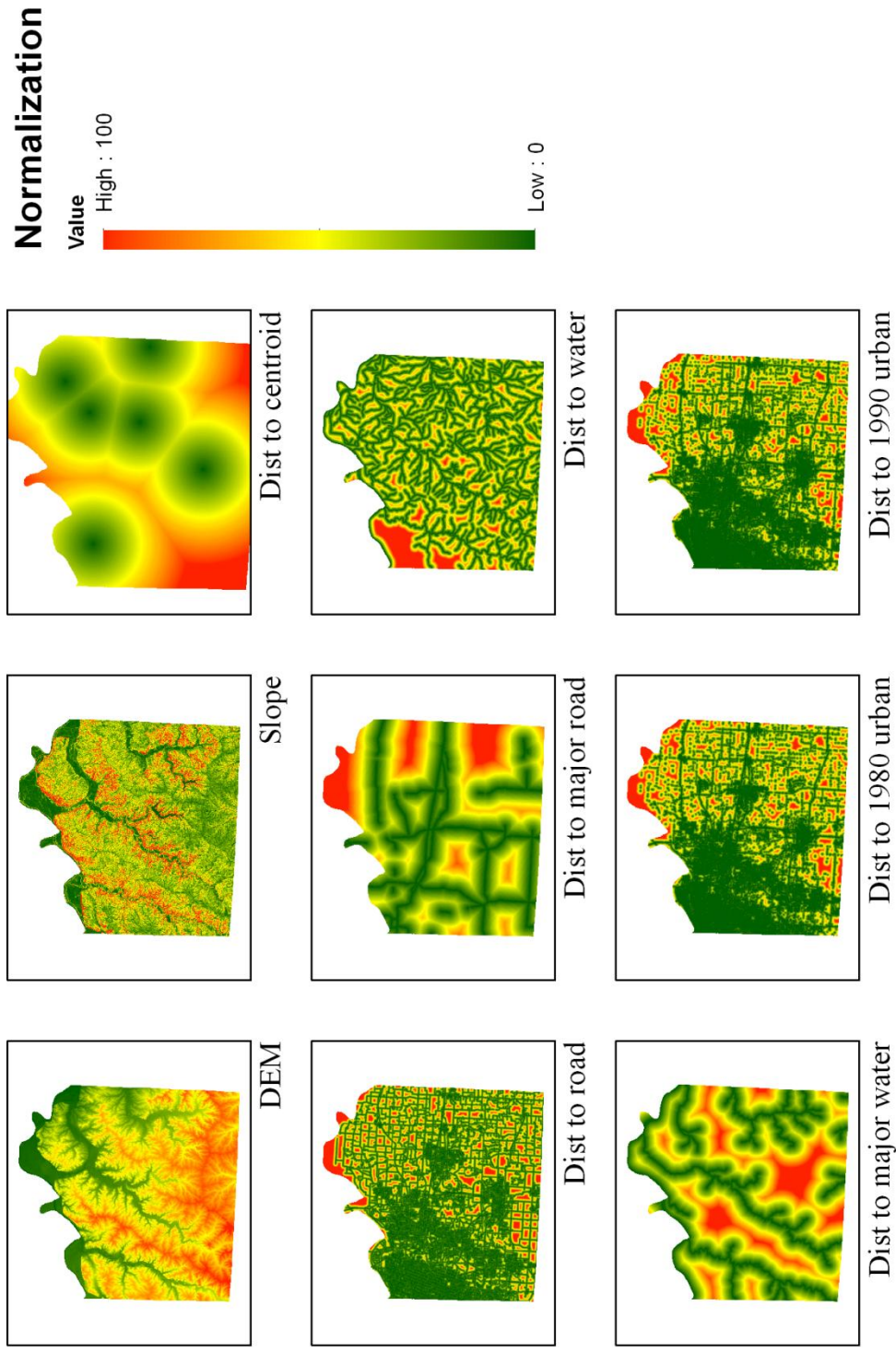


Figure 6. Output of distance analysis and terrain analysis module normalized predictor variables: elevation, slope, distance to centroids, distance to road, distance to major road, distance to water, distance to major water, distance to 1980 imperviousness and distance to 1990 imperviousness.

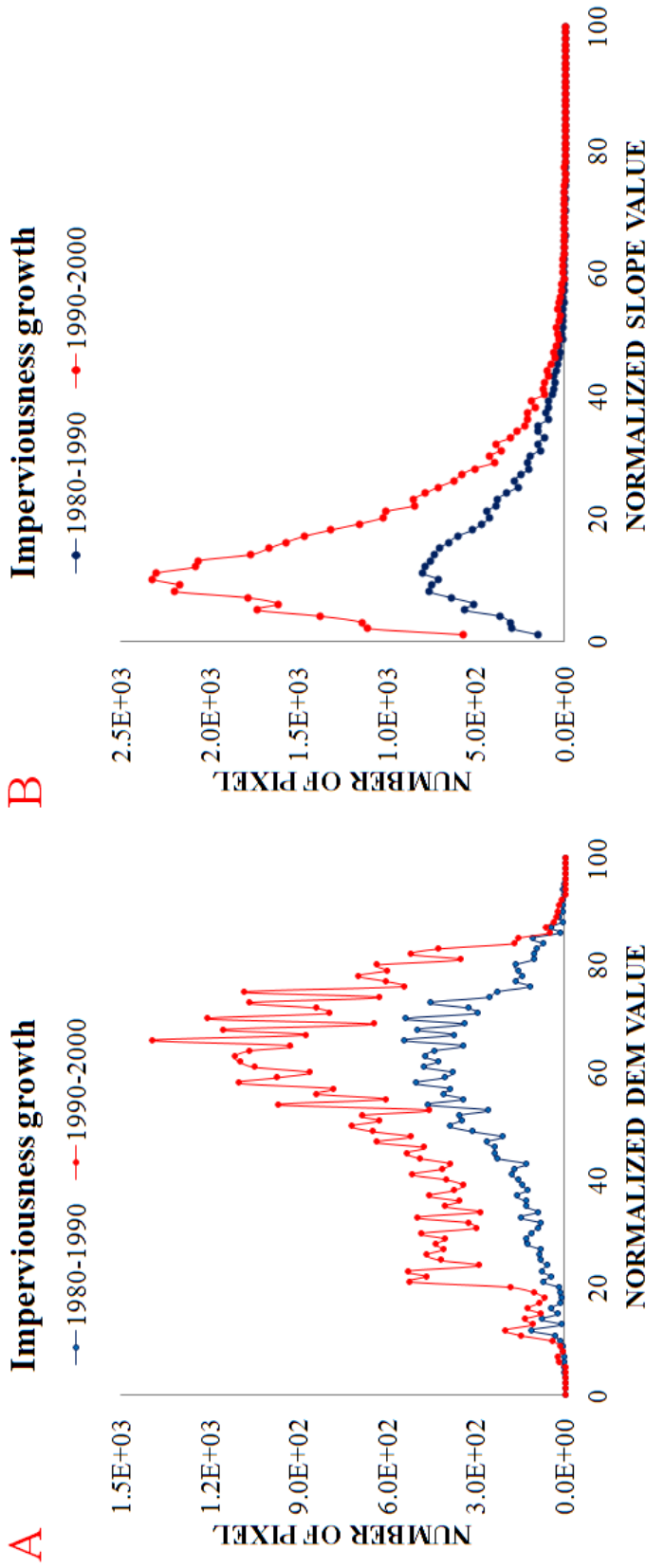


Figure 7. The frequencies of impervious surface growth summarized by normalized elevation in 1980s and 1990s (A). The frequencies of impervious surface growth summarized by normalized slope in the 1980s and 1990s (B).

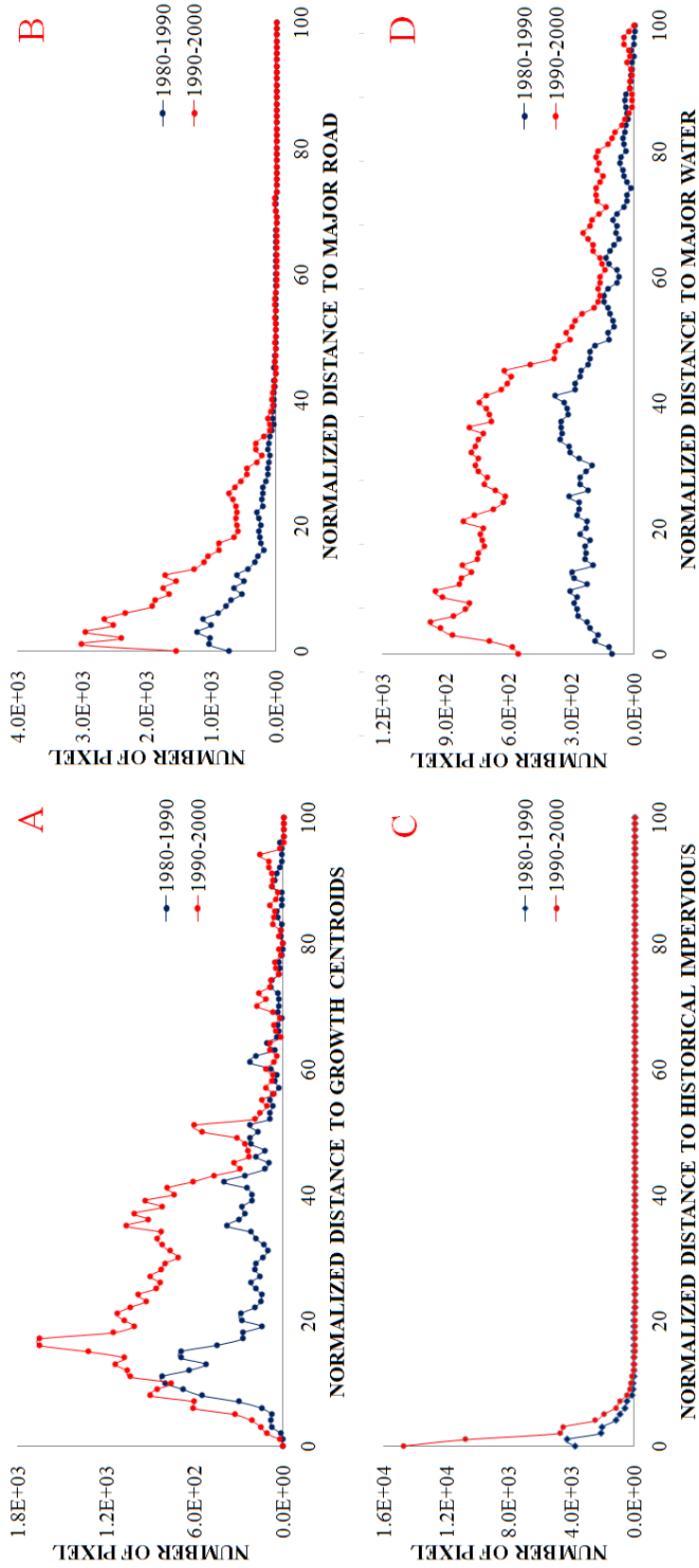


Figure 8. The frequencies of impervious surface growth summarized by normalized distance to growth centroids (A), major road (B), historical impervious surface (C), and major water (D) in the 1980s and 1990s.

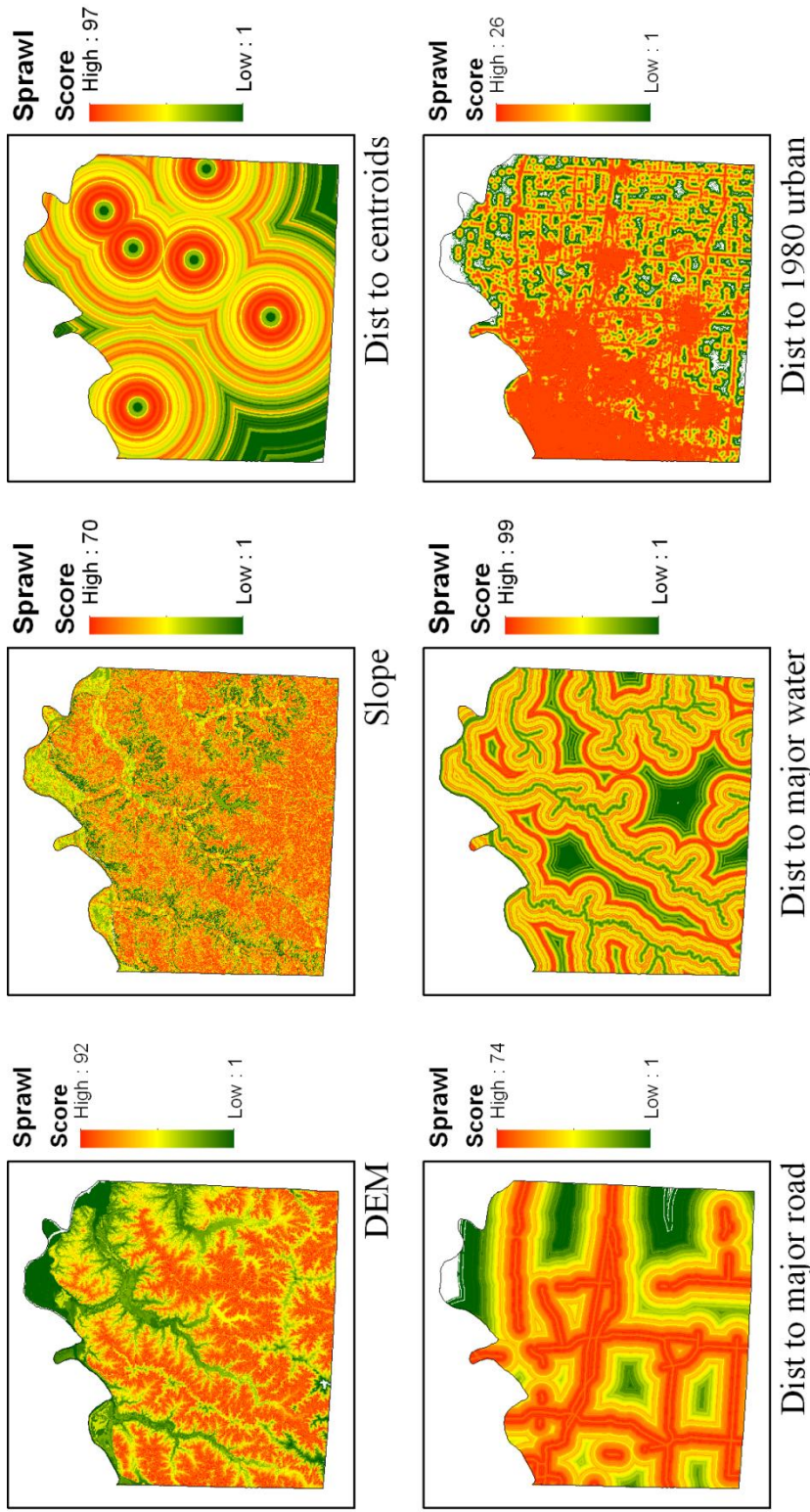


Figure 9. Reclassified transition probability surface values based on normalized elevation, slope, distance to centroids, distance to major road, distance to major water and distance to 1980 impervious surface and multi-criteria evaluation derived statistical results. High values are corresponding to high possibility to change from non-urban to urban based on historical impervious surface growth in the 1980s.

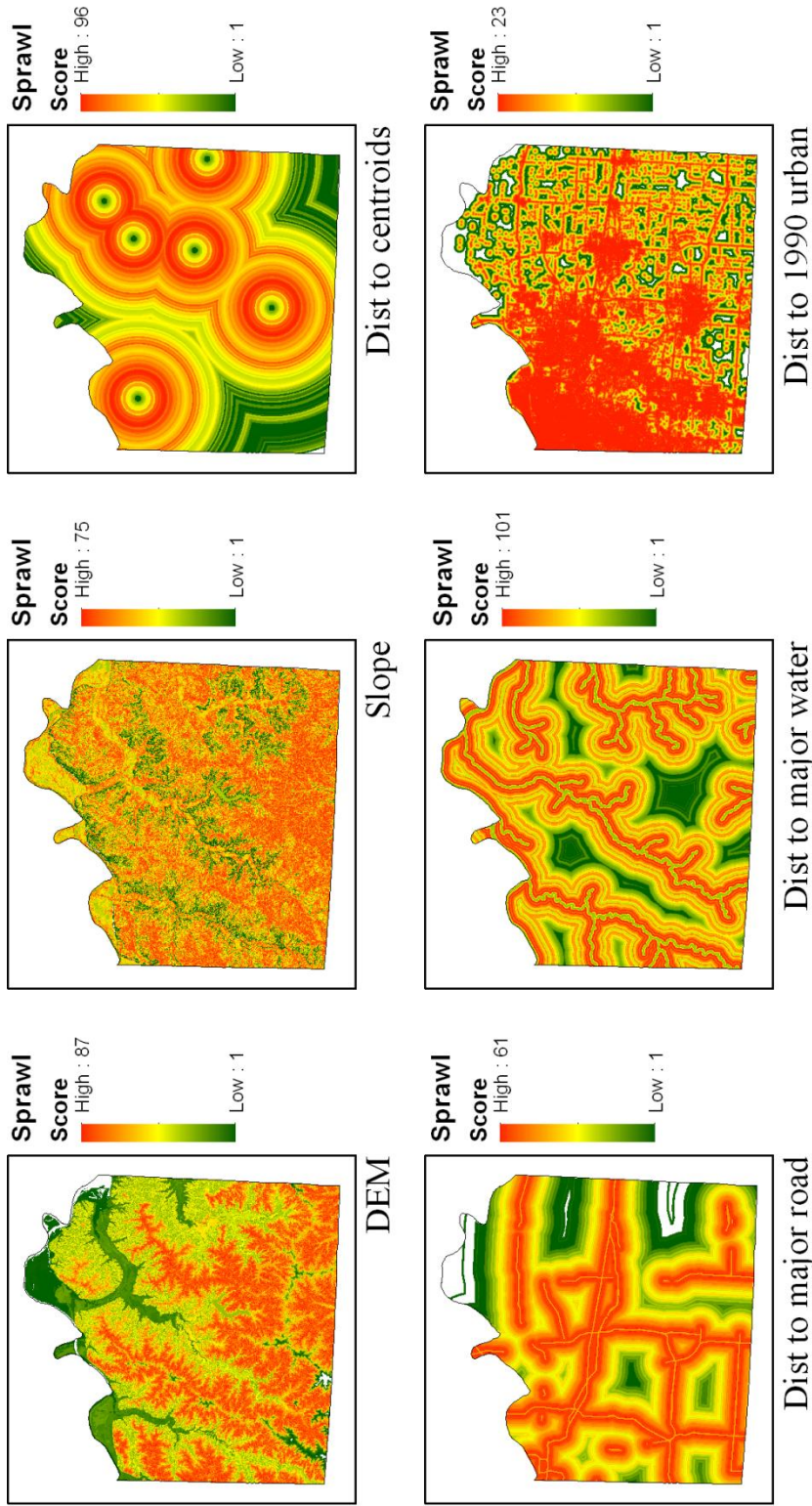
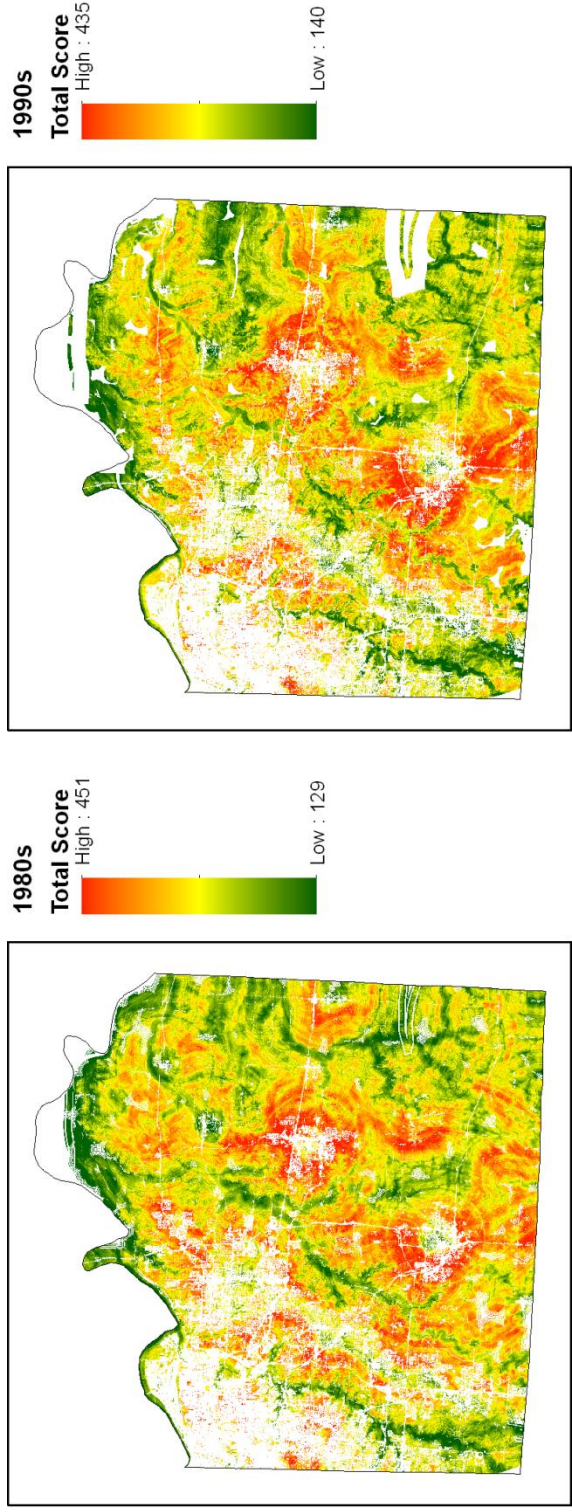


Figure 10. Reclassified transition probability values based on normalized elevation, slope, distance to centroids, distance to major road, distance to major water and distance to 1990 impervious surface and multi-criteria evaluation derived statistical results. High values are corresponding to high possibility to change from non-urban to urban based on historical impervious surface growth in the 1990s.



1980-1990

1990-2000

Figure 11. Total transition probability values for all developable pixels for the decade of 1980s and 1990s. High total values are corresponding to high possibility to change from non-urban to urban based on historical impervious surface growth in the 1980s and 1990s correspondingly.

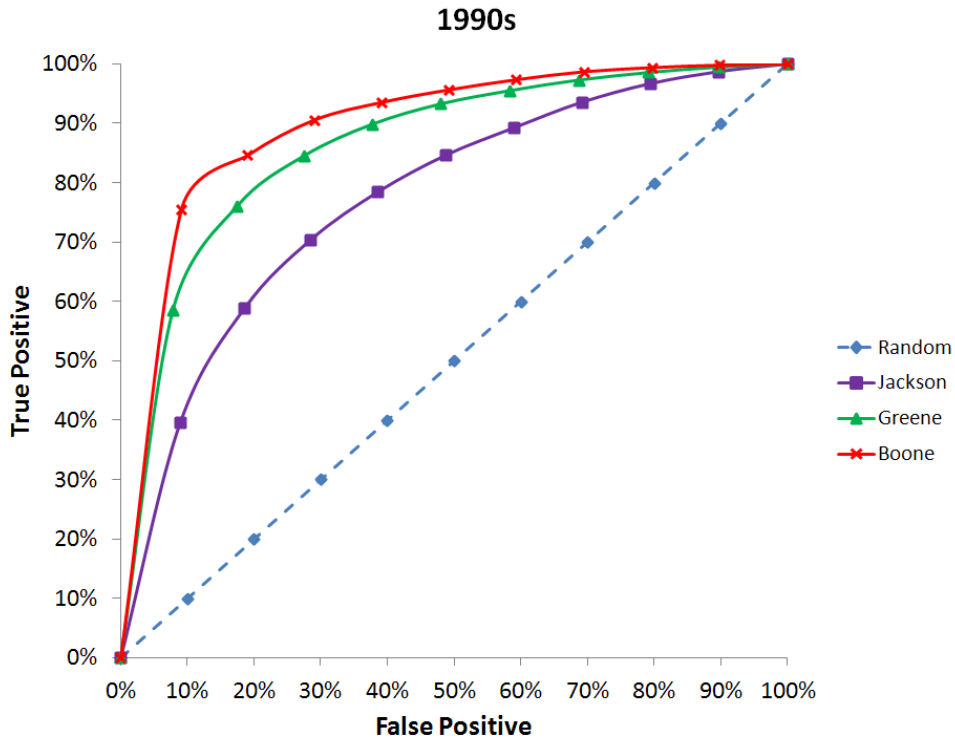
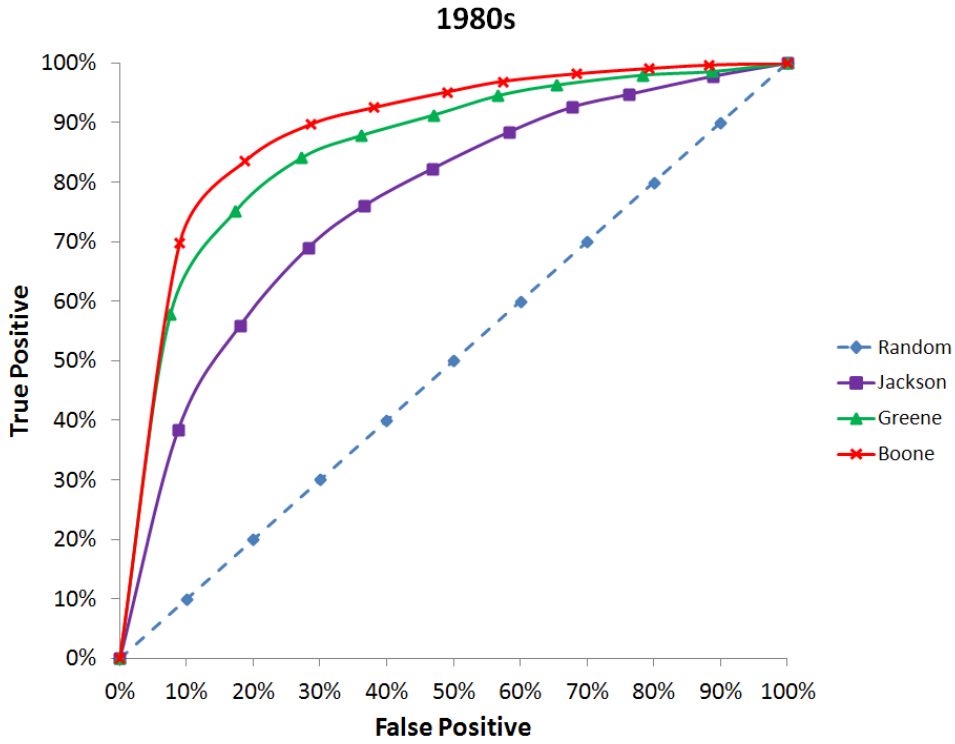
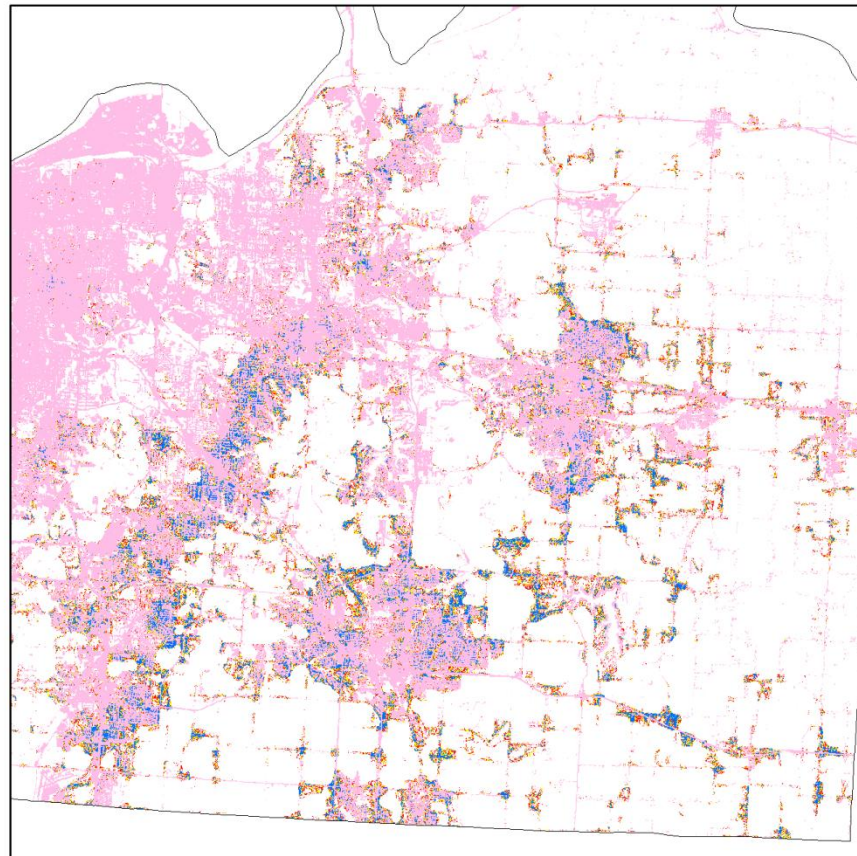


Figure 12. ROC curves for model simulation of impervious surface growth calibration in 1980s (upper) and 1990s (lower) for Jackson, Greene, and Boone Counties compared with random growth of impervious surface.



Legend

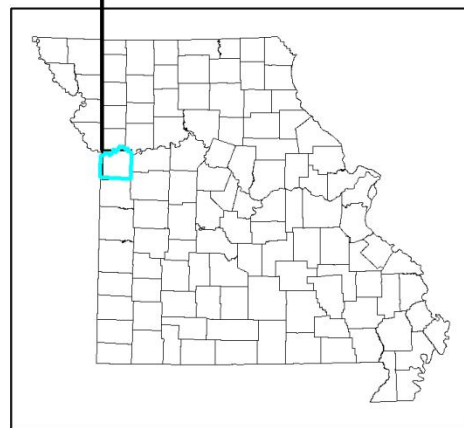
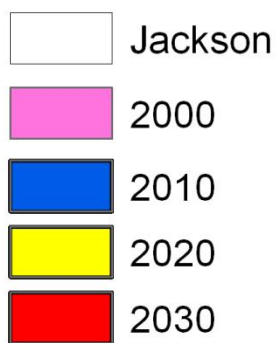
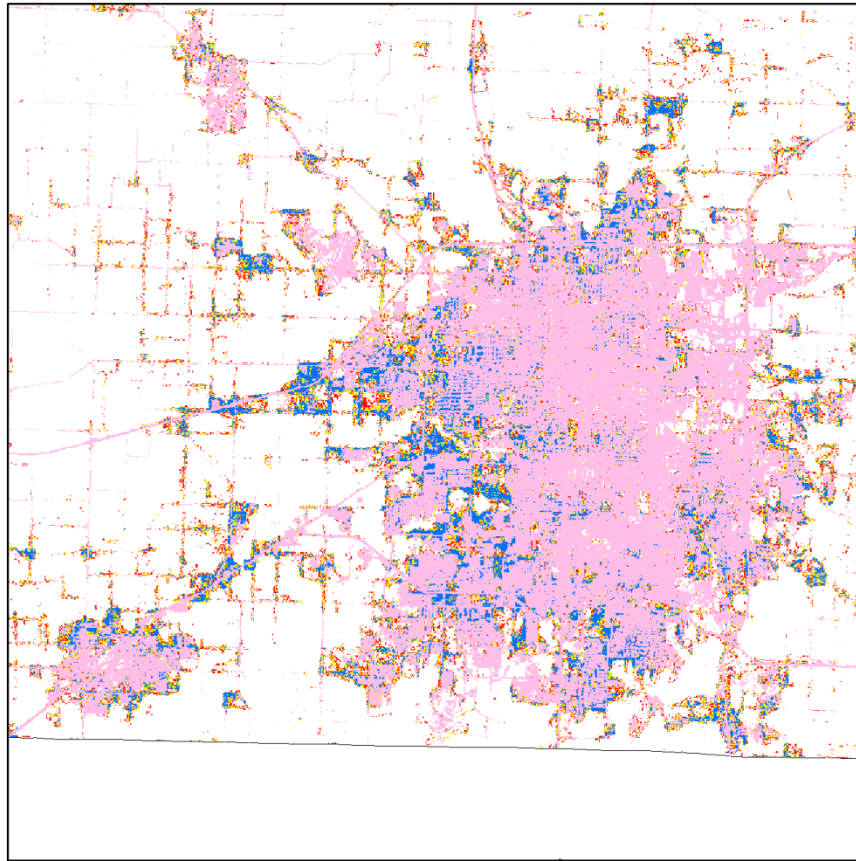


Figure 13. Model simulation for future urban growth in the form of impervious surface growth for Jackson County for 2010, 2020 and 2030 with historical impervious surface extent of 2000 for reference and an inset to illustrate the exact location of the simulation in the spatial context of Missouri.



Legend

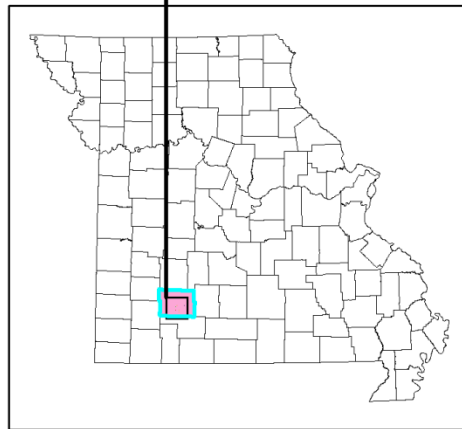
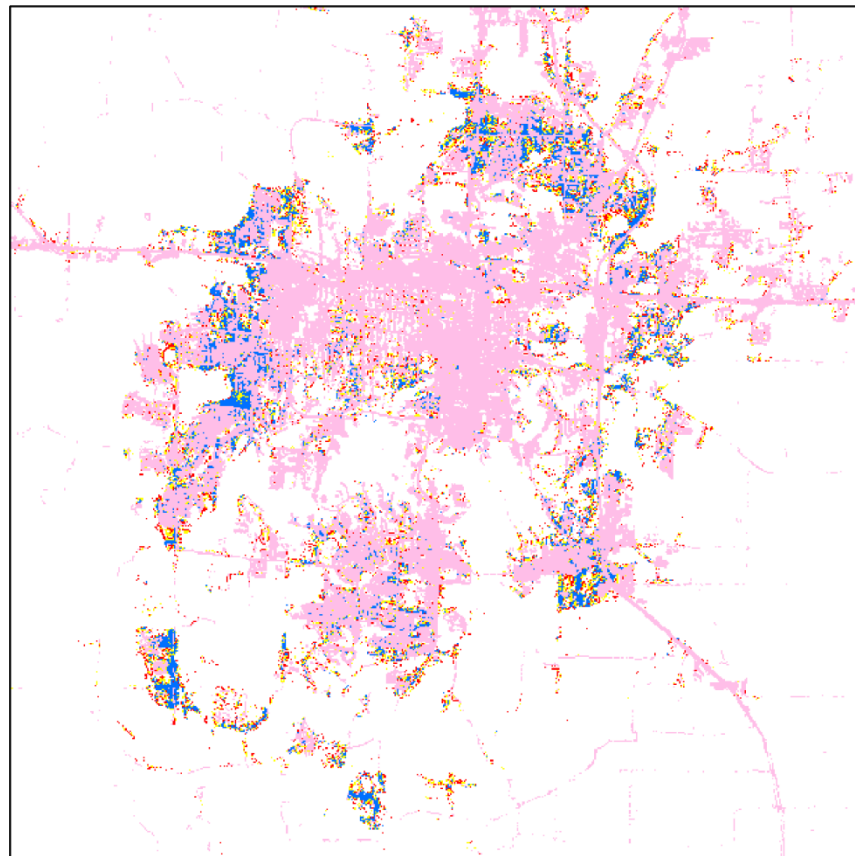


Figure 14. Model simulation for future urban growth in the form of impervious surface growth for Greene County for 2010, 2020 and 2030 with historical impervious surface extent of 2000 for reference and an inset to illustrate the exact location of the simulation in the spatial context of Missouri.



Legend

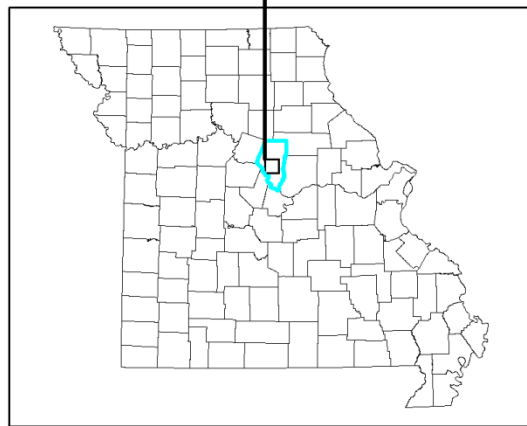
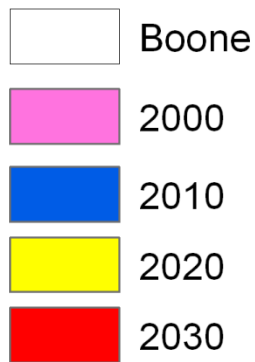


Figure 15. Model simulation for future urban growth in the form of impervious surface growth for Boone County for 2010, 2020 and 2030 with historical impervious surface extent of 2000 for reference and an inset to illustrate the exact location of the simulation in the spatial context of Missouri.

VITA

Bo Zhou was born July 20th, 1983 in Wuhan, China. After graduating with his undergraduate degree in China, he came to the US to pursue graduate studies in the University of Missouri. His seven years in the graduate school is very eventful and productive. He has attended various academic conferences and presented in each. He has published two peer reviewed papers and two more papers are under review. He received the following degrees: a B.S. in Remote Sensing and Photogrammetry from Wuhan University in Wuhan China (2005); a M.A. in Geography from University of Missouri at Columbia, Missouri (2007); and a Ph.D. in Forestry from University of Missouri at Columbia, Missouri (2012).